

Planet formation: key mechanisms and global models

Sean N. Raymond and Alessandro Morbidelli

Abstract

Models of planet formation are built on underlying physical processes. In order to make sense of the origin of the planets we must first understand the origin of their building blocks.

This review comes in two parts. The first part presents a detailed description of six key mechanisms of planet formation:

- The structure and evolution of protoplanetary disks
- The formation of planetesimals
- Accretion of protoplanets
- Orbital migration of growing planets
- Gas accretion and giant planet migration
- Resonance trapping during planet migration

While this is not a comprehensive list, it includes processes for which our understanding has changed in recent years or for which key uncertainties remain.

The second part of this review shows how global models are built out of planet formation processes. We present global models to explain different populations of known planetary systems, including close-in small/low-mass planets (i.e., *super-Earths*), giant exoplanets, and the Solar System's planets. We discuss the different sources of water on rocky exoplanets, and use cosmochemical measurements to constrain the origin of Earth's water. We point out the successes and failings of different models and how they may be falsified.

Finally, we lay out a path for the future trajectory of planet formation studies.

Sean N. Raymond

Laboratoire d'Astrophysique de Bordeaux, CNRS and Université de Bordeaux, Pessac, France
e-mail: rayray.sean@gmail.com

Alessandro Morbidelli

Laboratoire Lagrange, Observatoire de la Côte d'Azur, Nice, France
e-mail: morby@oca.eu

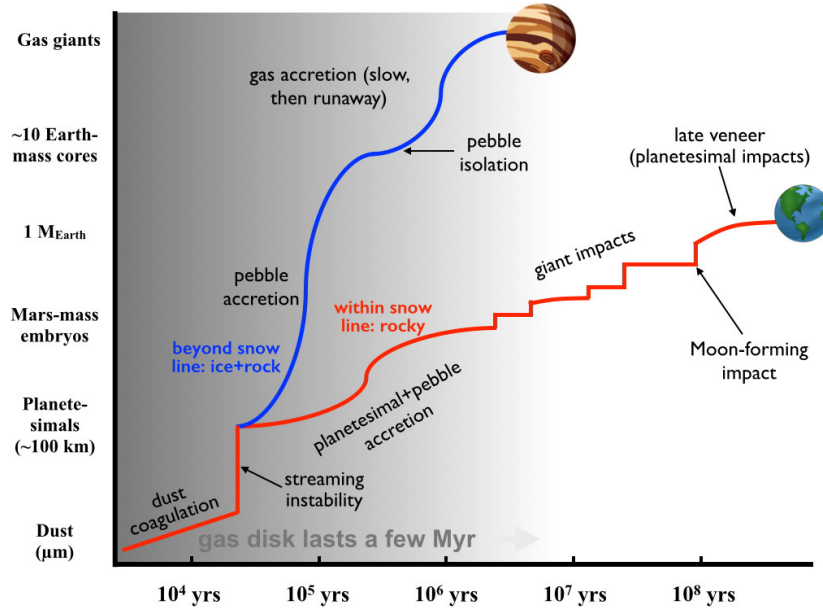


Fig. 1 Schematic view of some of the processes involved in forming Jupiter and Earth. This diagram is designed to present a broad view of the relevant mechanisms but still does not show a number of important effects. For instance, we know from the age distribution of primitive meteorites that planetesimals in the Solar System formed in many generations, not all at the same time. In addition, this diagram does not depict the large-scale migration thought to be ubiquitous among any planets more massive than roughly an Earth-mass (see discussion in text). Adapted from [322].

1 Observational constraints on planet formation models

If planet building is akin to cooking, then a review of planet formation is a cookbook. Planetary systems – like dishes – come in many shapes and sizes. Just as one cooking method cannot produce all foods, a single growth history cannot explain all planets. While the diversity of dishes reflects a range of cooking techniques and tools, they are all drawn from a common set of cooking methods. Likewise, the diversity of planetary systems can be explained by different combinations of processes drawn from a common set of physical mechanisms. Our goal in this review is first to describe the key processes of planet formation and then to show how they may be combined to generate global models, or recipes, for different types of planetary systems.

To illustrate the processes involved, Fig. 1 shows a cartoon picture of our current vision for the growth of Earth and Jupiter. Both planets are thought to have formed from planetesimals in different parts of the Solar System. In our current understanding, the growth tracks of these planets diverge during the pebble accretion process, which is likely to be much more efficient past the snow line [254, 335]. There exists a much larger diversity of planets than just Jupiter and Earth, and many vital processes

are not included in the Figure, yet it serves to illustrate how divergent formation pathways can contribute to planetary diversity.

We start this review by summarizing the key constraints on planet formation models. Constraints come from Solar System measurements (e.g., meteorites), observations of other planetary systems (e.g., exoplanets and protoplanetary disks), as well as laboratory measurements (e.g., to measure the sticking properties of small grains).

Solar System Constraints

Centuries of human observation have generated a census of the Solar System, albeit one that is still not 100% complete. The most important constraints for planet formation include our system’s orbital architecture as well as compositional and timing information gleaned from in-situ measurements. An important but challenging exercise is to distill the multitude of existing constraints into just a few large-scale factors to which resolution-limited models can be compared.

The central Solar System constraints are:

- **The masses and orbits of the terrestrial planets.**¹ The key quantities include their number, their absolute masses and mass ratios, and their low-eccentricity, low-inclination orbits. These have been quantified in studies that attempted to match their orbital distribution. For example the normalized angular momentum deficit *AMD* is defined as [260, 88]:

$$AMD = \frac{\sum_j m_j \sqrt{a_j} (1 - \cos(i_j) \sqrt{1 - e_j^2})}{\sum_j m_j \sqrt{a_j}}, \quad (1)$$

where a_j , e_j , i_j , and m_j correspond to planet j ’s semimajor axis, eccentricity, orbital inclination, and mass. The Solar System’s terrestrial planets have an *AMD* of 0.0018.

The radial mass concentration statistic *RMC* (called S_c by [88]) is a measure of the radial mass profile of the planets. It is defined as:

$$RMC = \max \left(\frac{\sum m_j}{\sum m_j [\log_{10}(a/a_j)]^2} \right). \quad (2)$$

The function in brackets is calculated sweeping a across all radii, and the *RMC* represents the maximum. For a one-planet system *RMC* is infinite. The *RMC* is higher when the planets’ masses are concentrated in narrow radial zones (as is the case in the terrestrial planets, with two large central planets and two small

¹ The terms “terrestrial” and “rocky” planet are interchangeable: the Solar System community generally uses the term *terrestrial* and the exoplanet community uses *rocky*. We use both terminologies in this review to represent planets with solid surfaces that are dominated (by mass) by rock and iron.

exterior ones). The *RMC* becomes smaller for systems that are more spread out and systems in which all planets have similar masses. The Solar System's terrestrial planets' *RMC* is 89.9.

Confronting distributions of simulated planets with these empirical statistics (as well as other ones) has become a powerful and commonly-used discriminant of terrestrial planet formation models [88, 373, 428, 426, 423, 104, 291].

- **The masses and orbits of the giant planets.** As for the terrestrial planets, the number (two gas giant, two ice giant), masses and orbits of the giant planets are the central constraints. The orbital spacing of the planets is also important, for instance the fact that no pair of giant planets is located in mean motion resonance. An important, overarching factor is simply that the Solar System's giant planets are located far from the Sun, well exterior to the orbits of the terrestrial planets.
- **The orbital and compositional structure of the asteroid belt.** While spread over a huge area the asteroid belt contains only $\sim 4.5 \times 10^{-4} M_{\oplus}$ in total mass [246, 252, 125], orders of magnitude less than would be inferred from models of planet-forming disks such as the very simplistic minimum-mass solar nebula model [495, 189]. The orbits of the asteroids are excited, with eccentricities that are roughly evenly distributed from zero to 0.3 and inclinations evenly spread from zero to more than 20° (a rough stability limit given the orbits of the planets). While there are a number of compositional groups within the belt, the general trend is that the inner main belt is dominated by S-types and the outer main belt by C-types [171, 125, 126]. S-type asteroids are associated with ordinary chondrites, which are quite dry (with water contents less than 0.1% by mass), and C-types are linked with carbonaceous chondrites, some of which (CI, CM meteorites) contain $\sim 10\%$ water by mass [436, 236, 10].
- **The cosmochemically-constrained growth histories of rocky bodies in the inner Solar System.** Isotopic chronometers have been used to constrain the accretion timescales of different solid bodies in the Solar System. Ages are generally measured with respect to CAIs (Calcium and Aluminum-rich Inclusions), mm-sized inclusions in chondritic meteorites that are dated to be 4.568 Gyr old [67]. Cosmochemical measurements indicate that chondrules, which are similar in size to CAIs, started to form at roughly the same time [107, 371]. Age dating of iron meteorites suggests that differentiated bodies – large planetesimals or planetary embryos – were formed in the inner Solar System within 1 Myr of CAIs [181, 251, 448]. Isotopic analyses of Martian meteorites show that Mars was fully formed within 5-10 Myr after CAIs [368, 117], whereas similar analyses of Earth rocks suggest that Earth's accretion did not finish until much later, roughly 100 Myr after CAIs [476, 240].

There is evidence that two populations of isotopically-distinct chondritic meteorites – the so-called carbonaceous and non-carbonaceous meteorites – have similar age distributions [250]. Given that chondrules are expected to undergo very fast radial drift within the disk [494, 253], this suggests that the two populations were kept apart and radially segregated, perhaps by the early growth of Jupiter's core [250].

Constraints from Observations of Planet-forming disks around other stars

Gas-dominated protoplanetary disks are the birthplaces of planets. Disks' structure and evolution plays a central role in numerous processes such as how dust drifts [47], where planetesimals form [135, 134], and what direction and how fast planets migrate [51].

We briefly summarize the main observational constraints from protoplanetary disks for planet formation models (see also dedicated reviews [506, 25, 11]):

- **Disk lifetime.** In young clusters virtually all stars have detectable hot dust, which is used as a tracer for the presence of gaseous disks [179, 70]. However, in old clusters very few stars have detectable disks. Analyses of a large number of clusters of different ages indicate that the typical timescale for disks to dissipate is a few Myr [179, 70, 192, 294, 390]. Fig. 2 shows this trend, with the fraction of stars with disks decreasing as a function of cluster age. It is worth noting that observational biases are at play, as the selection of stars that are members of clusters can affect the interpreted disk dissipation timescale [392].
- **Disk masses.** Most masses of protoplanetary disks are measured using sub-mm observations of the outer parts of the disk in which the emission is thought to be optically thin [506]. Disk masses are commonly found to be roughly equivalent to 1% of the stellar mass, albeit with a 1-2 order of magnitude spread [140, 17, 18, 21, 506]. It has recently been pointed out that there is tension between the inferred disk masses and the masses of exoplanet systems, as a large fraction of disks do not appear to contain enough mass to produce exoplanet systems [295, 352], even assuming a very high efficiency of planet formation (see Fig. 2).
- **Disk structure and evolution.** ALMA observations suggest that disks are typically 10-100 au in scale [36], similar to the expected dimensions of the Sun's protoplanetary disk [189, 168, 247]. Sub-mm observations at different radii indicate that the surface density of dust Σ in the outer parts of disks follows a roughly $\Sigma \sim r^{-1}$ radial surface density slope [353, 287, 19, 20], consistent with simple models for accretion disks. Many disks observed with ALMA show ringed substructure [14, 22, 16]. Disks are thought to evolve by accreting onto their host stars, and the accretion rate itself has been measured to vary as a function of time; indeed, the accretion rate is often used as a proxy for disk age [185, 25]. As disks age, they evaporate from the inside-out by radiation from the central star [12, 382, 11] and, depending on the stellar environment, may also evaporate from the outside-in due to external irradiation [194, 4].
- **Dust around older stars.** Older stars with no more gas disks often have observable dust, called *debris disks* (recent reviews: [315, 200]). Roughly 20% of Sun-like stars are found to have dust at mid-infrared wavelengths [74, 478, 329]. This dust is thought to be associated with the slow collisional evolution of outer planetesimal belts akin to our Kuiper belt but generally containing much more mass [515, 248]. The occurrence rate of dust is observed to decrease with the stellar age [324, 79]. More [less] massive stars have significantly higher [lower] occurrence of debris disks [463, 268]. There is no clear observed correlation between debris disks and planets [347, 300, 348]. A significant fraction of old stars have been found to

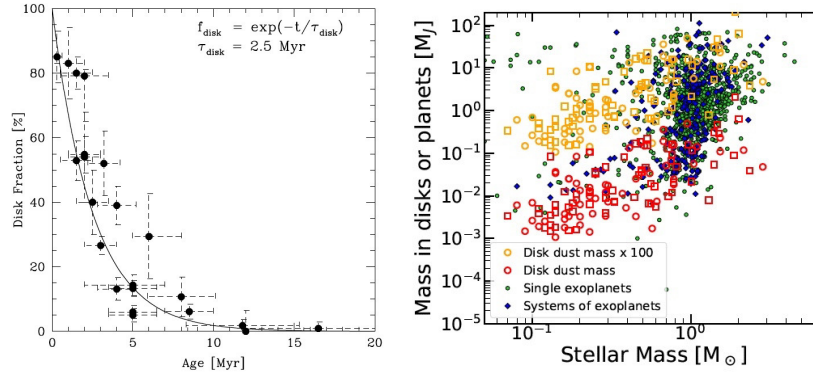


Fig. 2 Two observational constraints on planet-forming disks. **Left:** The fraction of stars that have detectable disks in clusters of different ages. This suggests that the typical gaseous planet-forming disk only lasts a few Myr [179, 70, 192]. From [294]. **Right:** A comparison between inferred disk masses and the mass in planets in different systems, as a function of host star mass. The dust mass (red) is measured using sub-mm observations (and making the assumption that the emission is optically thin), and the gas mass is inferred by imposing a 100:1 gas to dust ratio. There is considerable tension, as the population of disks does not appear massive enough to act as the precursors of the population of known planets. The solution to this problem is not immediately obvious. Perhaps disk masses are systematically underestimated [172], or perhaps disks are continuously re-supplied with material from within their birth clusters via Bondi-Hoyle accretion [473, 327]. From [295].

have warm or hot *exo-zodiacal* dust [2, 142, 245]. The origin of this dust remains mysterious as there is no clear correlation between the presence of cold and hot dust [142].

Constraints from Extra-Solar Planets

With a catalog of thousands of known exoplanets, the constraints from planets around other stars are extremely rich and constantly being improved. Figure 3 shows the orbital architecture of a (non-representative) selection of known exoplanet systems. While there exist biases in the detection methods used to find exoplanets [508], their sheer number form the basis of a statistical framework with which to confront planet formation theories.

We can grossly summarize the exoplanet constraints as follows:

- **Occurrence and demographics.** Over the past few decades it has been shown using multiple techniques that exoplanets are essentially ubiquitous [318, 85, 38]. Despite the observational biases, a huge diversity of planetary systems has been discovered. Yet when drawing analogies with the Solar System, it is worth noting that, if our Sun were to have been observed with present-day technology Jupiter is the only planet that could have been detected [339, 422]. This makes the Solar System unusual at roughly the 1% level. In addition, the Solar System is

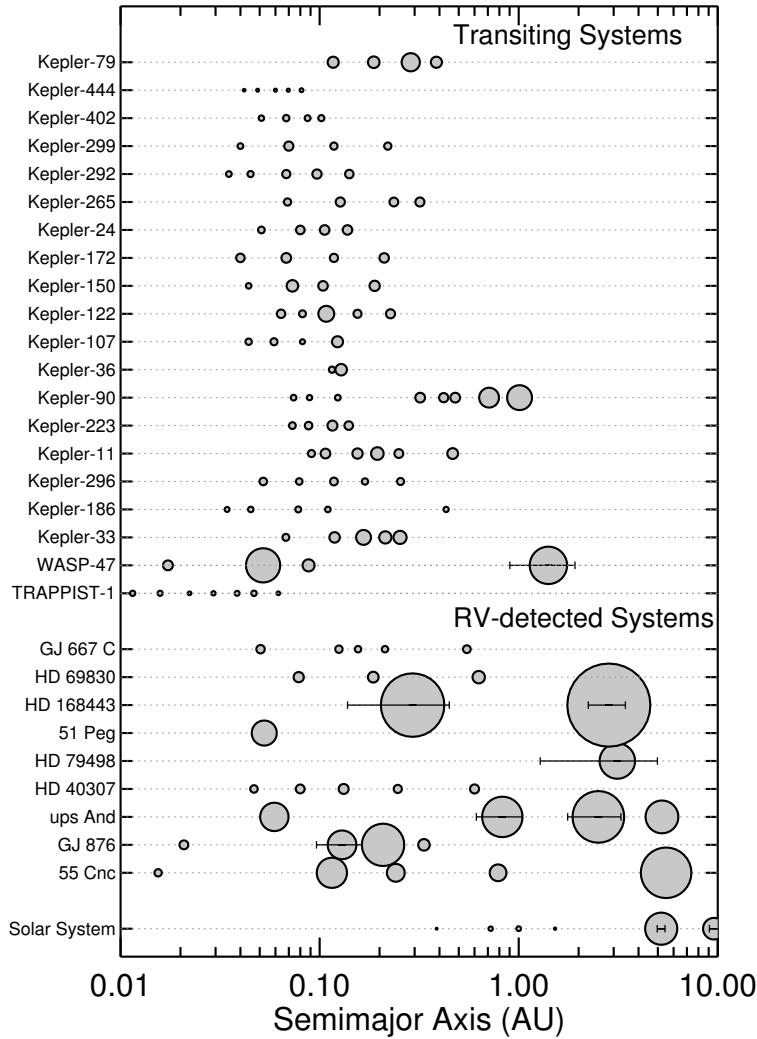


Fig. 3 A sample of exoplanet systems selected by hand to illustrate their diversity (from [422]). The systems at the top were discovered by the transit method and the bottom systems by radial velocity (RV). Of course, some planets are detected in both transit and RV (e.g. 55 Cnc e; [127]). A planet's size is proportional to its actual size (but is not to scale on the x-axis). For RV planets without transit detections we used the $M \sin i \propto R^{2.06}$ scaling derived by [284]. For giant planets ($M > 50 M_{\oplus}$) on eccentric orbits ($e > 0.1$; also for Jupiter and Saturn), the horizontal error bar represents the planet's pericenter to apocenter orbital excursion. The central stars vary in mass and luminosity; e.g., TRAPPIST-1 is an ultracool dwarf star with mass of only $0.08 M_{\odot}$ [162]. A handful of systems have \sim Earth-sized planets in their star's habitable zones, such as Kepler-186 [407], TRAPPIST-1 [162], and GJ 667 C [24]. Some planetary systems – for example, 55 Cancri [146] – are found in multiple star systems.

borderline unusual in *not* containing any close-in low-mass planets [302, 352]. For the purposes of this review we focus on two categories of planets: gas giants and close-in low-mass planets, made up of high-density ‘super-Earths’ and puffy ‘mini-Neptunes’.

- **Gas giant planets: occurrence and orbital distribution.** Radial velocity surveys have found giant planets to exist around roughly 10% of Sun-like stars [113, 318]. Roughly one percent of Sun-like stars have *hot Jupiters* on very short-period orbits [196, 512], very few have *warm Jupiters* with orbital radii of up to 0.5-1 au [77, 481], and the occurrence of giant planets increases strongly and plateaus between 1 to several au, and there are hints that it decreases again farther out [318, 145]; see Fig. 16. Direct imaging surveys have found a dearth of giant planets on wide-period orbits, although only massive young planets tend to be detectable [68]. Microlensing surveys find a similar overall abundance of gas giants as radial velocity surveys and have shown that ice giant-mass planets appear to be far more common than their gas giant counterparts [170, 464]. Giant planet occurrence has also been shown to be a strong function of stellar metallicity, with higher metallicity stars hosting many more giant planets [169, 443, 261, 147, 121].
- **Close-in low-mass planets: occurrence and orbital distribution.** Perhaps the most striking exoplanet discovery of the past decade was the amazing abundance of close-in small planets. Planets between roughly Earth and Neptune in size or mass with orbital periods shorter than 100 days have been shown to exist around roughly 30-50% of all main sequence stars [318, 195, 157, 131, 391, 508]. Both the masses and radii have been measured for a subset of planets [297] and analyses have shown that the smaller planets tend to have high densities and the larger ones have low densities, which has been interpreted as a transition between rocky ‘super-Earths’ and gas-rich ‘mini-Neptunes’ with a transition size or mass of roughly $1.5-2 R_{\oplus}$ or $\sim 3-5 M_{\oplus}$ [499, 497, 437, 511, 97]. For the purposes of this review we generally lump together all close-in planets smaller than Neptune and call them *super-Earths* for simplicity. The super-Earth population has a number of intriguing characteristics that constrain planet formation models. While they span a range of sizes, within a given system super-Earths tend to have very similar sizes [325, 498]. Their period ratios form a broad distribution and do not cluster at mean motion resonances [284, 143]. Finally, in the Kepler survey the majority of super-Earth systems only contain a single super-Earth [38, 440], which contrasts with the high-multiplicity rate found in radial velocity surveys [318].

Outline of this review

The rest of this chapter is structured as follows.

In Section 2 we will describe six essential mechanisms of planet formation. These are:

- The structure and evolution of protoplanetary disks (Section 2.1)
- The formation of planetesimals (Section 2.2)
- Accretion of protoplanets (Section 2.3)

- Orbital migration of growing planets (Section 2.4)
- Gas accretion and giant planet migration (Section 2.5)
- Resonance trapping during planet migration (Section 2.6)

This list does not include every process related to planet formation. These processes have been selected because they are both important and are areas of active study.

Next we will build global models of planet formation from these processes (Section 3). We will first focus on models to match the intriguing population of close-in small/low-mass planets: the *super-Earths* (Section 3.1). Next we will turn our attention to the population of giant planets, using the population of known giant exoplanets to guide our thinking about the formation of our Solar System's giant planets (Section 3.2). Next we will turn our attention to matching the Solar System itself (Section 3.3), starting from the classical model of terrestrial planet formation (Section 3.3.1) and then discussing newer ideas: the Grand Tack (Section 3.3.2), Low-mass Asteroid belt (Section 3.3.3) and Early Instability (Section 3.3.4) models. Then we will discuss the different sources of water on rocky exoplanets, and use cosmochemical measurements to constrain the origin of Earth's water (Section 3.4). Finally, in Section 4 we will lay out a path for the future trajectory of planet formation studies.

2 Key processes in planet formation

In this Section we review basic properties that affect the disk's structure, planetesimals and planet formation as well as dynamical evolution. These processes build the skeleton of our understanding of how planetary systems are formed. As pieces of a puzzle, they will then be put together to develop models on the origin of the different observed structures of planetary systems in Sec. 3.

2.1 Protoplanetary disks: structure and evolution

Planet formation takes place in gas-dominated disks around young stars. These disks were inferred by Laplace [259] from the near-perfect coplanarity of the orbits of the planets of the Solar System and of angular momentum conservation during the process of contraction of gas towards the central star. Disks are now routinely observed (imaged directly or deduced through the infrared excess in the spectral energy distribution) around young stars. The largest among protoplanetary disks are now resolved by the ALMA mm-interferometer ([16]). Here we briefly review the viscous-disk model and the wind-dominated model. For more in depth reading we recommend [25] and [480].

2.1.1 Viscous-disk model(s)

The simplest model of a protoplanetary disk is a donut of gas and dust in rotation around the central star evolving under the effect of its internal viscosity. This is hereafter dubbed the *viscous-disk model*. Because of Keplerian shear, different rings of the disk rotate with different angular velocities, depending on their distance from the star. Consequently, friction is exerted between adjacent rings. The inner ring, rotating faster, tends to accelerate the outer ring (i.e. it exerts a positive torque) and the outer ring tends to decelerate the inner ring (i.e. exerting a negative torque of equal absolute strength). It can be demonstrated (see for instance [178]) that such a torque is

$$T = 3\pi\Sigma\nu r^2\Omega, \quad (3)$$

where Σ is the surface density of the disk at the boundary between the two rings, ν is the viscosity, and Ω is the rotational frequency at the distance r from the star.

A fundamental assumption of a viscous-disk model is that it is in steady state, which means the the mass flow of gas \dot{M} is the same at any distance r . Under this assumption it can be demonstrated that the gas flows inwards with a radial speed

$$v_r = -\frac{3}{2}\frac{\nu}{r} \quad (4)$$

and that the product $\nu\Sigma$ is independent of r . That is, the radial dependence of Σ is the inverse of the radial dependence of ν . Of course the steady-state assumption is valid only in an infinite disk. In a more realistic disk with a finite size, this assumption is good only in the inner part of the disk, whereas the outer part expands into the vacuum under the effect of the viscous torque [292].

If viscosity rules the radial structure of the disk, pressure rules the vertical structure. At steady state, the disk has to be in hydrostatic equilibrium, which means that the vertical component of the gravitational force exerted by the star has to be equal and opposite to the pressure force, i.e.:

$$\frac{GM_*}{r^3}z = -\frac{1}{\rho}\frac{dP}{dz}, \quad (5)$$

where M_* is the mass of the star, z is the height over the disk's midplane, ρ is the volume density of the disk and P is its pressure. Using the perfect gas law $P = \mathcal{R}/\rho T/\mu$ (where \mathcal{R} is the gas constant, μ is the molecular weight of the gas and T is the temperature) and assuming that the gas is vertically isothermal (i.e. T is a function of r only), equation (5) gives the solution:

$$\rho(z) = \rho(0) \exp\left(-\frac{z^2}{2H^2}\right), \quad (6)$$

where $H = \sqrt{\mathcal{R}r^3T/\mu}$ is called the *pressure scale-height* of the disk (the gas extends to several scale-heights, with exponentially vanishing density).

We now need to compute $T(r)$. The simplest way is to assume that the disk is solely heated by the radiation from the central star (passive disk assumption, see [100]). Most of the disk is opaque to radiation, so the star can illuminate and deposit heat only on the surface layer of the disk, here defined as the layer where the integrated optical depth along a stellar ray reaches unity. For simplicity we assume that the stellar radiation hits a hard surface, whose height over the midplane is proportional to the pressure scale-height H . Then, the energy deposited on this surface between r and $r + \delta r$ from the star is:

$$E_+^{Irr} = \left(\frac{L_*}{4\pi r^2} \right) (2\pi r)(r\delta h), \quad (7)$$

where δh is the change in aspect ratio H/r over the range δr , namely $d(H/r)/dr\delta r$; the parentheses have been put in (7) to regroup the terms corresponding respectively to (i) stellar brightness L_* at distance r , (ii) circumference of the ring and (iii) projection of $H(r + \delta r) - H(r)$ on the direction orthogonal to the stellar ray hitting the surface. On the other hand, the same surface will cool by black-body radiation in space at a rate

$$E_-^{Irr} = 2\pi r\delta r\sigma T^4 \quad (8)$$

where σ is Boltzmann's constant. Equating (7) and (8) and remembering the definition of H as a function of r and T leads to

$$T(r) \propto r^{-3/7} \quad \text{and} \quad H/r \propto r^{2/7}. \quad (9)$$

The positive exponent in the dependence of the aspect ratio H/r on r implies that the disk is *flared*. Notice that neither quantities in Eq. 9 depend on disk's surface density, opacity or viscosity.

However, because we are dealing with a viscous disk, we cannot neglect the heat released by viscous dissipation, i.e. in the friction between adjacent rings rotating at different speeds. Over a radial width δr , this friction dissipates energy at a rate ([25])

$$E_+^{Visc} = \frac{9}{8}\Sigma\nu\Omega^2 2\pi r\delta r. \quad (10)$$

This heat is dissipated mostly close to the midplane, where the disk's volume density is highest. This changes the cooling with respect to Eq. 8. The energy cannot be freely irradiated in space; it has first to be transported from the midplane through the disk, which is opaque to radiation, to the "surface" boundary with the optically thin layer. Thus the cooling term in Eq. 8 has to be divided by $\kappa\Sigma$, where κ is the disk's opacity. Again by balancing heating and cooling and the definition of H we find:

$$H/r \propto (\dot{M}^2\kappa/\nu r)^{1/8}, \quad (11)$$

where we have used that $\dot{M} = 2\pi r v_r \Sigma = -3\pi\nu\Sigma$.

To know the actual radial dependence of this expression, we need to know the radial dependences of κ and ν (remember that \dot{M} is assumed to be independent of r).

The opacity depends on temperature, hence on r in a complicated manner, with abrupt transitions when the main chemical species (notably water) condense [43]. Let's ignore this for the moment. Concerning $\nu(r)$, Shakura and Sunyaev [454] proposed from dimensional analysis that the viscosity is proportional to the square of the characteristic length of the system and is inversely proportional to the characteristic timescale. At a distance r from the star, the characteristic length of a disk is $H(r)$ and the characteristic timescale is the inverse of the orbital frequency Ω . Thus they postulated $\nu = \alpha H^2 \Omega$, where α is an unknown coefficient of proportionality. If one adopts this prescription for the viscosity, the viscous-disk model is qualified as an *α -disk model*. Injecting this definition of ν into Eq. 11 one obtains

$$H/r \propto \left(\frac{\kappa \dot{M}^2}{\alpha} \right)^{1/10} r^{1/20} . \quad (12)$$

This result implies that the aspect ratio of a viscously heated disk is basically independent of r (and $T \propto 1/r$), in sharp contrast with the aspect ratio of a passive disk. Because the disk is both heated by viscosity and illuminated by the star, its aspect ratio at each r will be the maximum between Eq. 12 and Eq. 9: it will be flat in the inner part and flared in the outer part. Because Eq. 12 depends on opacity, accretion rate and α , the transition from the flat disk and the flared disk will depend on these quantities. In particular, given that \dot{M} decreases with time as the disk is consumed by accretion of gas onto the star [185], this transition moves towards the star as time progresses [51]. The effects of non-constant opacity introduce wiggles of H/r over this general trend [51].

The viscous disk model is simple and neat, but its limitation is in the understanding of the origin of the disk's viscosity. The molecular viscosity of the gas is by orders of magnitude insufficient to deliver the observed accretion rate \dot{M} onto the central star [185] given a reasonable disk's density, comparable to that of the Minimum Mass Solar Nebula model (MMSN: [495], [189]). It was thought that the main source of viscosity is turbulence and that turbulence was generated by the magneto-rotational instability (see [34]). But this instability requires a relatively high ionization of the gas, which is prevented when grains condense in abundance, at a temperature below $\sim 1,000\text{K}$ [128]. Thus, only the very inner part of the disk is expected to be turbulent and have a high viscosity. Beyond the condensation line of silicates, the viscosity should be much lower. Remembering that $\nu\Sigma$ has to be constant with radius, the drop of ν at the silicate line implies an abrupt increase of Σ . As we will see, this property has an important role in the drift of dust and the migration of planets. It was expected that near the surface of the disk, where the gas is optically thin and radiation from the star can efficiently penetrate, enough ionization may be produced to sustain the Magneto Rotational Instability (MRI) [462]. However, these low-density regions are also prone to other effects of non-ideal magneto-hydrodynamics (MHD), like ambipolar diffusion and the Hall effect [32], which are expected to quench turbulence. Thus, turbulent viscosity does not seem to be large enough beyond the silicate condensation line to explain the stellar accretion rates that are

observed. This has promoted an alternative model of disk structure and evolution, dominated by the existence of disk winds, as we review next.

2.1.2 Wind-dominated disk models

Unlike viscous disk models, which can be treated with simple analytic formulae, the emergence of disk winds and their effects are consequence of non-ideal MHD. Thus their mathematical treatment is complicated and the results can be unveiled only through numerical simulations. Thus, this Section will remain at a phenomenological level. For an in-depth study we recommend [32, 31, 480].

As we have seen above, the ionized regions of the disk have necessarily a low density. If the disk is crossed by a magnetic field, the ions atoms in these low-density regions can travel along the magnetic field lines without suffering collision with neutral molecules. This is the essence of *ambipolar diffusion*.

Consider a frame co-rotating with the disk at radius r_0 from the central star. In this frame, fluid parcels feel an effective potential combining the gravitational and centrifugal potentials. If poloidal (r, z) magnetic field lines act as rigid wires for fluid parcels (which happens as long as the poloidal flow is slower than the local Alfvén speed)², then a parcel initially at rest at $r = r_0$ can undergo a runaway if the field line to which it is attached is more inclined than a critical angle. Along such a field line, the effective potential decreases with distance, leading to an acceleration of magnetocentrifugal origin. This yields the inclination angle criterion $\theta > 30^\circ$ for the disk-surface poloidal field with respect to the vertical direction. Here fluid parcels rotate at constant angular velocity and so increase their specific angular momentum. Angular momentum is thus extracted from the disk and transferred to the ejected material. As the disk loses angular momentum, some material has to be transferred towards the central star, driving the stellar accretion. The efficiency of this process is directly connected to the disk's magnetic field strength, with a stronger field leading to faster accretion.

In wind-dominated disk models the viscosity can be very low and the disk's density can be of the order of that of the MMSN. The observed accretion rate onto the central star is not due to viscosity (the small value of $\nu\Sigma$ provides only a minor contribution) but is provided by the radial, fast advection of a small amount of gas, typically at 3-4 pressure scale heights H above the disk's midplane [174]. The global structure of the disk can be symmetric (Fig. 4a) or asymmetric (Fig. 4b) depending on simulation parameters and the inclusion of different physical effects (e.g. the Hall effect). The origin of the asymmetry is not fully understood. In some cases, the magnetic field lines can be concentrated in narrow radial bands that can fragment the disk into concentric rings ([46]; see Fig. 4b). This effect is intriguing in

² The Alfvén speed is defined as the ratio between the magnetic field intensity B and $\sqrt{\mu_0\rho}$, where μ_0 is the permeability of vacuum and ρ is the total mass density of the charged plasma particles. Apart from relativity effects, the Alfvén speed is the phase speed of the Alfvén wave, which is a magnetohydrodynamic wave in which ions oscillate in response to a restoring force provided by an effective tension on the magnetic field lines.

light of the recent ALMA observations of the ringed structure of protoplanetary disks [14, 22, 16]. It should be stressed, however, that there is currently no consensus on the origin of the observed rings. An alternative possibility is that they are the consequence of planet formation [521] or of other disk instabilities [474]. Understanding whether ring formation in protoplanetary disks is a prerequisite for, or a consequence of, planet formation is an essential goal of current research.

Depending on assumptions on the radial gradient of the magnetic field, and hence of the strength of the wind, the gas density of the disk may be partially depleted in its inner part [465] or preserve a global power-law structure similar to that of viscous-disk models [30] (see Fig. 5). A positive surface density gradient as in [465] has implication for the radial drift of dust and planetesimals [377] and for the migration of protoplanets [376]. In addition in [465] the maximum of the surface density (where dust and migrating planets tend to accumulate) moves outwards as time progresses and the disk evolves.

Disk winds do not generate an appreciable amount of heat. In wind-dominated models the disk temperature is close to that of a passive disk [343, 87], which has a snowline inward of 1 au [51]. The deficit of water in inner solar system bodies (the terrestrial planets and the parent bodies of enstatite and ordinary chondrites) demonstrates that the protoplanetary solar disk inwards of 2-3 au was warm, at least initially [333]. This implies that either the viscosity of the disk was quite high or another form of heating – for instance the adiabatic compression of gas as it fell onto the disk from the interstellar medium – was operating early on.

2.1.3 Dust dynamics

The dynamics of dust particles is largely driven by gas drag. Any time that there is a difference in velocity between the gas and the particle, a drag force is exerted on the particle which tends to erase the velocity difference. The *friction time* t_f is defined as the coefficient which relates the accelerations felt by the particle to the gas-particle velocity difference, namely:

$$\dot{\mathbf{v}} = -\frac{1}{t_f}(\mathbf{v} - \mathbf{u}), \quad (13)$$

where \mathbf{v} is the particle velocity vector and \mathbf{u} is the gas velocity vector, while $\dot{\mathbf{v}}$ is the particle's acceleration. The smaller a dust particle the shorter its t_f . In the Epstein regime, where the particle size is smaller than the mean free path of a gas molecule, t_f is linearly proportional to the particle's size R . In the Stokes regime the particle size is larger than the mean free path of a gas molecule and $t_f \propto \sqrt{R}$. It is convenient to introduce a dimensionless number, called the *Stokes number*, defined as $\tau_s = \Omega t_f$, which represents the ratio between the friction time and the orbital timescale.

The effects of gas drag are mainly the sedimentation of dust towards the midplane and its radial drift towards pressure maxima.

To describe an orbiting particle as it settles in a disk, cylindrical coordinates are the natural choice. The stellar gravitational force can be decomposed into a radial

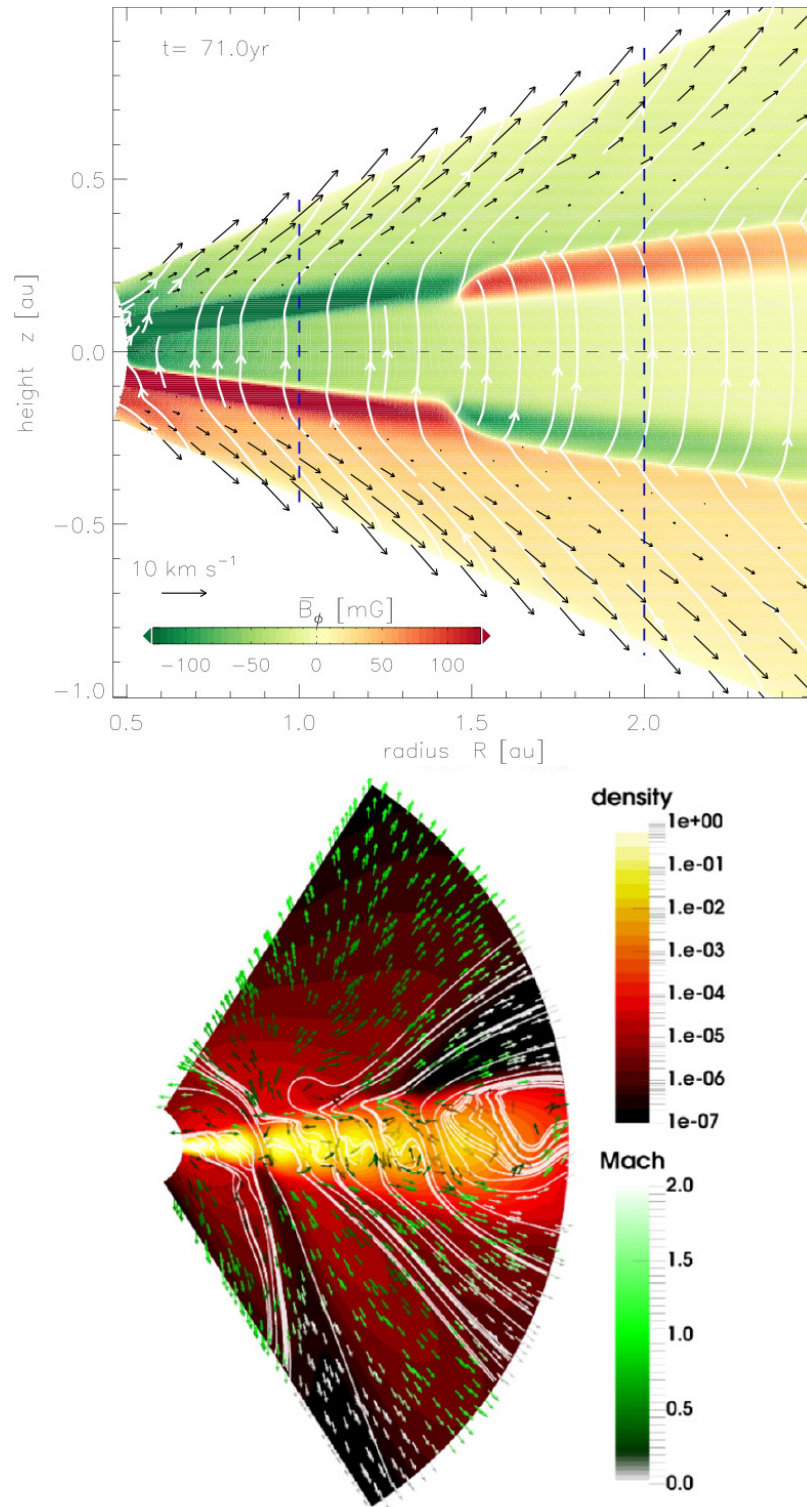


Fig. 4 Disk structure in two different wind-dominated disk global models. In the top panel from [174] shows the intensity and polarity of the magnetic field, the field lines and the velocity vectors of the wind. This disk model is symmetric relative to the mid-plane (anti-symmetric in polarity). The bottom panel from [46] shows the gas density, the magnetic field lines and the wind velocity vectors. This model has no symmetry relative to the midplane. Moreover, the disk is fragmented in rings by the accumulation of magnetic field lines in specific radial intervals.

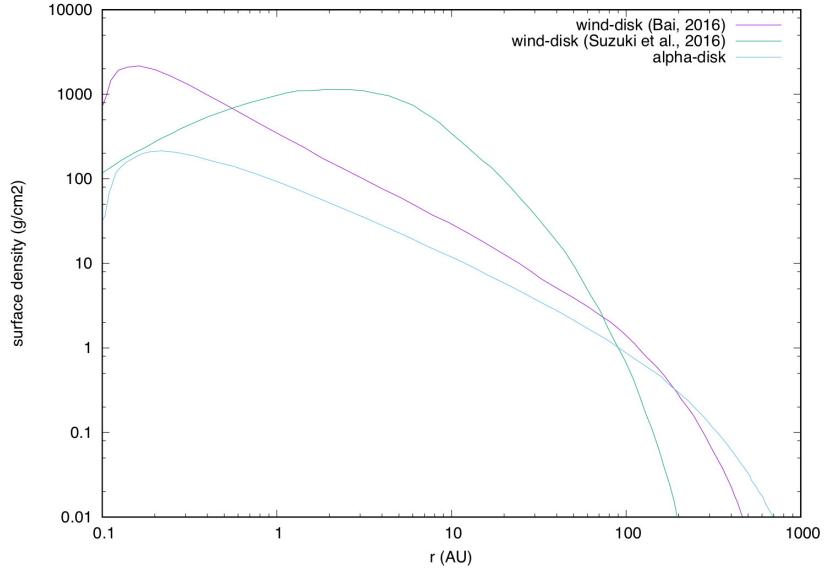


Fig. 5 Comparison between the radial surface density distribution of the wind-dominated disk models of ([465]), ([30]) and an α -disk model.

and a vertical component. The radial component is cancelled by the centrifugal force due to the orbital motion. The vertical component, $F_{g,z} = -m\Omega^2 z$, where m is the mass of the particle and z its vertical coordinate, instead accelerates the particle towards the midplane, until its velocity v_{settle} is such that the gas drag force $F_D = mv_{settle}/t_f$ cancels $F_{g,z}$. This sets $v_{settle} = \Omega^2 z t_f$ and gives a settling time $T_{settle} = z/v_{settle} = 1/(\Omega^2 t_f) = 1/(\Omega \tau_s)$. Thus, for a particle with Stokes number $\tau_s = 1$ the settling time is the orbital timescale. However, turbulence in the disk stirs up the particle layer, which therefore has a finite thickness. Assuming an α -disk model, the scale height of the particle layer is [99]:

$$H_p = \frac{H}{\sqrt{1 + \tau_s/\alpha}}. \quad (14)$$

Dust particles undergo radial drift due to a small difference of their orbital velocity relative to the gas. The gas feels the gravity of the central star and its own pressure. The pressure radial gradient exerts a force $F_r = -(1/\rho)dP/dr$ which can oppose or enhance the gravitational force. As we saw above, $P \propto \rho T$, and $\rho \sim \Sigma/H$. Because Σ and T in general decrease with r , $dP/dr < 0$. The pressure force opposes to the gravity force, diminishing it. Consequently, the gas parcels orbit the star at a speed

that is slightly slower than the Keplerian speed at the same location. The difference between the Keplerian speed v_K and the gas orbital speed is ηv_K , where

$$\eta = -\frac{1}{2} \left(\frac{H}{r} \right)^2 \frac{d \log P}{d \log r} \quad (15)$$

The radial velocity of a particle is then:

$$v_r = -2\eta v_K \tau_s / (\tau_s^2 - 1) + u_r / (\tau_s^2 - 1), \quad (16)$$

where u_r is the radial component of the gas velocity. Except for extreme cases u_r is very small and hence the second term in the right-hand side of Eq. 16 is negligible relative to the first term. Consequently, the direction of the radial drift of dust depends on the sign of η , i.e., from Eq. 15, on the sign of the pressure gradient. If the gradient is negative as in most parts of the disk, the drift is inwards. But in the special regions where the pressure gradient is positive, the particle's drift is outwards. Consequently, dust tends to accumulate at pressure maxima in the disk. We have seen above that the MHD dynamics in the disk can create a sequence of rings and gaps, where the density is alternatively maximal and minimal (Fig. 4b). Each of these rings therefore features a pressure maximum along a circle. In absence of diffusive motion, the dust would form an infinitely thin ring at the pressure maximum. Turbulence produces diffusion of the dust particles in the radial direction, as it does in the vertical direction. Thus, as dust sedimentation produces a layer with thickness given by Eq. 14, dust migration produces a ring with radial thickness $w_p = w / \sqrt{1 + \tau_s / \alpha}$ around the pressure maximum, where w is the width of the gas ring assuming that it has a Gaussian profile [138].

Consequently, observations of the dust distribution in protoplanetary disks can provide information on the turbulence in the disk. The fact that the width of the gaps in the disk of HL Tau appears to be independent of the azimuth despite the fact that the disk is viewed with an angle smaller than 90° , suggests that the vertical diffusion of dust is very limited such that α in Eq. 14 must be 10^{-4} or less [399]. In contrast, the observation that dust is quite broadly distributed in each ring of the disks, suggest that α could be as large as 10^{-3} , depending on the particles Stokes number τ_s , which is not precisely known [138]. These observations therefore suggest that turbulence in the disks is such that the vertical diffusion it produces is weaker than the radial diffusion. It is yet unclear which mechanism could generate turbulence with this property.

2.2 Planetesimal formation

Dust particles orbiting within a disk often collide. If collisions are sufficiently gentle, they stick through electrostatic forces, forming larger particles [57]. One could imagine that this process continues indefinitely, eventually forming macroscopic bodies called planetesimals. However, as we have seen above, particles drift through

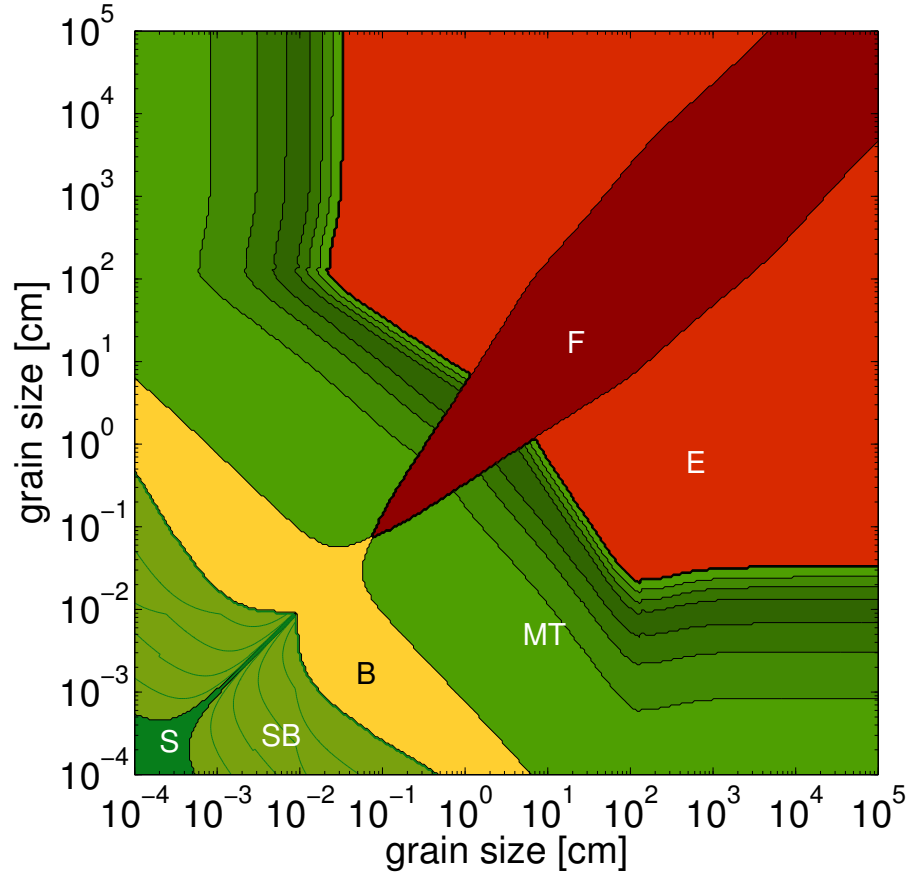


Fig. 6 Map of collisional outcome in the disk. The sizes of colliding particles are reported on the axes. The colours denote the result of each pair-wise collision. Green denotes growth, red denotes erosion and yellow denotes neither of the above (i.e. a bounce). The label S stands for sticking, SB for stick and bounce, B for bounce, MT for mass transfer, E for erosion and F for fragmentation. Form ([507]). This map is computed for compact (silicate) particles, at 3 au.

the disk at different speeds depending on their size (or Stokes number). Thus, there is a minimum speed at which particles of different sizes can collide. Particles of equal size also have a distribution of impact velocities due to turbulent diffusion.

Fig. 6 shows a map of the outcome of dust collisions within a simple disk model, from [507]. Using laboratory experiments on the fate of collisions as a function of particle sizes and mutual velocities, and considering a disk with turbulent diffusion $\alpha = 10^{-3}$ and drift velocities as in a MMSN disk, Windmark et al. computed the growth/disruption maps for different heliocentric distances. The one from Fig. 6 is for a distance of 3 au. The figure shows that, in the inner part of the disk, particles cannot easily grow beyond a millimeter in size. A bouncing barrier prevents particles to grow beyond this limit. If a particle somehow managed to grow to ~ 10 cm, its

growth could potentially resume by accreting tiny particles. But as soon as particles of comparable sizes hit each other, erosion or catastrophic fragmentation occurs, thus preventing the formation of planetesimal-size objects.

The situation is no better in the outer parts of the disk. In the colder regions, due to the lower velocities and the sticking effect of water ice, particles can grow to larger sizes. But this size is nevertheless limited to a few centimeters due to the so-called *drift barrier* (i.e. large enough particles start drifting faster than they grow: [47]). It has been proposed that if particles are very porous, they could absorb better the collisional energy, thus continuing to grow without bouncing or breaking [380]. Very porous planetesimals could in principle form this way and their low densities would make them drift very slowly through the disk. But eventually these planetesimals would become compact under the effect of their own gravity and of the ram pressure of the flowing gas [235]. This formation mechanism for planetesimals is still not generally accepted in the community. At best, it could work only in the outer part of the disk, where icy monomers have the tendency to form very porous structures, but not in the inner part of the disk, dominated by silicate particles. Moreover, meteorites show that the interior structure of asteroids is made mostly of compact particles of 100 microns to a millimeter in size, called chondrules, which is not consistent with the porous formation mode.

A mechanism called the *streaming instability* [518] can bypass these growth bottlenecks to form planetesimals. Although originally found to be a linear instability (see [219]), this instability raises even more powerful effects which can be qualitatively explained as follows. This instability arises from the speed difference between gas and solid particles. As the differential makes particles feel drag, the friction exerted from the particles back onto the gas accelerates the gas toward the local Keplerian speed. If there is a small overdensity of particles, the local gas is in a less sub-Keplerian rotation than elsewhere; this in turn reduces the local headwind on the particles, which therefore drift more slowly towards the star. Consequently, an isolated particle located farther away in the disc, feeling a stronger headwind and drifting faster towards the star, eventually joins this overdense region. This enhances the local density of particles and reduces further its radial drift. This process drives a positive feedback, i.e. an instability, whereby the local density of particles increases exponentially with time.

Particle clumps generated by the streaming instability can become self-gravitating and contract to form planetesimals. Numerical simulations of the streaming instability process [224, 456, 457, 446, 1] show that planetesimals of a variety of sizes are produced, but those that carry most of the final total mass are those of ~ 100 km in size. This size is indeed prominent in the observed size-frequency distributions of both asteroids and Kuiper-belt objects. Thus, these models suggest that planetesimals form (at least preferentially) big, in stark contrast with the collisional coagulation model in which planetesimals would grow progressively from pair wise collisions. If the amount of solid mass in small particles is large enough, even Ceres-size planetesimals can be directly produced from particle clumps (Fig. 7).

While Fig. 7 shows that the streaming instability can clearly form planetesimals, a concern arises from the initial conditions of such simulations. Simulations find

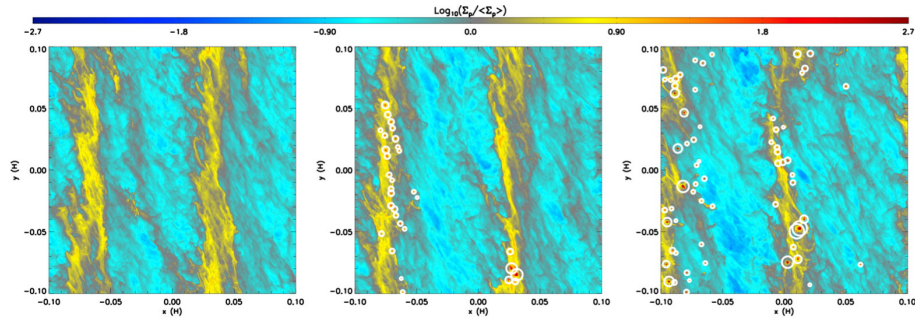


Fig. 7 Snapshots in time of a simulation of the streaming instability (from [456]). The color scale shows the vertically integrated particle surface density normalized to the average particle surface density (log scale). Time increases from left to right. The left panel shows the clumping due to the streaming instability in the absence of self-gravity but right before self-gravity is activated ($t = 110\Omega^1$). The middle panel corresponds to a point shortly after self-gravity was activated ($t = 112.5\Omega^1$), and the right panel corresponds to a time in which most of the planetesimals have formed ($t = 117.6\Omega^{-1}$). In the middle and right panel, each planetesimal is marked via a circle of the size of the Hill sphere.

that quite large particles are needed for optimal concentration, corresponding to at least decimeters in size when applied to the asteroid belt. Chondrules – a ubiquitous component of primitive meteorites – typically have sizes from 0.1 to 1 mm but such small particles are hard to concentrate in vortices or through the streaming instability. High-resolution numerical simulations [83, 517] show that chondrule-size particles can trigger the streaming instability only if the initial mass ratio between these particles and the gas is larger than about 4%. The initial solid/gas ratio of the Solar System disk is thought to have been $\sim 1\%$. At face value, planetesimals should not have formed as agglomerates of chondrules. A possibility is that future simulations with even-higher resolution and run on longer timescales will show that the instability can occur for a smaller solid/gas ratio, approaching the value measured in the Sun.

Certain locations within the disk may act as preferred sites of planetesimal formation. Drifting particles may first accumulate at distinct radii in the disc where their radial speed is slowest and then, thanks to the locally enhanced particle/gas ratio, locally trigger the streaming instability. Two locations have been identified for this preliminary radial pile-up. One is in the vicinity of the snowline, where water transitions from vapor to solid form [201, 26, 450]. The other is in the vicinity of 1 au [135]. These could be the two locations where planetesimals could form very early in the proto-planetary disk [136]. Elsewhere in the disk, the conditions for planetesimal formation via the streaming instability would only be met later on, when gas was substantially depleted by photo-evaporation from the central star, provided that the solids remained abundant ([473] [82]).

At least at the qualitative level, this picture is consistent with available data for the Solar System. The meteorite record reveals that some planetesimals formed very early (in the first few 10^5 y [240, 251, 448]). Because of the large abundance of short-lived radioactive elements present at the early time [175, 330], these first

planetesimals melted and differentiated, and are today the parent bodies of iron meteorites. But a second population of planetesimals formed 2 to 4 My later [487]. These planetesimals did not melt and are the parent bodies of the primitive meteorites called the chondrites. We can speculate that differentiated planetesimals formed at the two particle pile-up locations mentioned above, whereas the undifferentiated planetesimals formed elsewhere, for instance in the asteroid belt while the gas density was declining. Yet these preferred locations were certainly themselves evolving in time [136].

Strong support for the streaming instability model comes from Kuiper belt binaries. These binaries are typically made of objects of similar size and identical colors (see [369]). It has been shown [367] that the formation of a binary is the natural outcome of the gravitational collapse of the clump of pebbles formed in the streaming instability if the angular momentum of the clump is large. Simulations of this process can reproduce the typical semi-major axes, eccentricities and size ratios of the observed binaries. The color match between the two components is a natural consequence of the fact that both are made of the same material. This is a big strength of the model because such color identity cannot be explained in any capture or collisional scenario, given the observed intrinsic difference in colors between any random pair of Kuiper belt objects (KBOs - this statement holds even restricting the analysis to the cold population, which is the most homogenous component of the Kuiper belt population). Additional evidence for the formation of equal-size KBO binaries by streaming instability is provided by the spatial orientation of binary orbits. Observations [369] show a broad distribution of binary inclinations with $\approx 80\%$ of prograde orbits ($i_b < 90^\circ$) and $\approx 20\%$ of retrograde orbits ($i_b > 90^\circ$). To explain these observations, Nesvorný et al. [362] analyzed high-resolution simulations and determined the angular momentum vector of the gravitationally bound clumps produced by the streaming instability. Because the orientation of the angular momentum vector is approximately conserved during collapse, the distribution obtained from these simulations can be compared with known binary inclinations. The comparison shows that the model and observed distributions are indistinguishable. This clinches an argument in favor of the planetesimal formation by the streaming instability and binary formation by gravitational collapse. No other planetesimal formation mechanism has been able so far to reproduce the statistics of orbital plane orientations of the observed binaries.

2.3 Accretion of protoplanets

Once planetesimals appear in the disk they continue to grow by mutual collisions. Gravity plays an important role by bending the trajectories of the colliding objects, which effectively increases their collisional cross-section by a factor

$$F_g = 1 + V_{esc}^2/V_{rel}^2, \quad (17)$$

where V_{esc} is the mutual escape velocity defined as $V_{esc} = [2G(M_1 + M_2)/(R_1 + R_2)]^{1/2}$, M_1, M_2, R_1, R_2 are the masses and radii of the colliding bodies, V_{rel} is their relative velocity before the encounter and G is the gravitational constant. F_g is called the gravitational focussing factor [442].

The mass accretion rate of an object becomes

$$\frac{dM}{dt} \propto R^2 F_g \propto M^{2/3} F_g \quad (18)$$

where the bulk density of planetesimals is assumed to be independent of their mass, so that the planetesimal physical radius $R \propto M^{1/3}$. These equations imply two distinct growth modes called runaway and oligarchic growth.

2.3.1 Runaway growth

If one planetesimal (of mass M) grows quickly then its escape velocity V_{esc} becomes much larger than its relative velocity V_{rel} with respect to the rest of the planetesimal population. Then one can approximate F_g as V_{esc}^2/V_{rel}^2 . Notice that the approximation $R \propto M^{1/3}$ makes $V_{esc}^2 \propto M^{2/3}$.

Substituting this expression into Eq. 18 leads to:

$$\frac{dM}{dt} \propto \frac{M^{4/3}}{V_{rel}^2}, \quad (19)$$

or, equivalently:

$$\frac{1}{M} \frac{dM}{dt} \propto \frac{M^{1/3}}{V_{rel}^2}. \quad (20)$$

This means that the relative mass-growth rate is a growing function of the body's mass. In other words, small initial differences in mass among planetesimals are rapidly magnified, in an exponential manner. This growth mode is called *runaway growth* [173, 504, 505, 241, 242].

Runaway growth occurs as long as there are objects in the disk for which $V_{esc} \gg V_{rel}$. While V_{esc} is a simple function of the largest planetesimals' masses, V_{rel} is affected by other processes. There are two dynamical damping effects that act to decrease the relative velocities of planetesimals. The first is gas drag. Gas drag not only causes the drift of bodies towards the central star, as seen above, but it also tends to circularize the orbits, thus reducing their relative velocities V_{rel} . Whereas orbital drift vanishes for planetesimals larger than about 1 km in size, eccentricity damping continues to influence bodies up to several tens of kilometers across. However, in a turbulent disk gas drag cannot damp V_{rel} down to zero: in presence of turbulence the relative velocity evolves towards a size-dependent equilibrium value [204]. The second damping effect is that of collisions. Particles bouncing off each other tend to acquire parallel velocity vectors, reducing their relative velocity to zero. For a given

total mass of the planetesimal population, this effect has a strong dependence on the planetesimal size, roughly $1/r^4$ [505].

Meanwhile, relative velocities are excited by the largest growing planetesimals by gravitational scattering, whose strength depends on those bodies' escape velocities. A planetesimal that experiences a near-miss with the largest body has its trajectory permanently perturbed and will have a relative velocity $V_{rel} \sim V_{esc}$ upon the next return. Thus, the planetesimals tend to acquire relative velocities of the order of the escape velocity from the most massive bodies, and when this happens runaway growth is shut off (see below)

To have an extended phase of runaway growth in a planetesimal disk, it is essential that the bulk of the solid mass is in small planetesimals, so that the damping effects are important. Because small planetesimals collide with each other frequently and either erode into small pieces or grow by coagulation, this condition may not hold for long. Moreover, if planetesimals really form with a preferential size of ~ 100 km, as in the streaming instability scenario, the population of small planetesimals would have been insignificant and therefore runaway growth would have only lasted a short time if it happened at all.

2.3.2 Oligarchic growth

When the velocity dispersion of planetesimals becomes of the order of the escape velocity from the largest bodies, the gravitational focussing factor (Eq. 17) becomes of order unity. Consequently the mass growth equation (Eq. 18) becomes

$$\frac{1}{M} \frac{dM}{dt} \propto \frac{M^{-1/3}}{V_{rel}^2}. \quad (21)$$

In these conditions, the relative growth rate of the large bodies slows with the bodies' growth. Thus, the mass ratios among the large bodies tend to converge to unity.

In principle, one could expect that the small bodies also narrow down their mass difference with the large bodies. But in reality, the large value of V_{rel} prevents the small bodies from accreting each other. Small bodies only contribute to the growth of the large bodies (i.e. those whose escape velocity is of the order of V_{rel}). This phase is called *oligarchic growth* [242, 243].

In practice, oligarchic growth leads to the formation of a group of objects of roughly equal masses, embedded in the disk of planetesimals. The mass gap between oligarchs and planetesimals is typically of a few orders of magnitude. Because of dynamical friction – an equipartition of orbital excitation energy [91] – planetesimals have orbits that are much more eccentric than the oligarchs. The orbital separation among the oligarchs is of the order of 5 to 10 mutual Hill radii R_H , where:

$$R_H = \frac{a_1 + a_2}{2} \left(\frac{M_1 + M_2}{3M_*} \right)^{1/3}, \quad (22)$$

and a_1, a_2 are the semi-major axes of the orbits of the objects with masses M_1, M_2 , and M_* is the mass of the star.

2.3.3 The need for an additional growth process

In the classic view of planet formation [502, 281, 282] the processes of runaway growth and oligarchic growth convert most of the planetesimals mass into a few massive objects: the protoplanets (sometimes called *planetary embryos*). However, this picture does not survive close scrutiny.

In the Solar system, two categories of protoplanets formed within the few Myr lifetime of the gas component of the protoplanetary disk (see Fig. 2). In the outer system, a few planets of multiple Earth masses formed and were massive enough to be able to gravitationally capture a substantial mass of H and He from the disk and become the observed giant planets, from Jupiter to Neptune. In the inner disk, instead, the protoplanets only reached a mass of the order of the mass of Mars and eventually formed the terrestrial planets after the disappearance of the gas (see Section 3.3.1). Thus, the protoplanets in the outer part of the disk were 10-100 times more massive of those in the inner disk. This huge mass ratio is even more surprising if one considers that the orbital periods, which set the natural clock for all dynamical processes including accretion, are ten times longer in the outer disk.

The snowline represents a divide between the inner and the outer disk. The surface density of solid material is expected to increase beyond the snowline due to the availability of water ice [189]. However, this density-increase is only of a factor of ~ 2 [286], which is insufficient to explain the huge mass ratio between protoplanets in the outer and inner parts of the disc [335].

In addition, whereas in the inner disk oligarchic growth can continue until most of the planetesimals have been accreted by protoplanets, the situation is much less favorable in the outer disc. There, when the protoplanets become sufficiently massive (about 1 Earth mass), they tend to scatter the planetesimals away, rather than accrete them. In doing this they clear their neighboring regions, which in turn limits their own growth [273]. In fact, scattering dominates over growth when the ratio $V_{esc}^2/2V_{orb}^2 > 1$, where V_{esc} is the escape velocity from the surface of the protoplanet and V_{orb} is its orbital speed (so that $\sqrt{2}V_{orb}$ is the escape velocity from the stellar potential well from the orbit of the protoplanet). This ratio is much larger in the outer disc than in the inner disc because $V_{orb}^2 \propto 1/a$, where a is the orbital semi major axis.

Consequently, understanding the formation of the multi-Earth-mass cores of the giant planets and their huge mass ratio with the protoplanets in the inner Solar System is a major problem of the runaway/oligarchic growth models, and it has prompted the elaboration of a new planet growth paradigm, named *pebble accretion*.

2.3.4 Pebble accretion

Let's take a step back to what seems to be most promising planetesimal formation model: that of self-gravitating clumps of small particles (hereafter called pebbles even though in the inner disc they are expected to be at most mm-size, so that grains would be a more appropriate term). Once a planetesimal forms it remains embedded in the disk of gas and pebbles and it can keep growing by accreting individual pebbles. This process was first envisioned by Ormel and Klahr [381] and then studied in detailed by Lambrechts and Johansen [253, 254, 223]. To avoid confusion, we call below the accreting body a *protoplanet* and we denote the accreted body as a pebble or a planetesimal, depending on whether it feels strong gas drag.

Pebble accretion is more efficient than planetesimal accretion for two reasons. First, the accretion cross-section for a protoplanet-pebble encounter is much larger than for a protoplanet-planetesimal encounter. As seen above, in a protoplanet-planetesimal encounter the accretion cross-section is $\pi R^2 F_g$, where R is the physical size of the protoplanet and F_g is the gravitational focussing factor. But in a protoplanet-pebble encounter it can be as large as πr_d^2 , where r_d is the distance at which the protoplanet can deflect the trajectories of the incoming objects. This is because, as soon as the pebble's trajectory starts to be deflected, its relative velocity with the gas increases and gas-drag becomes very strong. Thus, the pebble's trajectory spirals towards the protoplanet. This is shown in the inlet of Fig. 8, whereas the outer panel of the figure shows the value of r_d as a function of the pebble's friction time, normalized to the Bondi radius $r_B = GM/v_{rel}^2$ (v_{rel} being the velocity of the pebble relative to the protoplanet, typically of order ηv_K).

The second reason that pebble accretion is more efficient than planetesimal accretion is that pebbles drift in the disk. Thus, the orbital neighborhood of the protoplanet cannot become empty. Even if the protoplanet accretes all the pebbles in its vicinity, the local population of pebbles is renewed by particles drifting inward from larger distances. This does not happen for planetesimals because their radial drift in the disk is negligible.

Provided that the mass-flux of pebbles through the disk is large enough, pebble accretion can grow protoplanets from about a Moon-mass up to multiple Earth-masses, i.e. to form the giant planets cores within the disc's lifetime [253, 254]. The large mass ratio between protoplanets in the outer vs. inner parts of the disc can be explained by remembering that icy pebbles can be relatively large (a few centimeters in size), whereas in the inner disc the pebble's size is limited to sub-millimetre by the bouncing silicate barrier (chondrule-size particles) and by taking into account that pebble accretion is more efficient for large pebbles than for chondrule-size particles [335].

For all these reasons, while some factors remain unknown (particularly the pebble flux and its evolution during the disk lifetime), pebble accretion is now considered to the dominant process of planet formation.

An important point is that pebble accretion cannot continue indefinitely. When a planet grows massive enough it starts opening a gap in the disk. This eventually creates a pressure bump at the outer edge of the gap which stops the flux of pebbles.

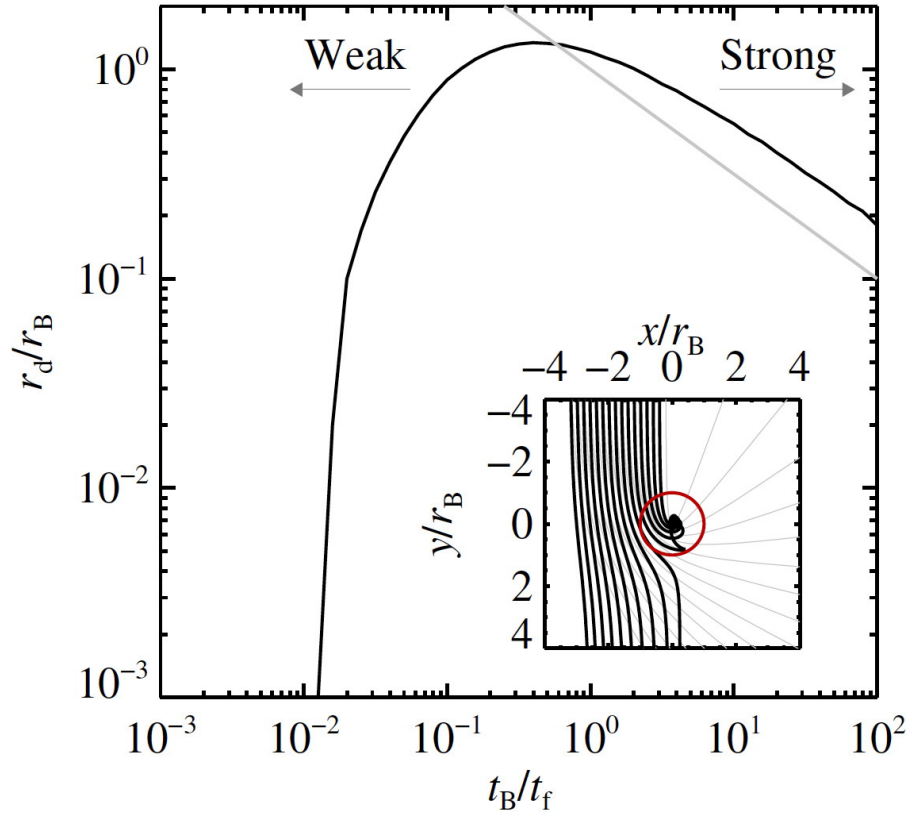


Fig. 8 Efficiency of pebble accretion. The outer plot shows the accretion radius r_d , normalized to the Bondi radius r_B , as a function of t_B/t_f , where t_f is the friction time and t_B is the time required to cross the Bondi radius at the encounter velocity v_{rel} . The smaller is the pebble the larger is t_B/t_f . The inset shows pebble trajectories (black curves) with $t_B/t_f = 1$, which can be compared with those of objects with $t_B/t_f \rightarrow 0$ (grey curves). Clearly the accretion radius for the former is much larger. A circle of Bondi radius is plotted in red. From ([253]).

The mass at which this happens is called *pebble isolation mass* [337, 255] and depends on disk's viscosity and scale height [53]. Once a planet reaches the pebble isolation mass it stops accreting pebbles. Given that it blocks the inward pebble flux, this means that all protoplanets on interior orbits are starved of pebbles, regardless of their masses. Turbulent diffusion can allow some pebbles to pass through the pressure bump [493], particularly the smallest ones, because the effects of diffusion are proportional to $\sqrt{\alpha/\tau_s}$.

2.4 Orbital migration of planets

Once a massive body forms in the disk, it perturbs the distribution of the gas in which it is embedded. We generically denote the perturbing body as a *planet*. In this Section we consider planets smaller than a few tens of Earth masses. The case of giant planets will be discussed in the next Section.

Analytic and numerical studies have shown that a planet generates a spiral density wave in the disk, as shown in Fig. 9 [165, 166, 277, 490, 467]. The exterior wave trails the planet. The gravitational attraction that the wave exerts on the planet produces a negative torque that slows the planet down. The interior wave leads the planet and exerts a positive torque. The net effect on the planet depends on the balance between these two torques of opposite signs. It was shown by [490] that for axis-symmetric disks with any power-law radial density profiles, the negative torque exerted by the wave in the outer disk wins. This is because a power-law disk is in slight sub-keplerian rotation, so that the gravitational interaction of the planet with a disk's ring located at $a_p + \delta a$ (a_p being the orbital radius of the planet) is stronger than with the ring located at $a_p - \delta a$, given that the relative velocity with the former is smaller. As a consequence of this imbalance, the planet must lose angular momentum and its orbit shrinks: the planet migrates towards the central star. This process is called *Type-I migration*. The planet migration speed is:

$$\frac{da}{dt} \propto M_p \Sigma_g \left(\frac{a}{H} \right)^2, \quad (23)$$

where a is the orbital radius of the planet (here assumed to be on a circular orbit), M_p is its mass, Σ_g is the surface density of the gas disk and H is its height at the distance a from the central star. A precise migration formula, function of the power-law index of the density and temperature radial profiles, can be found in Paardekooper et al. [386, 387]. The planet-disk interaction also damps the planet's orbital eccentricity and inclination if these are initially non-zero. These damping timescales are a factor $(H/a)^2$ smaller than the migration timescale [468, 111].

Precise calculations show that an Earth-mass body at 1 au, in a Minimum Mass Solar Nebula ($\Sigma_g = 1700 \text{g/cm}^2$) with scale height $H/a = 5\%$, migrates into the star in 200,000 y. For different planets or different disks, the migration time can be scaled using the relationship reported in Eq. 23. So, Lunar- to Mars-mass protoplanets are only mildly affected by Type-I migration because their migration timescales exceed the few Myr lifetime of the gas disk. Conversely, for more massive planets, migration should be substantial and should bring them close to the star before that the disk disappears.

Planet-disk interactions through the spiral density wave are only part of the story. An important interaction occurs along the planet's orbit due to fluid elements that are forced to do horseshoe-like librations in a frame corotating with the planet. Along these librations, as a fluid element passes from inside the planet's orbit to outside, it receives a positive angular momentum kick and exerts an equivalent but negative kick onto the planet. The opposite happens when a fluid element passes from outside

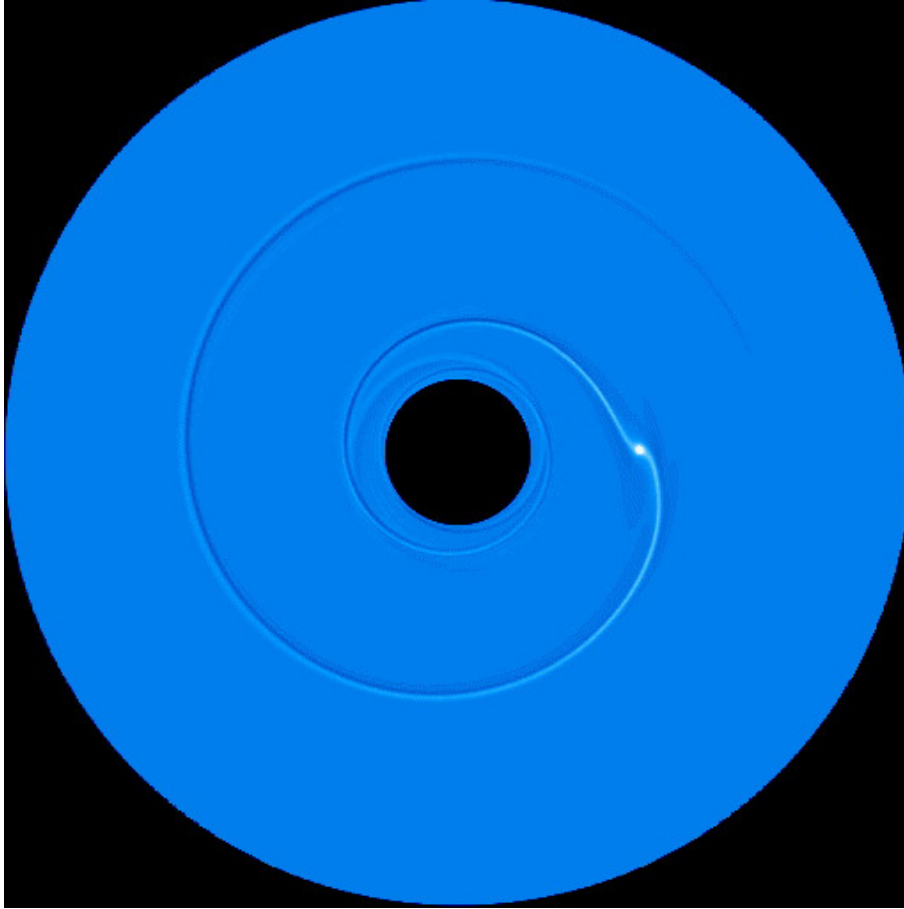


Fig. 9 The spiral density wave launched by a planet in the gas disk. The colour brightness is proportional to the gas surface density. Courtesy of F. Masset.

of the planet's orbit to inside. It can be proven [311] that, if the radial surface density gradient at the planet's location is proportional to $1/r^{3/2}$ (i.e. the *vortensity* of the disk is constant with radius) the positive and negative kicks cancel out perfectly, and there is no net effect on the planet. But for different radial profiles there is a net torque on the planet, named the *vortensity-driven corotation torque* [386, 387]. If the disk's profile is shallower than $1/r^{3/2}$ this corotation torque is positive and it slows down migration relative to the rate from Eq. 23. Moreover, if the disk's radial surface density gradient is positive and sufficiently steep, the corotation torque (positive) can exceed the (negative) torque exerted by the wave and reverse migration [311]. This implies the existence of a location in the disk – typically near the density maximum – where migration stops, dubbed *planet trap* [293]. Positive surface density gradients could exist at the inner edge of the protoplanetary disk, where the disk is truncated

by the stellar magnetic torque [92], or at transition from the MRI-active to the MRI-inactive parts of the disk [150, 151] – also very close to the central star – or at the inner edge of each ring observed in MHD simulations (see Fig. 4b). Therefore, there can be several *planet traps* in the disk [188, 33].

The corotation region can also exert a positive torque on the planet in a region of the disk where the radial temperature gradient is steeper than $1/r$ [388]. This torque is called *entropy-driven corotation torque* [386, 387]. Steep temperature gradients exist behind the “bumps” of the disk’s aspect ratio that are generated by opacity transitions [51]. However, because the disk evolves over time towards a passive disk, with a temperature gradient shallower than $1/r$, the outward migration regions generated by the entropy-driven corotation torque exist only temporarily [51].

Other torques can act on the planet and affect its migration in specific cases. If the viscosity of the disk is very small, *dynamical torques* are produced as a feedback of planet migration [385, 394, 397]. The feedback is negative, i.e. it acts to decelerate the migration, if the disk’s surface density profile is shallower than $1/r^{3/2}$ and migration is inwards, or if the profile is steeper than $1/r^{3/2}$ and migration is outwards. In the opposite cases, the dynamical torque accelerates the migration.

Low-viscosity disks are also prone to a number of instabilities generating vortices when submitted to the perturbation of a planet. As a result, the migration of the planet can become stochastic, due to the interaction with these variable density structures [320].

As it approaches the planet gas is compressed then decompressed so that its temperature first increases then decreases. Because hot gas loses energy by irradiation, the situation is not symmetric and the gas is colder (i.e. denser) after the conjunction with the planet than it was before conjunction. This generates a negative torque [267]. On the other hand, if a planet is accreting solids, gravitational energy is released as heat. This source of heat modifies the density of the gas in the vicinity of the planet. In some conditions, this *heating torque* can exceed the previous effect, so that the net effect is positive and can even overcome the negative torque exerted by the wave [44]. This torque, however, also enhances the orbital eccentricity of the planet [141], which in turn reduces its accretion rate. Thus some self-regulated regime can be achieved [310].

Finally, even the steady-state dust distribution can be perturbed by the presence of the planet, acquiring asymmetries that can exert torques on the planet [45].

To summarize, although the migration of a small-mass planet is typically inward and fast, there can be locations in the disk where migration is halted, as well as a number of temporary mechanisms that can reduce or enhance the migration rate. Therefore, the actual migration of a planet must be investigated in a case-by-case basis and requires a realistic modeling of the disk, given that its density and temperature gradients, opacity, viscosity and dust distribution play a key role. Unfortunately, so far our limited theoretical and observational knowledge of disks hampers our ability to model planet migration quantitatively.

2.5 Gas accretion and giant planet migration

A massive planet immersed in a gas disk can attract gas by gravity and build up an atmosphere. To distinguish between the solid part of the planet from its atmosphere, we will call the formed the *core*.

The closed set of equations that govern the distribution of gas in the atmosphere are:

$$\frac{dP}{dr} = \frac{GM(r)\rho(r)}{r}, \quad (24)$$

where $\rho(r)$ is the density of the gas at a distance r from the center of the planet, which describes hydrostatic equilibrium (gravity balanced by the internal pressure gradient);

$$\frac{dM}{dr} = 4\pi r^2 \rho(r), \quad (25)$$

which describes the planet's mass-radius relationship $M(r)$ from $M(r_c) = M_c$, where r_c is the radius of the core and M_c is its mass;

$$\frac{dT}{dr} = -\frac{3\kappa L\rho}{64\pi\sigma r^2 T^3}, \quad (26)$$

where σ is Boltzman's constant, κ the gas opacity and $L \propto M_c \dot{M}_c / r_c$ is the luminosity of the core, due to the release of the gravitational energy delivered by the accretion of solids at a rate \dot{M}_c ;

$$P = \frac{\mathcal{R}}{\mu\rho T}, \quad (27)$$

which is the equation of state, here for a perfect gas (\mathcal{R} being the perfect gas constant and μ the molecular weight).

One can attempt to solve this set of equations using boundary condition $\rho(r_b) = \rho_0$ and $T(r_b) = T_0$, where ρ_0 and T_0 are the disk's values for gas density and temperature, respectively, and r_b is the disk-planet boundary, typically the Bondi radius $r_b = 2GM/c_s^2$ (c_s being the sound speed). A solution exists only for $M_c < M_{crit}(\kappa, L)$ where $M_{crit}(\kappa, L)$ is a threshold value depending on opacity and luminosity (and disk's properties), as shown in Fig. 10 [401, 254].

M_{crit} tends to zero as the core's accretion rate tends to zero. If $L = 0$ no hydrostatic solution can exist. Recall from the previous Section that when a planet reaches the pebble isolation mass the accretion pebbles effectively stops [337, 53]. This drastically changes the value of L and hence M_{crit} . If the atmosphere of the planet was in hydrostatic equilibrium up to that point, it may be out of equilibrium. As a rule of thumb, when M_c approaches M_{crit} the mass of the atmosphere in hydrostatic equilibrium approaches that of the core. This triggers runaway gas accretion[254].

When the atmosphere is no longer in hydrostatic equilibrium, it contracts under the effect of gravity. The compression of gas releases energy, so the atmosphere can only contract on the Kelvin-Helmoltz timescale, which is effectively the atmosphere's cooling timescale through irradiation. As the atmosphere contracts, new gas can be captured within the Bondi radius r_b . This increases the mass of the atmosphere and

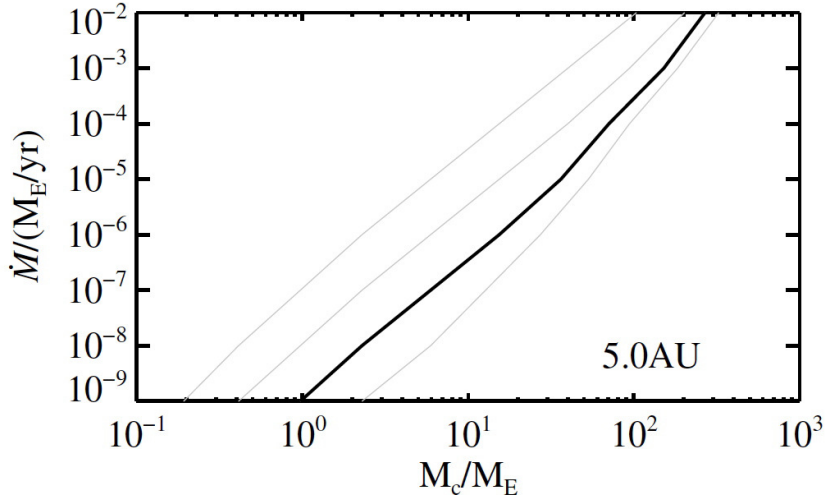


Fig. 10 The value of M_{crit} (on the horizontal axis) as a function of core's accretion rate (on the vertical axis), for different values of the opacity – increasing from left to right. The atmosphere can be in hydrostatic equilibrium only if $M_c < M_{crit}$. From [254].

hence the gravity of the full planet. This triggers a positive feedback on the accretion rate, so that the mass of the planet's atmosphere increases exponentially with time (see Fig. 11) [404, 199, 283].

A number of studies have modeled atmospheric accretion during the runaway phase [209, 106, 257] using different approaches. All have confirmed the runaway gas accretion with a mass-doubling timescales for Jupiter-mass planets of order 10^4 – 10^5 y in a MMSN disk. This raises the question of why Saturn-mass exoplanets outnumber Jupiter-mass ones, which drastically outnumber super-Jupiters [77, 481]. One possibility is that giant planets enter in their runaway phase late, as the disk is disappearing [404, 52]. Given that the mass doubling timescale in the runaway phase is so much shorter than the disk's lifetime, this appears to be a surprising coincidence. The other possibility is that the growth of a planet is limited by the ability of the disk to transport gas radially. We know from observations, however, that the gas accretion rate onto the central star is typically of the order of $10^{-8} M_\odot/y$ [185], which means that a Jupiter-mass of gas passes through the orbit of a giant planet in only 10^5 y, again much shorter than the disk's lifetime. Perhaps the study of giant planet growth in low-viscosity disks dominated by winds can bring a solution to the problem, given the different geometry and mechanism of transport for the accreting gas relative to a classic, viscous disk.

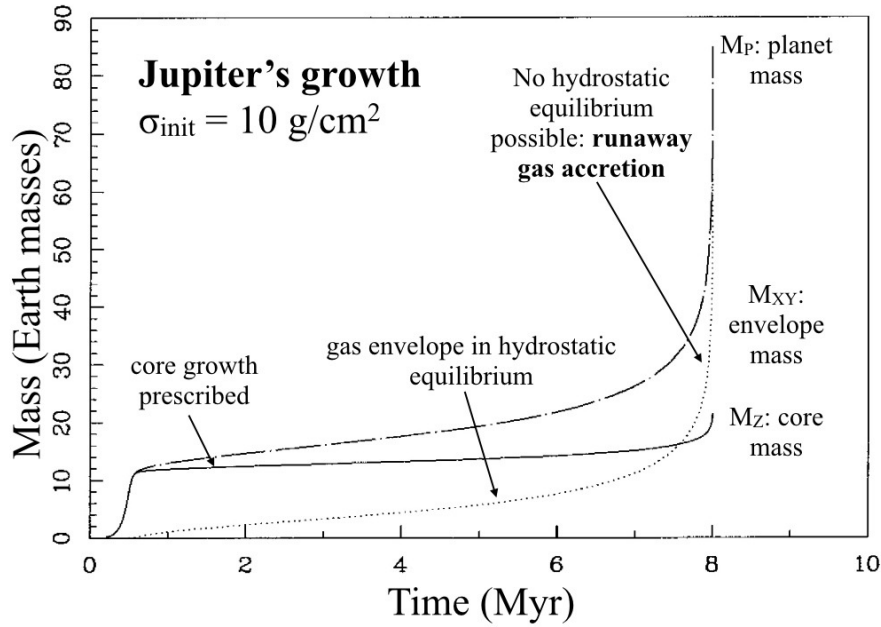


Fig. 11 Runaway growth of a giant planet near Jupiter’s orbital radius. The solid curve shows the mass of the solid core, the dotted curve the mass of the atmosphere and the dashed curve the total mass of the planet. Here the accretion of solids onto the core is prescribed according to a now obsolete planetesimal accretion model. The approximate boundary in time between the hydrostatic regime and the runaway regime is at ~ 7.5 Myr. While the runaway gas accretion regime is not in hydrostatic equilibrium it can be modeled as a series of equilibrium states. Adapted from [404].

2.5.1 Gap opening and Type-II migration

As we have seen in Sect. 2.4 a planet embedded in a disk exerts a positive torque on the outer part of the disk and a negative torque on the inner part. The torque is proportional to the planet’s mass. If the planet is small, its torque is easily overcome by the viscous torque that the annuli of the disk exert on each other. The global surface density profile of the disk is not changed and only the spiral density wave appears. But if the planet is massive enough the torque it exerts on the disk overwhelms the disk’s viscous torque. In this case, the planet effectively pushes gas away from its orbit: outer gas outwards and inner gas inwards. A gap opens in the gas distribution around the orbit of the planet.

As gas is removed, the gap becomes deeper and wider. But as the gradients of the disk’s surface density distribution become steeper at the edges of the gap, the disk’s viscous torque is enhanced. In fact, the viscous torque acting on elementary rings can be computed by differentiation of Eq. 3 to give:

$$\delta T_\nu = -\frac{3}{2}\nu\Omega \left[\frac{r}{\Sigma} \frac{d\Sigma}{dr} + \frac{1}{2} \right] (2\pi r \Sigma). \quad (28)$$

Once the density gradient becomes steep enough, the viscous torque balances the torque that the planet exerts on the same annulus of the disk [484].

The depth of a gap – defined as the ratio between the surface density of the disk perturbed by the planet Σ_p and the original value Σ_u – is [234]:

$$\frac{\Sigma_p}{\Sigma_u} = \frac{1}{1 + 0.04K}, \quad (29)$$

where

$$K = \left(\frac{M_p}{M_*} \right)^2 \left(\frac{H}{r} \right)^{-5} \alpha^{-1} \quad (30)$$

and M_p, M_* are the masses of the planet and the star, respectively, the aspect ratio of the disk H/r is taken at the planet’s location, and as usual $\alpha = \nu/(H^2\Omega)$. This formula holds up to $K \sim 10^4$ (see Fig. 11 in [234]). However it cannot hold indefinitely, in particular in the limit of low α . This is because if the density gradients at the edges of the gap become too steep, the rotational properties of the gas change so much under the effect of the pressure gradient that the specific angular momentum of the disk $r^2\Omega(r)$ is no-longer a growing function of r [233]. When this happens the disk becomes Rayleigh unstable and develops local turbulence, in turn enhancing the local viscosity. This effectively limits the steepness of the gap “walls” and the depth of the gap. Because the pressure gradient is also proportional to $(H/r)^2$, this narrative implies that, in the limit of vanishing viscosity, the denser the disk the shallower the gap. Thus, a gap opening criterion –i.e. the minimal mass of a planet to cause a depletion of 90% of the gas in the gap– must depend not only on viscosity but also on the disk’s aspect ratio. An often-quoted criterion is the following:

$$\frac{3}{4} \frac{H}{R_H} + \frac{50}{qR_e} < 1, \quad (31)$$

where $q = M_p/M_*$, $R_H = (q/3)^{1/3}$ and $R_e = r_p^2\Omega_p/\nu$ [112].

The formation of a gap profoundly changes a planet’s migration. This migration mode has been dubbed *Type-II migration*. The gap must migrate along with the planet. In particular, as the planet moves inwards, the disk has to refill the portion of the gap “left behind” by the planet’s radial motion. Because the radial velocity of the gas in a viscous unperturbed disk is $v_r = -(3/2)\nu/r$, this was the expected migration speed of the planet, independent of the planet’s mass and disk’s scale aspect ratio [491].

However, the planet’s migration rate is not so simple [137, 139]. It depends on the ratio between the disk’s density and the mass of the planet, exemplified by the dimensionless ratio $r_p^2\Sigma/M_p$ (see Fig. 12), and also on the disk’s aspect ratio. Depending on these quantities, the radial velocity of the planet can be smaller or larger than the “idealized” Type-II migration speed of $-(3/2)\nu/r$.

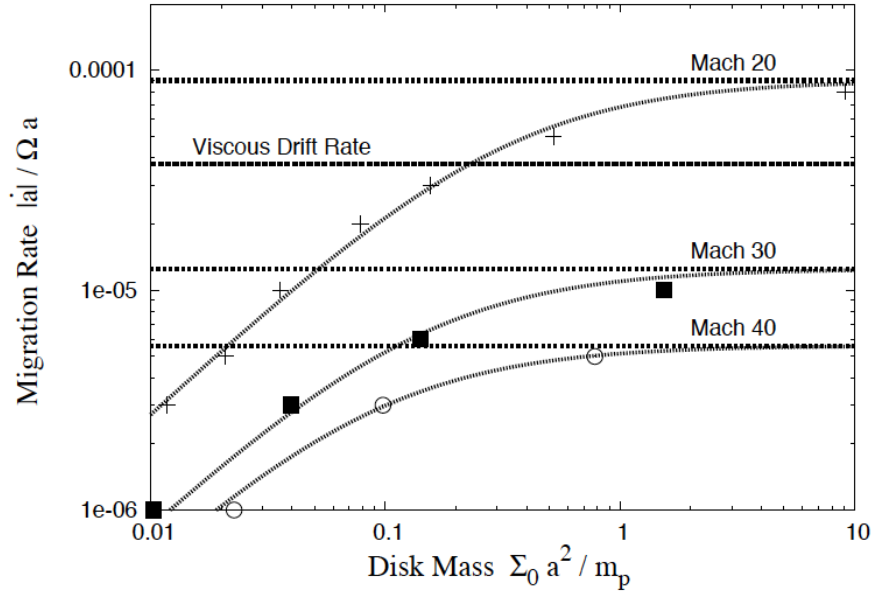


Fig. 12 The migration rate as a function of the ratio $r_p^2 \Sigma / M_p$ for a giant planet in a disk with $\alpha = 3 \times 10^{-3}$, for three different disk's aspect ratios. Notice that the migration rate can be smaller or larger than the viscous drift rate of the gas, i.e. the idealized Type-II migration speed. From [137].

It is easy to understand that a planet's migration speed is slower than the idealized speed for the case of a low disk mass. A light disk obviously cannot push a heavy planet. This is the inertial limit: the planet is an obstacle to the flow of the gas. But how can a planet migrate faster than the radial speed of the gas? In principle the gas should remain behind and the planet, losing contact from the outer disk, should feel a weaker negative torque, eventually slowing down its migration until it moves at the same speed of the gas. The explanation given in [137, 139] was that, as the planet migrates inwards, the gas from the inner disk can pass through the gap, refilling the left-behind part of the gap. In this way, the planet does not have to wait for the gas to drift-in at viscous speed. But the passage of gas through the gap is insignificant if the gap is significantly wider than the planet's horseshoe region [435], which is the case for massive planets in low-viscosity disks. In that case, as the planet moves inwards, the gap must be refilled from the outer disk. However, the steep density gradient at the edge of the gap enhances the viscous torque, as discussed above, so that the gas radial speed can be several times faster than $-(3/2)v/r$. This explains why the planet can exceed the idealized Type-II migration rate. Nevertheless, the migration rate of the planet must linearly proportional to the viscosity of the disk [435].

The dependence of the migration rate of giant planets on disk's viscosity opens the possibility that, in low-viscosity disks, the migration timescale can exceed the

disk's lifetime. This would be convenient to explain why most giant planets are warm/cold Jupiters and not hot Jupiters [77, 481].³ However, recall from Sect. 2.1.1 that low-viscosity disks cannot explain the accretion rates observed for the central stars. If viscosity is low, there must be some additional mechanism for the radial transport of gas, possibly induced by angular momentum removal in disk winds. The migration rate of giant planets in these kind of disks has not yet been studied.

2.6 Resonance trapping during planet migration

Numerical simulations show that multiple planets migrating in a disk have the tendency to lock into mutual mean motion resonance, where the period ratio is very close to the ratio of integer numbers [470, 395, 214]. Typically, these numbers differ by just one such that the period ratios are 2:1, 3:2, 4:3 etc. These are called *first-order* resonances.

To understand this propensity to form resonant chains we need to dive into the complex world of dynamical planet-planet interactions. To stay simple, we will consider the planar three body problem, where two planets orbit a star on coplanar orbits. This is the simplest example of dynamics of a planetary system, yet it already captures most of the complexities of real systems. The best mathematicians made huge efforts to find an analytic solution of this problem, until Poincaré [402] demonstrated that this was impossible. A general analytic solution does not exist. The system can exhibit chaotic behavior [191]. Yet, some description can be provided, such as for instance for the dynamics of resonant planets with small libration amplitude, which is that of interest to understand the formation of resonant chains. This is what we attempt to do in this Section.

To study the three body problem, the most effective approach is to use the Hamiltonian formalism. A system of first-order differential equations

$$\frac{d\mathbf{x}}{dt} = \mathbf{f}(\mathbf{x}, \mathbf{y}), \quad \frac{d\mathbf{y}}{dt} = \mathbf{g}(\mathbf{x}, \mathbf{y}) \quad (32)$$

is said to be in Hamiltonian forms, if there exists a scalar function $\mathcal{H}(\mathbf{x}, \mathbf{y})$ such as

$$f_i(\mathbf{x}, \mathbf{y}) = \frac{\partial \mathcal{H}}{\partial y_i}, \quad g_i(\mathbf{x}, \mathbf{y}) = -\frac{\partial \mathcal{H}}{\partial x_i}, \quad (33)$$

for each component $i = 1, \dots, N$ of the vectors $\mathbf{x}, \mathbf{y}, \mathbf{f}, \mathbf{g}$. The function \mathcal{H} is called the *Hamiltonian* of the problem; \mathbf{x} is called the vector of *coordinates* and \mathbf{y} the vector of *momenta*. If \mathcal{H} is periodic on \mathbf{x} , the coordinates are also called *angles* and the momenta *actions*.

³ We define a hot Jupiter as a giant planet within 0.1 au from its star and warm/cold Jupiters as those that are beyond 0.5 au. Very few giant planets fall between 0.1 and 0.5 au so the exact values of these boundaries are not important. Debaised observations suggest that hot Jupiters are about 1/10th or less as abundant as warm/cold Jupiters [145, 509, 510].

An important property of Hamiltonian dynamics is that \mathcal{H} is constant over the flow $\mathbf{x}(t), \mathbf{y}(t)$ that is solution of the equations of motion. This means that, in the special case where \mathcal{H} is a function of only one component of \mathbf{x} , namely $\mathcal{H} \equiv \mathcal{H}(x_1, \mathbf{y})$, the evolution of the system can be easily computed: y_2, \dots, y_N are constant of motion from (32) and (33); the motion of x_1, y_1 can be obtained from the level curve of $\mathcal{H}(x_1, y_1, y_2, \dots, y_N) = \mathcal{H}(\mathbf{x}(0), \mathbf{y}(0))$, which is a 1D curve in a 2D x_1, y_1 space (called *phase space*). In this case, the problem is integrable (i.e. the solution is provided with analytic functions of time).

In studying a problem written in Hamiltonian form, a typical goal is to find a transformation of variables $\mathbf{x} \rightarrow \mathbf{x}', \mathbf{y} \rightarrow \mathbf{y}'$ that transforms the Hamiltonian function into one that is independent of x'_2, \dots, x'_N . However, only transformations that preserve the form of Hamilton equations (Eqns 32 and 33), called *canonical transformations*, are allowed. There are many forms of canonical transformations. In this Section we will use only linear transformations $\mathbf{x}' = A\mathbf{x}, \mathbf{y}' = B\mathbf{y}$ where A, B are $N \times N$ matrices. It can be proven that the transformation is canonical if and only if

$$B = [A^{-1}]^T . \quad (34)$$

In general, it is not possible to find a canonical transformation that makes the Hamiltonian independent of $N - 1$ coordinates. Then, a goal in *perturbation theory* is to find a canonical transformation that turns $\mathcal{H}(\mathbf{x}, \mathbf{y})$ into

$$\mathcal{H}'(\mathbf{x}', \mathbf{y}') = \mathcal{H}'_0(x'_1, \mathbf{y}') + \epsilon \mathcal{H}'_1(\mathbf{x}', \mathbf{y}') . \quad (35)$$

In this case \mathcal{H}'_0 is called the *integrable approximation* and \mathcal{H}'_1 the *perturbation*. The latter can be neglected if one is interested in the dynamics up to a time $t < 1/\epsilon$. Depending on the goal in terms of accuracy, ϵ has to be sufficiently small.

After this broad and shallow introduction to Hamiltonian dynamics, let's turn to the planar three-body problem. The problem admits a Hamiltonian description, with Hamiltonian function:

$$\mathcal{H} = \sum_{j=1,2} \frac{\|\mathbf{p}_j\|^2}{2\mu_j} - \frac{G(M_* + m_j)\mu_j}{\|\mathbf{r}_j\|} + \frac{\mathbf{p}_1 \cdot \mathbf{p}_2}{M_*} - \frac{Gm_1m_2}{\|\Delta\|} , \quad (36)$$

where \mathbf{r}_j is the *heliocentric* position vector of planet j of reduced mass $\mu_j = m_j M_* / (m_j + M_*)$, $\mathbf{p}_j = m_j \mathbf{v}_j$ with \mathbf{v}_j being the *barycentric* velocity vector (not a typo!: positions and velocities have to be taken in different reference frames [403] if one wants a Hamiltonian description of the problem) and $\Delta = \mathbf{r}_1 - \mathbf{r}_2$.

Using the canonical Delaunay variables:

$$\begin{aligned} \Lambda_j &= \mu_j \sqrt{G(M_* + m_j) a_j} , & \lambda_j &= M_j + \varpi_j \\ \Gamma_j &= \Lambda_j (1 - \sqrt{1 - e_j^2}) , & \gamma_j &= -\varpi_j \end{aligned}$$

where a_j, e_j are the semi major axes and eccentricities, ϖ_j are the perihelion longitudes, M_j the mean anomalies and G is the gravitational constant, the Hamiltonian

(Eq. 36) becomes:

$$\mathcal{H} = -G^2 \sum_{j=1,2} \frac{\mu_j^3 (M_* + m_j)^2}{2\Lambda_j^2} + \mathcal{H}_1(\Lambda_{1,2}, \Gamma_{1,2}, \lambda_{1,2}, \gamma_{1,2}). \quad (37)$$

The first term in the r.h.s. of (Eq. 37), denoted \mathcal{K} hereafter, taken alone, is an integrable Hamiltonian, but the flow that it describes is trivially that of two uncoupled Keplerian motions: the actions $\Lambda_{1,2}, \Gamma_{1,2}$ are constant, the longitude of perihelia $\gamma_{1,2}$ are constants, and only the mean longitudes $\lambda_{1,2}$ move with constant frequency $G^2 \mu_j^3 (M_* + m_j)^2 / \Lambda_j^3 = \sqrt{G(M_* + m_j) / a_j^3}$. So, this kind of integrable approximation of the full Hamiltonian is not sufficient for our purposes and we need to find a better one.

To this end, we expand \mathcal{H}_1 in power series of $\sqrt{\Gamma_j} \sim \sqrt{\Lambda_j/2} e_j$ and in Fourier series of the angles λ_j, γ_j . The general form is therefore

$$\begin{aligned} \mathcal{H}_1 = & \sum_{l_1, l_2, k_1, k_2, j_1, j_2} c_{l_1, l_2, k_1, k_2, j_1, j_2}(\Lambda_1, \Lambda_2) \Gamma_1^{j_1/2} \Gamma_2^{j_2/2} \cos(k_1 \lambda_1 + k_2 \lambda_2 + l_1 \gamma_1, l_2 \gamma_2) \\ & + s_{l_1, l_2, k_1, k_2, j_1, j_2}(\Lambda_1, \Lambda_2) \Gamma_1^{j_1/2} \Gamma_2^{j_2/2} \sin(k_1 \lambda_1 + k_2 \lambda_2 + l_1 \gamma_1, l_2 \gamma_2) \end{aligned} \quad (38)$$

The so-called *D'Alembert rules* give us information on which terms of this series can have non-zero coefficients, namely:

- only the c coefficients can be non-zero, because the Hamiltonian must be invariant for a change of sign of all angles (measuring angles clockwise or counter-clockwise is arbitrary), so that the Fourier expansion can contain only cos terms;
- only the $c_{l_1, l_2, k_1, k_2, j_1, j_2}$ coefficients with $k_1 + k_2 - l_1 - l_2 = 0$ can be non-zero, because the Hamiltonian has to be invariant by a rotation of the reference frame, namely increasing all angles by an arbitrary phase δ_0 (remember that $\gamma = -\varpi$, so if all orbital angles are increased by δ_0 , γ is decreased by δ_0).
- only the $c_{l_1, l_2, k_1, k_2, j_1, j_2}$ coefficients with $j_1 = |l_1| + 2n$ and $j_2 = |l_2| + 2i$ (with n and i non-negative integer numbers) can be non-zero. This is because the Hamiltonian is not singular for circular orbits (i.e. $\Gamma_1 = 0$ and/or $\Gamma_2 = 0$) so that it has become a polynomial expression in the canonical variables $p_1 = \sqrt{2\Gamma_1} \cos \gamma_1, q_1 = \sqrt{2\Gamma_1} \sin \gamma_1, p_2 = \sqrt{2\Gamma_2} \cos \gamma_2, q_2 = \sqrt{2\Gamma_2} \sin \gamma_2$.

If we are interested in two planets near a mean motion resonance where $P_2 \sim k/(k-1)P_1$, where P_1 and P_2 are the orbital periods and k is a positive integer number, the angle $k\lambda_2 - (k-1)\lambda_1$ will have an almost null time-derivative (as one can see remembering that $\dot{\lambda} = 2\pi/P$ and using the relationship between the orbital periods written above). Thus, it is a slow angle, whereas both λ_1 and λ_2 are fast angles, as it is their difference. To highlight this difference in timescales, let us define new angles:

$$\delta\lambda = \lambda_1 - \lambda_2, \quad \theta = k\lambda_2 - (k-1)\lambda_1. \quad (39)$$

Using the rule (34) this linear transformation of the angles can be made canonical by changing the actions as:

$$\Delta\lambda = k\Lambda_1 + (k-1)\Lambda_2, \quad \Theta = \Lambda_1 + \Lambda_2, \quad (40)$$

so that $(\Delta\lambda, \delta\lambda)$ and (Θ, θ) are pairs of canonical action-angle variables.

Because we are interested in the long-term evolution of the dynamics, we can average the Hamiltonian over $\delta\lambda$, which means that the averaged Hamiltonian will be independent of this angle and, consequently, $\Delta\lambda$ will be a constant of motion. Because the units of semi-major axis are arbitrary, one can always chose them so that $\Delta\lambda = 1$. In other words, changing the values of $\Delta\lambda$ does not change the dynamics; it simply changes the unit of measure of the semi major axes.

Using the D'Alembert rules described above, the function in Eq. 38 takes the form

$$\mathcal{H}_1 = \sum_{m,n,i>0,j>0} d_{m,n,i,j}(\Theta, \Delta\lambda) \Gamma_1^{|n-m|/2+j} \Gamma_2^{|m|/2+i} \cos[n(\theta+\gamma_1)+m(\gamma_2-\gamma_1)], \quad (41)$$

where the coefficients $d_{m,n,i,j}$ come from the original coefficients $c_{l_1,l_2,k_1,k_2,j_1,j_2}$ through a simple index algebra that follows trivially from the redefinition of the angles (Eq. 39).

Because there are only two possible combinations of angles in the harmonics of Eq. 41 it is convenient to identify each of them with a single angle, namely:

$$\psi_1 = \theta + \gamma_1 \quad \delta\gamma = \gamma_2 - \gamma_1, \quad \gamma'_2 = \gamma_2 \quad (42)$$

Again, using the rule (Eq. 34) this linear transformation of the angles can be made canonical by changing the actions as:

$$\Psi_1 = \Theta, \quad \Psi_2 = \Theta - \Gamma_1, \quad \mathcal{L} = \Gamma_1 + \Gamma_2 - \Theta \quad (43)$$

Now, the Hamiltonian $\mathcal{K} + \mathcal{H}_1$ depends only on the angles ψ_1 and $\delta\gamma$, and \mathcal{L} is a new constant of motion (related to the angular momentum of the system).

This Hamiltonian is still not integrable, because it depends on two angles. An integrable approximation (dependent on only one angle) can be obtained if one retains in Eq. 41 only the terms linear in the planets' eccentricities, i.e. proportional to $\sqrt{\Gamma_{1,2}}$, and doing some cumbersome change of variables [453, 40]. In this case one can then trace global dynamical diagrams by plotting the level curves of the Hamiltonian (see for instance Fig. 3 in [40]). However, even in the general non-integrable case one can look for the stable equilibrium points in $(\Psi_1, \psi_1, \Psi_2, \delta\gamma)$ as a function of \mathcal{L} (recall that $\Delta\lambda$ can be fixed to unity). The locus of equilibrium points, once transformed back into the original orbital elements, describes a curve in $e_2, a_2/a_1$ or, equivalently, $e_1, a_2/a_1$, like that shown in Fig. 13. Note that on the curve $a_2/a_1 \rightarrow \infty$ as $e_1 \rightarrow 0, e_2 \rightarrow 0$. This feature comes from the fact that, from Hamilton's equations $\dot{\gamma}_{1,2} = \partial\mathcal{H}/\partial\Gamma_{1,2}$ applied to (41), one has $\dot{\gamma}_{1,2} \propto \Gamma_{1,2}^{-1/2}$, i.e. $\dot{\gamma}_{1,2} \rightarrow \infty$ as $\Gamma_{1,2} \propto e_{1,2}^2 \rightarrow 0$. Thus, to have the equilibrium $\dot{\psi}_1 = 0$ the value of $\dot{\theta}$ has to diverge, which means that a_2/a_1 has to diverge as well.

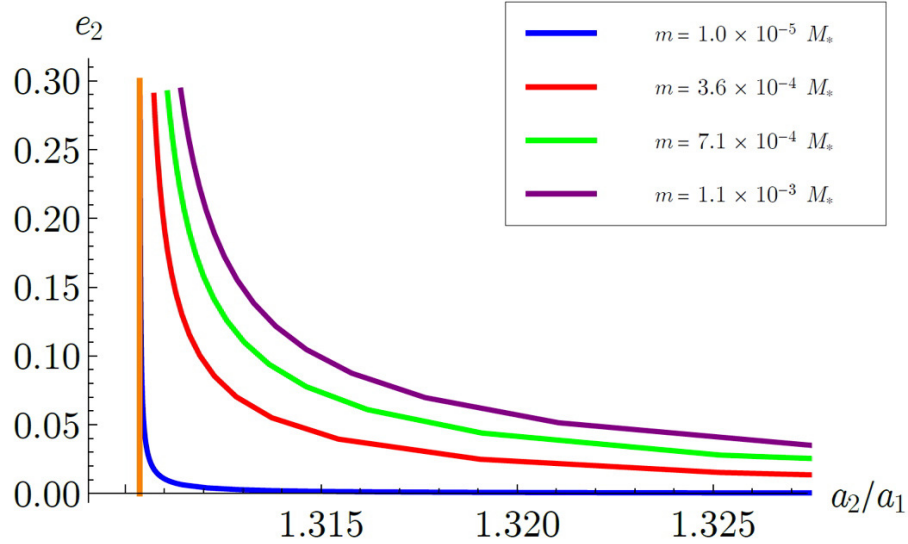


Fig. 13 The locus of equilibrium points for the 3:2 mean motion resonance in the plane e_2 vs. a_2/a_1 , for different planetary masses (here assumed to be equal to each other) in different colors. The vertical orange line shows the location of the resonance in the Keplerian approximation (the same a_2/a_1 for any eccentricity because the orbital frequencies depends only on semi major axes). Adapted from Pichierri et al. [393].

This feature of the curve of equilibrium points is the key to understand resonant capture. If the planets are far from resonance (i.e. a_2/a_1 is much larger than the resonant ratio assuming Keplerian motion; a 3:2 resonance being located at $a_2/a_1 = 1.3103$ in Fig. 13), the protoplanetary disk exerts damping forces on their eccentricities, so that the planet's orbits are basically circular. This means, from the shape of the curve of equilibrium points, that the planets will be on the equilibrium. As migration proceeds and a_2 approaches a_1 (this is the case if the outer planet migrates faster towards to the star, which happens in Type-I migration if it is more massive or if the inner planet is blocked at a planet trap), the ratio a_2/a_1 decreases. If this happens slowly compared to the libration period around the equilibrium point, the dynamical evolution has to react *adiabatically* [359]. This means that the amplitude of libration around the equilibrium point has to be conserved. Because initially the planets have vanishing amplitude of libration (their eccentricities are basically null as those characterizing the equilibrium point), this means that the planets have to evolve from one equilibrium point to the other, i.e. they have to follow the curve traced in Fig. 13. As a_2/a_1 asymptotically approaches the Keplerian resonant value, the eccentricities of the two planets increase.

If the convergent migration is too fast, the adiabatic condition is broken. The amplitude of libration is not conserved. The planets can jump off resonance and continue to approach each other more closely. But, because the libration frequency of a resonance $P_2 \sim k/(k-1)P_1$ increases with k , eventually the planets will find

a resonance with k large enough and libration frequencies fast enough that the adiabatic condition is satisfied. Then, they will be trapped in resonance. In essence, the faster is the convergent migration, the higher the index k of the resonance in which the planets will be trapped. But trapping always occurs, eventually. These arguments apply for each pair of neighboring planets in a multi-planet system. This is why the formation of configurations in resonant chains is a typical outcome of planet migration.

If the adiabatic condition is satisfied, is resonant trapping stable? Fig 13 suggests that the eccentricities of the planets should grow indefinitely. But in reality the disk exerts eccentricity damping, so that the eccentricities grow until an equilibrium is established between the eccentricity damping from the disk and the resonant conversion of convergent migration into eccentricity pumping. A precise formula to compute this equilibrium in a variety of configurations (damping exerted on both planets or only on one, inner planet at a planet-trap or not etc.) can be found in the appendix of [393]. The equilibrium eccentricity is typically of order $(H/r)^2$, where (H/r) is the aspect ratio of the protoplanetary disk.

There is a complication. For the adiabatic principle to be applied, the dissipative forces have to act on the parameters of the Hamiltonian, not on the dynamical variables. This is the case for migration. The change in semi major axis ratio changes the otherwise constant of motion \mathcal{L} , i.e. a parameter of the Hamiltonian. But the eccentricity damping affects $\Gamma_{1,2}$, i.e. dynamical variables. Then, the equilibrium point can become a focus, which means that the dynamical evolution spirals around it. The spiral can be inward if the focus is stable (which means that any initial amplitude of libration would shrink to 0) or outwards if the focus is unstable (which means that the amplitude of libration grows indefinitely, even if it is initially arbitrarily small). This unstable evolution, first pointed out in [164], is called *overstability*.

Fig. 14 shows a summary of the most detailed investigation of the stability/overstability of a resonance in presence of eccentricity damping [122]. If the eccentricity damping is proportional to the planetary masses (as in the case where both planets are embedded in the disk), for the 3:2 and higher- k resonances the resonant configuration is stable whenever $m_1 > m_2$. In the opposite case, the stability/overstability depends on the total mass ratio $\epsilon_p = (m_1 + m_2)/M_*$. There is a limit value of the ratio m_1/m_2 below which the system is overstable, and this ratio decreases with increasing ϵ_p (Fig. 14a). For the 2:1 resonance the situation is qualitatively similar, but the planets can be overstable even if $m_1/m_2 > 1$ if ϵ_p is small enough (Fig. 14b). On the other hand, if there is no eccentricity damping on the inner planet ($\tau_{e_1} \rightarrow \infty$, which happens if the inner planet has been pushed into a disk's cavity), the resonant configuration is always stable for any m_1/m_2 ratio.

Even if resonant planets are not in the overstable regime, they may be unstable because of other processes. Due to their proximity and eccentric orbits they may approach each other too much over their resonant trajectories and be destabilized by a close-encounter [393]. There can also be subtle secondary resonances between a combination of the libration frequencies and the synodic frequency $\lambda_1 - \lambda_2$. These secondary resonances cannot be described with the averaged Hamiltonian (Eq. 41) because the terms in $\lambda_1 - \lambda_2$ have been removed by the averaging procedure. But they

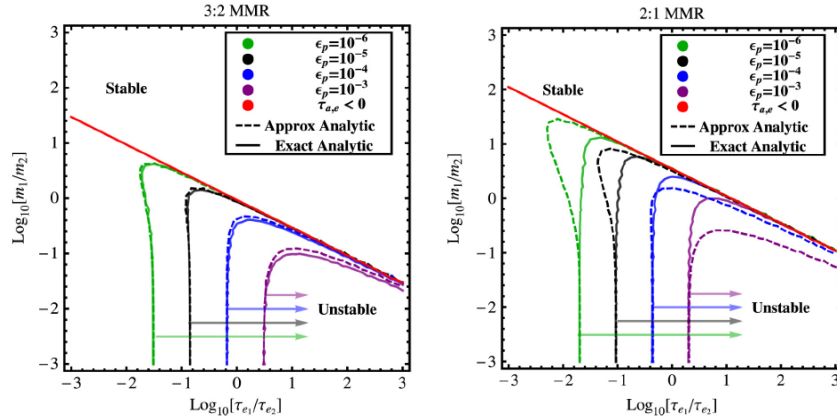


Fig. 14 Each plot shows the region of the parameter plane τ_{e1}/τ_{e2} and m_1/m_2 , where $\tau_{e1,2}$ is the damping timescale of the eccentricity of planets 1 and 2, respectively, with masses m_1 and m_2 , for different planetary masses $\epsilon_p = (m_1 + m_2)/M_*$. The left plot is for the 3:2 resonance, the right plot for the 2:1 resonance. For a planet of mass m at semi-major axis a the eccentricity damping timescale is $\tau_e \propto (H/a)^4 / (m\Sigma\sqrt{a})$, where Σ is the surface density of the disk and H/a its aspect ratio. Thus, if the disk has a constant aspect ratio and $\Sigma \propto 1/\sqrt{a}$ the system should place on the dashed diagonal line (i.e. $m_1/m_2 = \tau_{e1}/\tau_{e2}$). This shows, for instance, that a 3:2 system is stable if $m_1 < m_2$. If instead the inner planet is in a low-density region (i.e. a disk's cavity), $\tau_{e1} \rightarrow \infty$ and therefore the system is stable for all mass ratios. Adapted from ([122]).

can be studied following a more precise and convoluted approach. As the number of planets in a resonant chain increases, the number of libration frequencies increases as well and therefore a richer set of combined frequencies is possible. This explains, at least at the qualitative level, why long resonant chains are more fragile than short chains, as observed in numerical simulations [312, 110]. The long-term evolution of multi-planet resonant chains remains nevertheless an active area of research in celestial mechanics.

3 Global models of planet formation

Building global models of planet formation is akin to putting together a puzzle. We have a vague picture of what the puzzle should look like (i.e., from exoplanet demographics) but observational biases cloud our view. And the puzzle pieces – the planet formation mechanisms – often change in number and in shape. The puzzle-builders must constantly have an eye both on the evolution of the big picture and on the set of viable puzzle pieces. And one must not hesitate to discard a model when it no longer serves.

We will describe our current best global models for the origin of super-Earth systems (Section 3.1), giant planet systems (Section 3.2) and our own Solar System

(Section 3.3). Then we will look at how water may be delivered to rocky planets (Section 3.4).

3.1 Origin of close-in super-Earths

The key properties of super-Earth systems that must be matched by any formation model can be very simply summarized as follows:

- A large fraction (roughly one third to one half) of stars have close-in super-Earths (with periods shorter than 100 days; [157, 352]), but many (perhaps most) of them do not.
- Most super-Earth systems only have a single planet detected in transit, whereas a fraction of systems is found with many planets in transit [284, 144, 477].
- In multi-planet systems, pairs of neighboring super-Earths are rarely found to be in mean motion resonance [284, 143].
- The masses of super-Earths extend from Earth to Neptune, with a preference for a few M_{\oplus} [499, 297, 511, 97].

Models for the formation of super-Earths were developed before they were even discovered [416]. While certain models have been refined in recent years, only a single new model has been developed.

In-situ accretion is the most intuitive and simplest model for super-Earth formation yet it has a fatal flaw. That model proposes that super-Earths simply accreted from local material very close to their stars in a similar fashion to the classical model of terrestrial planet formation in the Solar System (see Section 3.3.1 below). In-situ accretion was proposed in 2008 [416] and discarded because the masses implied in the innermost parts of disks seemed prohibitively large. In 2013 this idea was revisited by Chiang and Laughlin [98], who used the population of known super-Earths to generate a “minimum-mass extrasolar nebula” representing a possible precursor disk that would have formed the population of super-Earths. The high masses inferred in inner disks conflicts with measurements, but those measurements are only of the outermost parts of disks [506]. While it is possible to imagine that inner disks can pile up material, there is a simply-understood timescale problem. With very high densities in the inner disk the growth timescale for super-Earths is extremely fast [285, 430, 419, 210, 449, 378]. In fact, the growth timescales are so fast and the requisite disks so massive that migration is simply unavoidable [378]. Even aerodynamic drag is strong enough to cause rapid orbital drift [210, 176]. Thus, we cannot consider the planets to have formed in-situ because they must have migrated and their final orbits cannot represent their starting ones. Nonetheless, it has been shown that if the right conditions were to arise, with the requisite amount of solid material close to the star, accretion should indeed produce planetary systems similar to the observed super-Earths [183, 184, 119, 120, 344, 265, 263, 264].

A number of the first processes to be explored for forming super-Earths relied on giant planets. For example, migrating giant planets can shepherd material interior

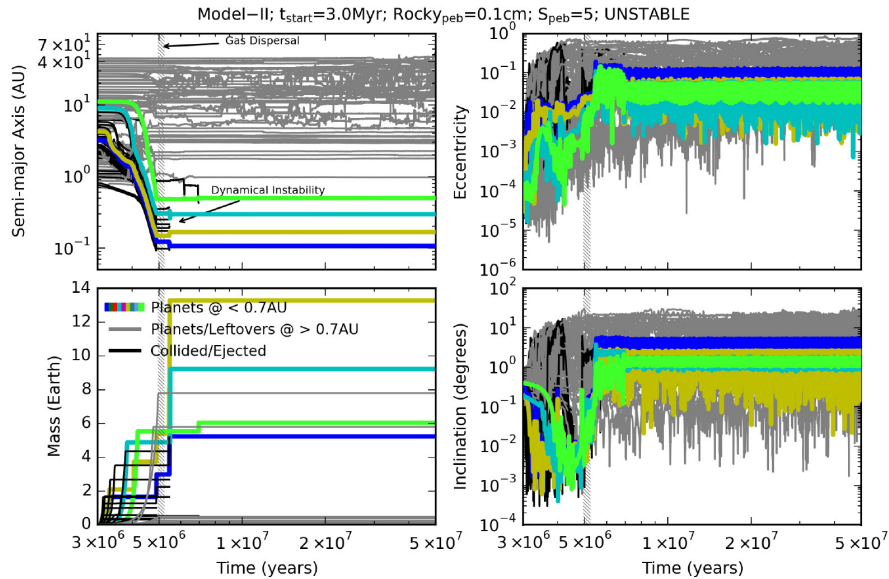


Fig. 15 Evolution of a simulation of the *breaking the chains* migration model for the origin of close-in super-Earths. The panels show the evolution of a population of \sim lunar-mass planetary embryos that grow by accreting pebbles, migrate inward and form a resonant chain anchored at the inner edge of the disk. The resonant chain is destabilized shortly after the dissipation of the gaseous disk, leading to a late phase of scattering and collisions that spreads out the planets and increases their eccentricities and inclinations. From [211].

to their orbits and stimulate the growth of super-Earths [522, 152, 153, 424, 296]. Moving secular resonances driven by giant planet interactions can do the same [522]. However, these models have been ruled out as the main formation pathways for super-Earths because most super-Earth systems do not appear to have an associated giant planet (although testing the correlation between super-Earths and outer gas giants is an active area of study [72, 523, 35]).

The migration model has proven quite successful model in reproducing the observed population of super-Earths[470, 375, 321, 205, 109, 214, 211, 418, 81]. In that model, large planetary embryos grow throughout the disk and migrate inward, driven by the gaseous disk (Fig. 15 shows an example of a simulation of the migration model). It is natural to think that embryos would form first past the snow line, where pebble accretion is thought to be more efficient (see Section 2.3 and [335]). However, it is also possible that in some disks large embryos can form very close to their stars. This might occur if inward-drifting pebbles are concentrated at a pressure bump, perhaps associated with the inner edge of a dead zone [95, 96].⁴ While the migration rate and direction depends on the disk model [293, 247, 49, 54],

⁴ This idea forms the basis of a model of super-Earth formation sometimes called *inside-out planet formation* [61, 95, 96, 198, 197]. That model invokes the direct formation of super-Earths from pebbles at pressure bumps in the inner disk.

inward migration is generally favored. The inner edge of the disk creates a strong positive torque [151] that acts to trap any inward-migrating embryo [311]. This leads to a convergence of bodies near the disk's inner edge. Convergent migration leads to resonant trapping (see Section 2.6) and tends to produce planets in long chains of resonances. Of course, the observed super-Earths are not found in resonance. However, most resonant chains become dynamically unstable as the gaseous disk dissipates. This leads to a phase of giant collisions between embryos that is quite similar to that simulated by studies that ignored the migration phase and invoked a large population of embryos in a dissipating gaseous disk [183, 184, 265, 119, 120]. The instability phase leads to scattering among embryos, breaks the resonant chains, and causes systems to spread out and become dynamically excited. A small fraction of resonant chains remain stable after the disk dissipates; these may represent iconic systems such as Trappist-1 [162, 290] and Kepler-223 [326].

Simulations of the migration model have shown that the surviving systems quantitatively match the population of observed super-Earths as long as more than 90% of resonant chains become unstable [214, 211]. When run through a simulated observing pipeline, the significant dynamical excitation of the surviving systems implies large enough inclinations such that most viewing geometries can only see a single planet in transit. This solves the so-called Kepler dichotomy problem [222, 144] and implies that all super-Earth systems are inherently multiple. The period ratio distribution of simulated systems matches observations, again taking observational biases into account [214, 211, 351].

Yet questions remain. If super-Earth formation is as efficient as in simulations, why don't all stars have them? One possibility is that when an outer gas giant planet forms, it blocks the inward migration of large embryos and those instead become ice giants [215, 213]. This implies an anti-correlation between the presence of outer gas giants and systems with many super-Earths, and it remains unclear if such an anti-correlation exists [72, 523, 35]. The fraction of stars with gas giants appears to be far less than the fraction of stars without super-Earths, which makes it difficult to imagine gas giants being the main cause. Is it possible, instead, that outer ice giants or super-Earths are the culprit? Probably not. While their occurrence rate is high [170, 464], outer ice giants cannot efficiently block the inward migration of other planets and are generally too low-mass to block the pebble flux [337, 254, 53]. Perhaps, instead, many disks are subdivided into radial zones [225]. Pebbles trapped within a given zone may not be able to drift past the zone boundary such that the pebble flux in certain regions of the disk would remain too low for planets to grow fast enough for long-range migration [258]. Such a scenario would also be compatible with the ringed structures seen in many ALMA disks [16].

The compositions of super-Earths may also provide a constraint for formation models. It naively seems that the migration model should produce very volatile-rich super-Earths because the main source of mass is beyond the snow line, where the efficiency of pebble accretion is higher [335, 211, 50, 55]. This need not be true in 100% of cases, as inward-migrating icy embryos can in some cases stimulate the growth of inner, purely rocky planets [418]. However, most super-Earths in the migration model should be ice-rich [211]. It is unclear whether this is consistent with

the observed distribution of bulk densities of super-Earths. While it has been claimed that most super-Earths appear to be “rocky” [383, 384, 288, 220], measurement uncertainties preclude any clear determination of the compositions of super-Earths [132, 133]. In addition, “rocky” planets may in some context include water contents up to $\sim 20\%$ by mass [177]. For context, that is similar to the approximate water contents of comet 67P [389], Pluto, and the most water-rich meteorites known (thought to originate from the outer Solar System [7, 8]). Finally, short-lived radionuclides such as Al-26 may efficiently dry out some super-Earths [274]. The rocky vs. icy nature of super-Earths remains an important outstanding issue.

The fact that super-Earths seem to ubiquitously have large radii consistent with atmospheres of a few percent H/He by mass [497, 511, 159, 158] confirm that these planets formed during the gaseous disk phase and certainly by a process quite different than the formation of our own terrestrial planets. Formation models are starting to be coupled to models of atmospheric accretion and loss [265, 210, 163, 263, 81]. However, given the complexities in these processes [256] this remains an ongoing challenge.

3.2 Giant exoplanets: formation and dynamics

Drawing from numerous radial velocity, transit and microlensing surveys for exoplanets, the essential constraints on giant planet formation are:

- Gas giants exist around roughly 10% of Sun-like stars [113, 318, 508, 155, 464, 145] and are more/less common around more/less massive stars [289, 227, 101, 102].
- Most gas giants are on relatively wide orbits past 0.5-1 au [77, 481, 318, 439, 509, 510].
- Gas giant exoplanets tend to have much higher eccentricities than Jupiter and Saturn, following a broad eccentricity distribution with a median of ~ 0.25 [77, 481, 514, 63].
- There is a strong correlation between a star’s metallicity and the probability that it hosts a gas giant planet [169, 443, 147], especially among hot Jupiters and gas giants with eccentric orbits [121].

There exist two categories of formation models for giant planets [60, 190]. The first is a top-down, collapse scenario in which a localized instability in a protoplanetary disk can lead to the direct formation of one or more giant planets. The second is the bottom-up, core accretion scenario (which we argue below should really be called the *core-migration-accretion* scenario). In recent years the core accretion model has become the dominant one, yet it is plausible that some systems may be explained by the disk instability model.

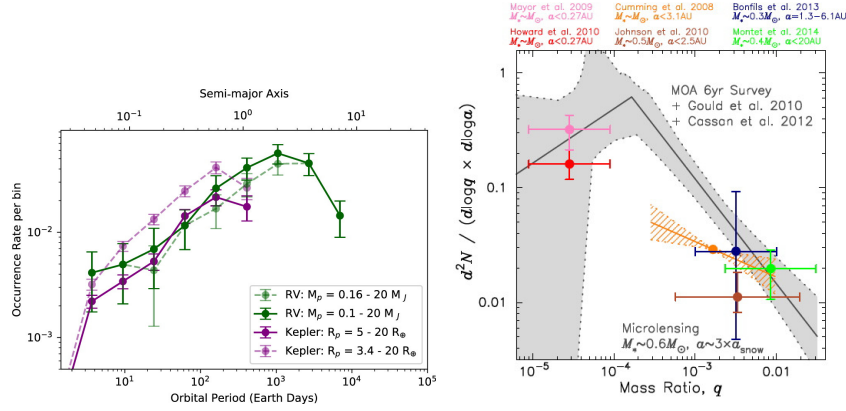


Fig. 16 Mass and orbital radius distributions of giant exoplanets. **Left:** The frequency of giant planets as a function of orbital distance from radial velocity surveys (green) and the Kepler transit statistics (purple). From [145]. **Right:** The occurrence rate of giant planets as a function of planet-to-star mass ratio q , from [464]. The different symbols correspond to different radial velocity studies whereas the black line and grey regions are the results from microlensing surveys.

Disk Instability

The disk instability scenario [64, 65, 66, 317, 316] invokes a localized region of the disk that becomes gravitationally unstable. This is usually quantified with the Toomre Q criterion [475]:

$$\frac{c_s \Omega}{\pi G \Sigma} < Q_{crit} \approx 1, \quad (44)$$

where c_s is the sound speed, Ω is the local orbital frequency, G is the gravitational constant, and Σ is the local surface density of the disk. Simulations show that in disks that have $Q \lesssim 1$, fragmentation does indeed occur and Jupiter-mass clumps form quickly [65, 316, 62]. To become true gas giants, these clumps must cool quickly to avoid being sheared apart by the Keplerian flow.

It is generally thought that only the outermost parts of massive disks are able to attain the criteria needed for instability [323, 25, 238]. The very distant, massive planets such as those of the HR8799 system [298, 299] may perhaps be explained by disk instability, as other mechanisms struggle to form such massive planets so far away from their stars. However, it is not clear whether disk instability can produce Jupiter-like planets (although the giant planet orbiting the low-mass star GJ3512 is a very good candidate – [332]). Planets or clumps that form very far out would also migrate inward rapidly [37] and it is unclear whether they would survive. In the *tidal downsizing model*, gravitational instability forms clumps in the outer parts of disks that migrate inward but are often disrupted to act as the seeds of much smaller planets [357].

Core-*Migration*-Accretion

The bottom-up, core accretion scenario forms the basis of the current paradigm of giant planet formation. In its standard form the core-accretion model essentially represents a combination of processes summarized in Sections 2.3 (growth of proto-planets) and 2.5 (gas accretion). As we shall see, another important process (orbital migration – described in Section 2.4) must be included.

Since its inception the canonical picture has suffered setbacks related to core growth, migration, and gas accretion (see Section 2.3). Early models that invoked planetesimals as the building blocks of large cores could not explain the rapid growth of the $\sim 10 M_{\oplus}$ cores needed to trigger rapid gas accretion [272, 471, 408, 86, 273]. Even in the most optimistic scenarios planetesimal accretion was simply too slow. In recent years it has been shown that pebble accretion is far more efficient and can indeed – given that there is a sufficiently massive and drawn-out supply of pebbles [223, 50] – explain the rapid growth of giant planet cores [381, 253, 254]. It has also been shown that gas accretion is actually not halted, and only modestly slowed down, by the generation of a gap in the disk [114, 482].

Migration remains a giant issue for the core accretion model, so much so that the model itself could plausibly be renamed the *core-migration*-accretion model. It is not so much a problem as an added dimension. The mass scale at which gas accretion becomes an important phenomenon is similar to that at which migration becomes important. Thus, planets that are undergoing gas accretion must necessarily be migrating at the same time. Growth tracks of planets must include both radial and mass growth.

Figure 17 shows the growth tracks of four different simulated planets. Starting from \sim lunar-mass cores, each planet's growth is initially determined simply by the flux of pebbles across its orbit [254, 202]. Once each planet reaches several Earth masses it starts to migrate inward. At the same time it starts to slowly accrete gas. Above the pebble isolation mass (defined in Sec 2.3) pebble accretion is stopped but migration and gas accretion continue. The two inner planets in the simulation grew fast enough to undergo rapid gas accretion and become gas giants, whereas the two outer planets did not accrete enough gas before the disk dispersed and thus ended up as ice giants.

Fig. 17 leads to a naive-sounding but surprisingly profound question: *Why is Jupiter at 5 au?* In the model from Fig. 17, any core that started within roughly 10 au ended up as a hot Jupiter. Likewise, in order to finish at 5 au a core needed to start at 15-20 au (see also [51, 358]). How, then did our own Jupiter avoid this fate? There are currently four possible solutions. First, perhaps Jupiter's core simply did form at 15-20 au [52]. While this is hard to rule out, it seems unlikely because most material that originated interior to Jupiter's orbit would have remained interior to Jupiter's final orbit [420, 400]. This would therefore require that only a few Earth masses of material formed in the entire Solar System interior to 15-20 au. Second, perhaps Jupiter's migration was much slower than that shown in Fig. 17. That could be the case if the disk's viscosity was much lower than generally assumed, which is consistent with new disk models (see Section 2.1). Third, perhaps Jupiter's migration

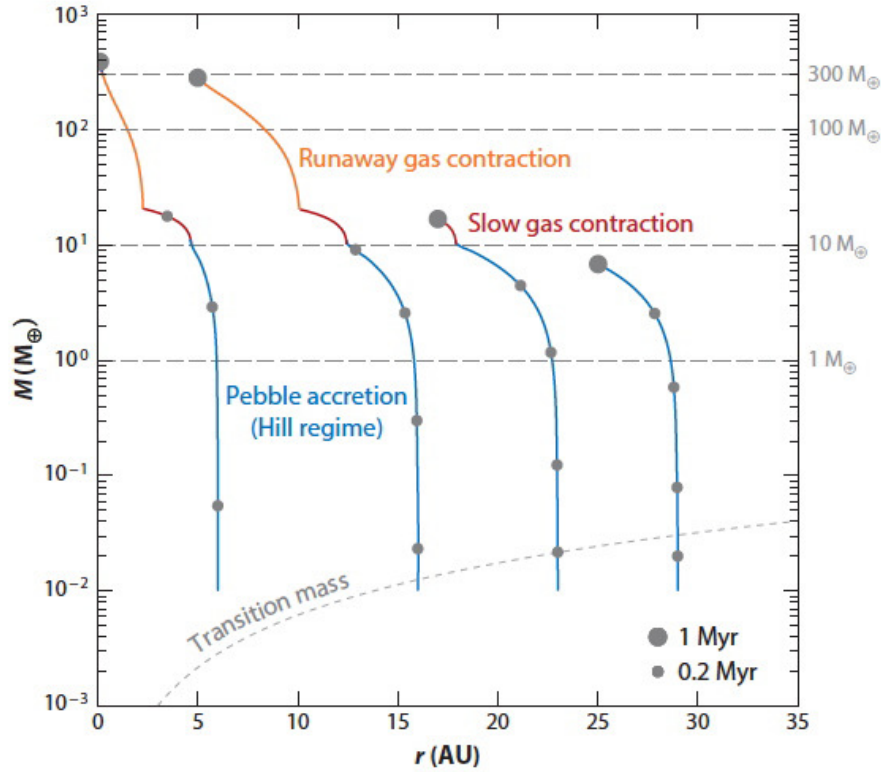


Fig. 17 Growth tracks for four different types of planets from simulations that include pebble accretion and migration and gas accretion. The leftmost planet grows fast enough to migrate a long distance and become a hot Jupiter. The second planet from the left starts as a core at $\sim 15\text{au}$ and ends up as a Jupiter-like planet at 5 au. The two planets on the right are ice giant analogs that never undergo rapid gas accretion. In this case the pebble isolation mass – the mass above which the pebble flux is blocked and pebble accretion shut off [255, 53] – was fixed at $10 M_{\oplus}$. Each small dot denotes a time interval of 0.2 Myr along the growth tracks and each large dot a time interval of 1 Myr. From [223].

was halted because the inner gas disk was evaporated away by energetic radiation from the active young Sun [13]. Indeed, disks are thought to disperse by being photo-evaporated by their central stars [11], and this may be a consequence. Fourth, perhaps Jupiter’s migration was held back by Saturn. Hydrodynamical simulations show that, while a Jupiter-mass planet on its own migrates inward, the Jupiter-Saturn pair can avoid rapid inward migration and sometimes even migrate outward [309, 340, 395, 520, 396, 398]. This forms the basis of the Grand Tack model of Solar System formation, which we will discuss in detail in Section 3.3.2. However, that model’s potential fatal flaw is that avoiding inward migration requires that Jupiter

and Saturn maintain a specific mass ratio of roughly 3-to-1 [309] and it is uncertain whether that ratio can be maintained in the face of gas accretion.

Despite these uncertainties, the core accretion model can match a number of features of the known exoplanet population [203, 342, 358], including the observed giant planet-metallicity correlation [147] and the much higher abundance of Neptune-mass compared with Jupiter-mass planets [77, 481, 464].

Unstable Giant Planet Systems and the Exoplanet Eccentricity Distribution

Gas giant exoplanets are often found on non-circular orbits. This is surprising because, as we saw in Section 2, planets form in disks and so on orbits similar to the disks' streamlines, which are all circular and coplanar. The broad eccentricity of giant planets was for years a subject of broad speculation (for a historical discussion and a comprehensive list of proposed mechanisms, see [154]). The most likely culprit is a mechanism often referred to as *planet-planet scattering* [409, 496, 276]. The planet-planet scattering model proposes that the giant exoplanets formed in systems with many planets and that those that we see are the survivors of dynamical instabilities. Instabilities lead to orbit crossing, followed by a phase of gravitational scattering that usually concludes when one or more planets are ejected from the system entirely, typically leaving the surviving planets with eccentric orbits [308, 5, 331, 94, 229, 355, 415, 417, 410, 411, 412, 42].

Whereas instabilities among systems of rocky planets tend to lead to collisions, among systems of giant planets they lead to scattering and ejection. This can be understood by simply considering the conditions required for a planet to be able to give a strong enough gravitational kick to eject another object. The Safronov number Θ is simply the ratio of the escape speed from a planet's surface to the escape speed from the star at that orbital radius. It is defined as:

$$\Theta^2 = \left(\frac{G m_p}{R_p} \right) \left(\frac{a_p}{G M_\star} \right) = \frac{m_p a_p}{M_\star R_p}, \quad (45)$$

where m_p and M_\star are the planet and star mass, respectively, a_p is the planet's orbital radius, and R_p its physical radius. When $\Theta < 1$ collisions are (statistically-speaking) favored over ejection, and when $\Theta > 1$ ejection is favored. Scattering and ejection are therefore favored for massive planets far from their stars. It is interesting to note that Θ is defined in the same way as the gravitational focussing factor F_G from Eq. 17 in Section 2.2, which described the gravitational cross section of a growing protoplanet such that $F_G = 1 + (V_{esc}/V_{rel})^2$. Here, in the context of scattering, the dynamics are the same but in reverse. While the gravitational focussing factor F_G describes how far away can a planet accrete another object, Θ is a measure of how far a planet can launch another object.

The planet-planet scattering model matches the observed eccentricity distribution of giant exoplanets [5, 229, 94, 417, 410]. The only requirement is that a large fraction of systems have undergone instabilities. In simulations performed to date, at least 75% – and probably more like 90-95% – of giant planets systems must have

undergone planet-planet scattering in their past [229, 410, 411]. Scattering can even explain the highest-eccentricity giant exoplanets [84].

There is an anti-correlation between giant exoplanet masses and eccentricities. More massive planets are observed to have higher eccentricities [228, 432, 513]. This is the opposite of what one would expect from planet-planet scattering. Given that scattering is a process of equipartition of energy, one would naturally expect the low-mass planets to end up with high eccentricities and the high-mass planets with low-eccentricities. This is indeed what is seen in simulations of unstable systems starting with a dispersion of different planet masses. The solution to this conundrum may be quite simply that massive planets form in systems with many, roughly equal-mass planets [410, 206]. In that case, the most massive planets do indeed end up on the most eccentric orbits, as observed.

A Breaking the Chains Scenario for Giant Planets

The evolution of giant planet systems may well parallel that of super-Earths. As we saw in Section 3.1, the prevailing model for super-Earth formation – called *breaking the chains* [214] – involves migration into resonant chains followed by instability. Could this same evolutionary pathway apply to giant planet systems (Fig. 18)?

The answer appears to be yes. Giant planets may indeed follow a *breaking the chains*-style evolution that is similar, but not identical, to that of super-Earth systems.

Survival of resonances after the gaseous disk phase may be somewhat more common for giant planet systems. Only a few dozen giant planets are known to be found in resonance (e.g., the GJ876 resonant chain of giant planets [434]). Yet it is possible that many more resonant pairs of giant planets are hiding in plain sight. The radial velocity signatures of resonant planets can mimic those of a single eccentric planet [23] and it is possible that up to 25% of the current sample of eccentric planets are actually pairs of resonant planets [59]. The PDS 70 protoplanetary disk may host a pair of young giant planets in resonance [29], and other disk signatures may require multi-resonant planets to explain them [129]. When multiple giant planets form within a given disk it may thus slow and limit migration. This contrasts with the case of super-Earths, which migrate all the way to the disk's inner edge.

Instabilities appear to be ubiquitous among both super-Earths and giant exoplanets. As discussed above, the eccentricities of giant exoplanets are easily matched if most systems are survivors of instability. Instabilities may be triggered by the dispersal of the gaseous disk [314], chaotic diffusion within the giant planets' orbits [308, 41], or external perturbations, e.g. from wide binary stars [232].

Connection with Rocky Planets and Debris Disks

When giant planets go unstable they affect their entire system. Given their large masses and the high eccentricities they reach during the scattering phase, giant planets can wreak havoc on their inner and outer systems. Giant planet scatter-

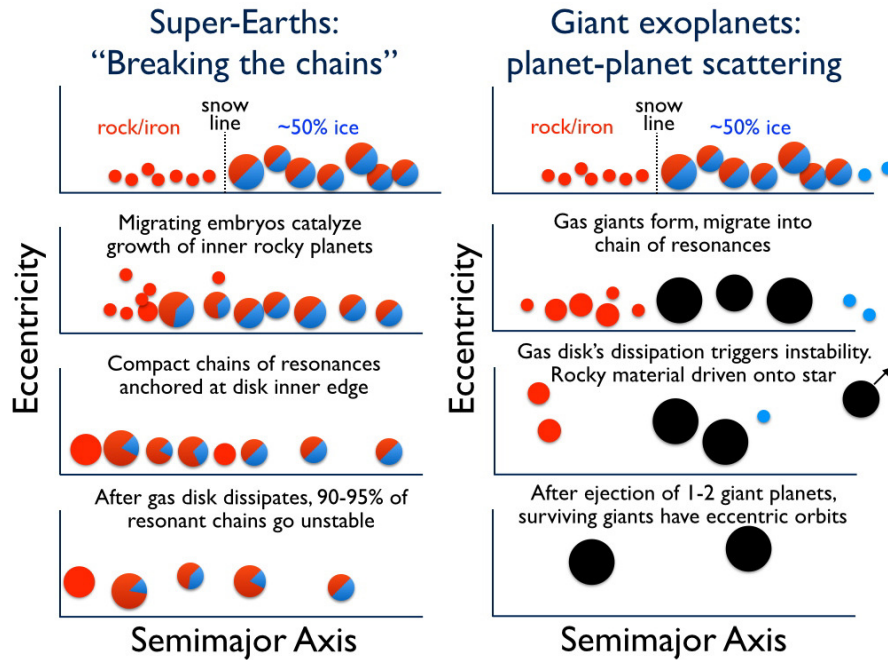


Fig. 18 Cartoon comparison of the evolution of super-Earth and giant planets systems. The same general processes could very well causing both populations to follow *breaking the chains*-like pathways. From [422].

ing systematically disrupts inner rocky planet systems [485, 486, 313, 80] or their building blocks [411, 412], usually by driving inner bodies onto such eccentric orbits that they collide with their host stars (see Fig. 19). Scattering also tends to destroy outer planetesimals disks by ejecting planetesimals into interstellar space [411, 412, 431, 307]. Outer planetesimal belts – when they survive and contain enough mass to self-excite to a moderate degree – evolve collisionally to produce cold dust observed as debris disks [515, 248, 315, 200], .

Raymond et al [411, 412] proposed that, by influencing both the inner and outer parts of their systems, giant planets induce a correlation between rocky inner planets and debris disks. Hints of a correlation have been found [516] but more data are needed. It has also been suggested that giant planets – especially those on very eccentric orbits – should anti-correlate with the presence of debris disks. While there may be a tendency for debris disks to be less dense in systems with eccentric giant planets[73], no strong correlation or anti-correlation between giant planets and debris disks has been observed to date [347, 348].

Nonetheless, connections between planetary system architecture and the presence and characteristics of dust remains an active area of study.

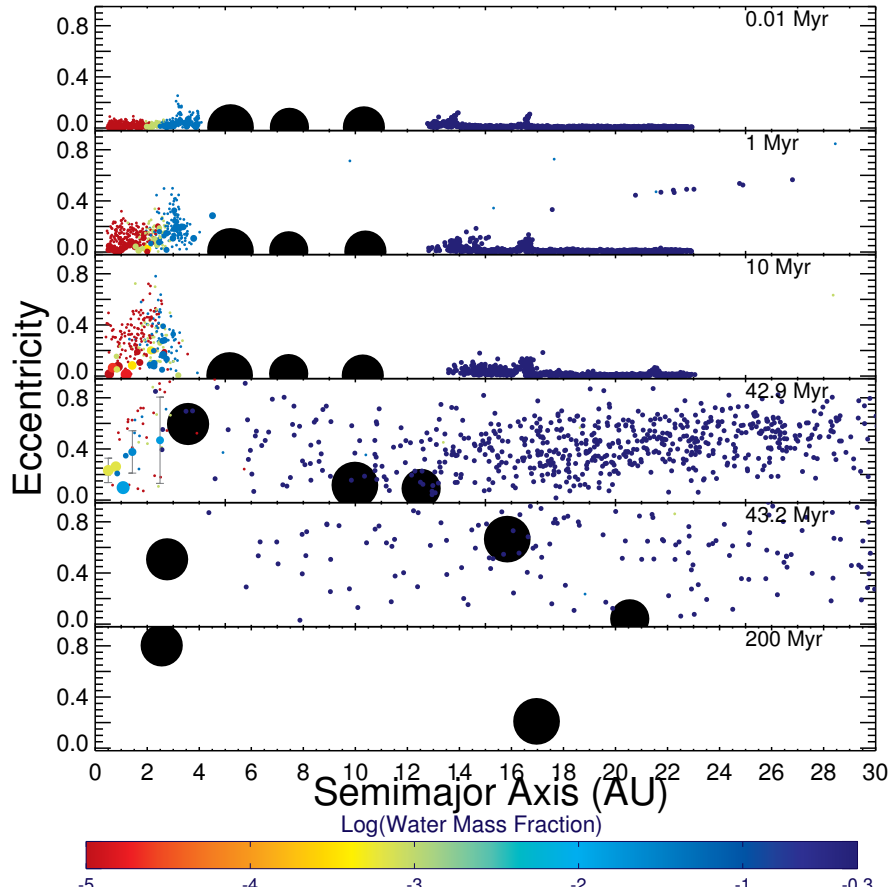


Fig. 19 Evolution of a simulation in which a system of gas giant went unstable, resulting in the destruction of both an inner system of growing terrestrial planets (that were driven into collisions with the central star) and an outer disk of ice-rich planetesimals (that was ejected into interstellar space; see [414, 413]. From [412].

3.3 Solar System formation

The standard timeline of Solar System formation proceeds as follows. Time zero is generally taken as the formation of Calcium- and Aluminum-rich Inclusions, or CAIs. CAIs are the oldest known inclusions in chondritic meteorites aged to be 4.568 Gyr old [15, 67, 108]. Radioactive ages of iron meteorites suggest that their parent bodies – several hundred to a thousand-km scale planetary embryos – were fully formed within 1 Myr after CAIs [181, 251, 448]. There are two isotopically distinct types of meteorites: the so-called carbonaceous and non-carbonaceous groups [492]. There is a broad distribution in the ages of both types of meteorites, whose overlap indicate

that these very different types of meteorites accreted simultaneously [15, 492, 250]. Chondrules – the primitive, mm-scale building blocks of chondritic meteorites – are found at the size scale at which objects drift rapidly through the disk due to aerodynamic drag [494, 253, 224]. The separation of the two different types of chondritic meteorites is interpreted as indicating that two isotopically-distinct reservoirs were kept spatially segregated, perhaps by the rapid growth of a large planetary embryo to the pebble isolation mass [75, 250]. This may thus constrain the timing of the growth of Jupiter’s core to have been very rapid, reaching the critical mass to block the pebble flux (of $\sim 10 - 20 M_{\oplus}$; [53]) within 1-1.5 Myr after CAIs [250].

The gaseous disk probably lasted for roughly 5 Myr. Gaseous disks around other stars are observed to dissipate on a few Myr timescale (see Fig. 2). The oldest chondritic meteorites are the CB chondrites, which formed roughly 5 Myr after CAIs albeit perhaps in the absence of gas [239, 249, 226]. Given that gas is thought to be needed for planetesimal formation [221], this implies 5 Myr as an upper limit on the gas disk lifetime (at least in some regions).

Hafnium-Tungsten (Hf/W) measurements of Martian meteorites indicate that Mars’ formation was basically finished within 5-10 Myr [368, 117], meaning that it grew very little after the disk had dispersed. In contrast, Hf/W measurements indicate that Earth’s last differentiation event – generally thought to have been the Moon-forming impact – did not take place until ~ 100 Myr after CAIs [476, 240]. However, uncertainties in the degree of equilibration of the Hf/W isotopic system during giant impacts make it hard to determine a more accurate timeframe [149].

Highly-siderophile (“iron-loving”) elements should in principle be sequestered in the core during differentiation events. Thus, any highly-siderophile elements in the terrestrial mantle and crust should in principle have been delivered *after* the Moon-forming impact [237]. Simulations show that there is a clear anti-correlation between the timing of the last giant impact on Earth and the mass in planetesimals delivered after the last giant impact [218]. The total amount of highly-siderophile elements can therefore constrain the timing of the impact. Assuming a chondritic composition, Earth accreted the last $\sim 0.5\%$ of its mass as a veneer after the Moon-forming impact [341]. This implies that the Moon-forming impact took place roughly 100 Myr after CAIs [218], consistent with the Hf/W chronometer.

The Solar System’s giant planets are thought to have undergone an instability. The so-called *Nice model* showed that the giant planets’ current orbital configuration [479, 363] – as well as the orbital properties of Jupiter’s Trojans [336, 366], the irregular satellites [365], and the Kuiper belt [271, 360] – could be explained by a dynamical instability in the giant planets’ orbits [361]. The instability is generally thought to have been triggered by interactions between the giant planets and a remnant planetesimal disk (essentially the primordial Kuiper belt [167, 340, 270, 405]), although a self-driven instability is also possible [410, 433]. The instability was first proposed to explain the so-called terminal lunar cataclysm, i.e. an abrupt increase in the flux of projectiles hitting the Moon roughly 500 Myr after CAIs [469, 167, 337]. However, newer analyses suggest that no terminal lunar cataclysm ever took place

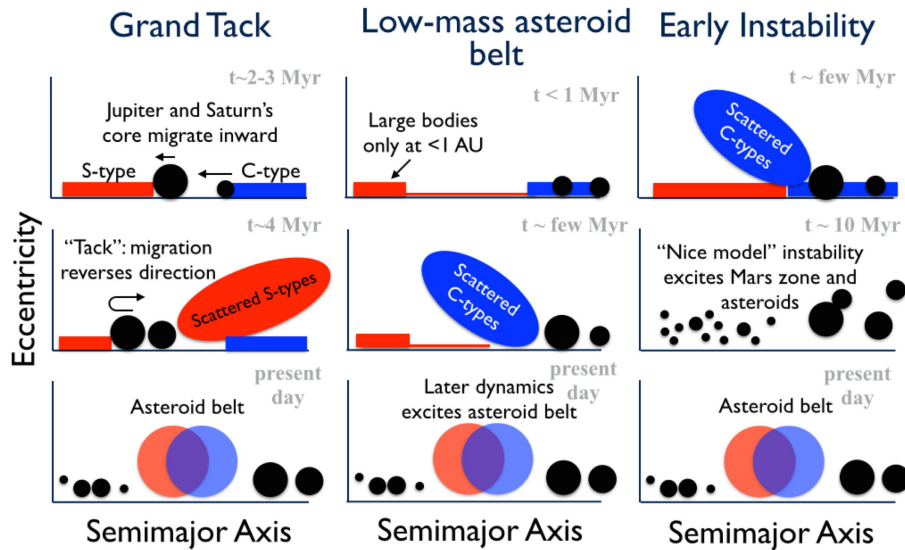


Fig. 20 Cartoon comparison between the global evolution of three plausible models for Solar System formation described in Sections 3.3.2-3.3.4. From [422].

[93, 58, 519, 338, 186], and that the instability may have taken place anytime in the first ~ 100 Myr after CAIs [338, 364, 328].

Over the past decade, global models of Solar System formation have been revolutionized (see Fig 20). Decades-old models that assumed local growth of the planets (i.e., the so-called *classical model* [495, 500, 502, 89, 88, 427, 373, 426, 423]) have been supplanted with models that explain the distribution of the planets and small body belts by invoking processes such as long-range migration of the giant planets (the *Grand Tack* model [488, 425, 69]), non-uniform planetesimal formation within the disk (the *Low-mass Asteroid belt* model [182, 135, 216, 421]) and an early instability among the giant planets' orbits (the *Early Instability* model [104, 103, 105]). Pebble accretion has been proposed to play an important role during the terrestrial planets' growth [269], the importance of which may be constrained by isotopic measurements of different types of meteorites as well as Earth samples [492, 250, 447, 76].

Here we first describe the classical model and then the other competing models. We then compare the predictions of different models.

3.3.1 The Classical model

The classical model of terrestrial planet formation makes two dramatically simplifying assumptions. First, it assumes that the planets formed roughly in place. This implies that one can reconstruct the approximate mass distribution of the protoplan-

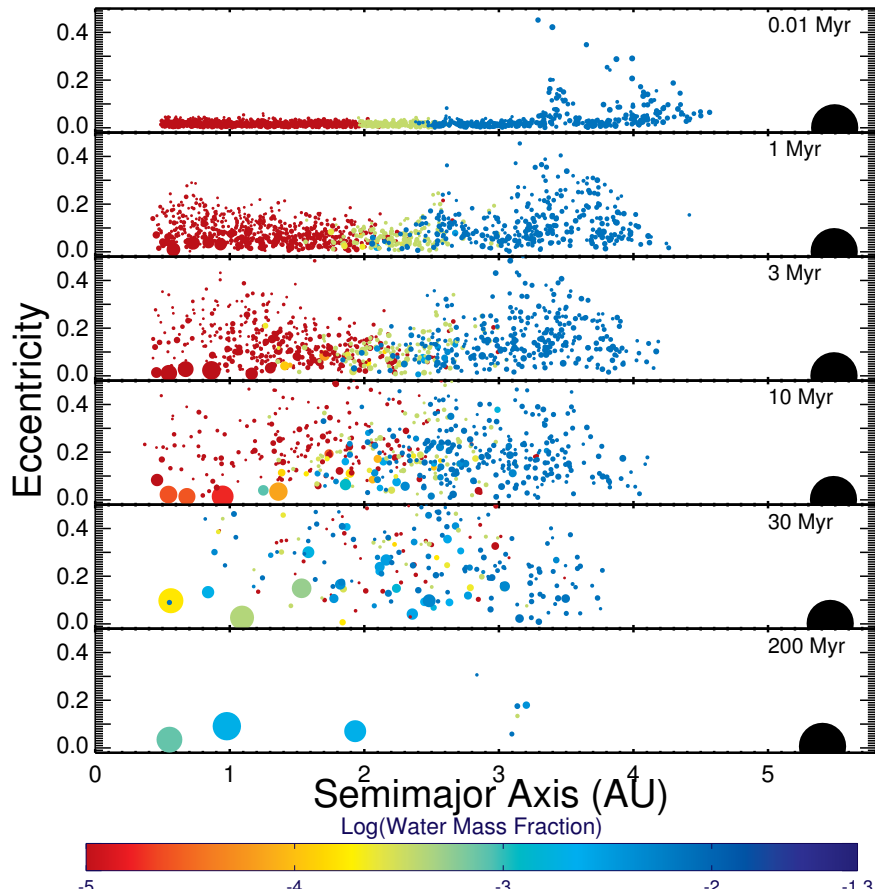


Fig. 21 Simulation of the classical model of terrestrial planet formation from [428]. The size of each planetary embryo scales with its mass m as $m^{1/3}$. Colors represent the water contents, initially calibrated to match the water contents of current orbital radii of different populations of primitive asteroids [171, 427]. Jupiter is the large black circle.

etary disk by simply spreading the planets' masses out in concentric annuli (the so-called 'minimum-mass solar nebula' model; [495, 189, 118]). Second, it assumes that giant- and terrestrial planet formation can be treated separately. Thus, one can study the influence of the giant planets' orbits on terrestrial planet formation after the gas disk had dispersed without the need to consider their earlier effects.

Figure 21 shows a simulation of the classical model of terrestrial planet formation (from [428]). In this case Jupiter is included on a supposed pre-instability orbital configuration, on a near-circular orbit. The terrestrial disk is initially composed of roughly 2000 planetary embryos with masses between that of Ceres and the Moon. Accretion is driven from the inside-out by gravitational self-stirring and from the outside-in by secular and resonant forcing from Jupiter. There is a long chaotic

phase of growth that involves many giant impacts between planetary embryos (see e.g. [6, 244, 406]). The planets grow on a timescale of 10-100 Myr. Remnant planetesimals are cleared out on a longer timeframe. There is sufficient radial mixing during growth for water-rich material from past 2.5 au to have been delivered to the growing Earth (see extensive discussion of the origin of Earth's water in Section 3.4).

The classical model has a fatal flaw: it systematically produces Mars analogs that are far more massive than the real Mars [501]. This can be seen in the simulation from Fig. 21, which formed passable Venus and Earth analog but a Mars analog roughly as massive as Earth. The true problem is not Mars' absolute mass but the large Earth/Mars mass ratio. The classical model tends to produce systems in which neighboring planets have comparable masses rather than the $\sim 9:1$ Earth/Mars ratio [428, 373, 426, 345, 346, 148, 231]. Classical model simulations tend to have two other problems related to the asteroid belt: large embryos are often stranded in the belt [426], and they do not match the belt's eccentricity and inclination distributions [216].

The building blocks of the terrestrial planets were roughly Mars-mass and thus the inner Solar System may only have contained roughly two dozen embryos [337]. One may wonder how often a small Mars arises because, by chance, it avoided any late giant impacts. Fischer & Ciesla [148] showed that this happens in a few percent of simulations. However, when one takes the asteroid belt constraints into consideration the success rate of the classical model in matching the inner Solar System drops by orders of magnitude [216].

The 'small Mars' problem – first pointed out by Wetherill [501] and re-emphasized in 2009 [426] – is thus the Achilles heel of the classical model. It prompted the development of alternate models whose goal was to explain how two neighboring planets could have such different masses.

3.3.2 The Grand Tack model

The Grand Tack model [488] proposed that Jupiter's migration during the gaseous disk phase was responsible for depleting Mars' feeding zone. The Grand Tack is based on hydrodynamical simulations of orbital migration (see Sections 2.4 and 2.5 for more details). Simulations show the giant planets carve annular gaps in the disk [278, 491, 112]. A single planet usually migrates inward on a timescale that is related to the disk's viscous timescale [114, 139]. Multiple planets often migrate convergently and become trapped in mean-motion resonances [458, 266], often sharing a common gap. When the inner planet is two to four times more massive than the outer one and both planets are in the gap-opening regime, gas piles up in the inner disk and a torque imbalance causes the two planets to migrate *outward* [309, 340, 395, 520, 396, 398].

The Grand Tack model proposes that Jupiter formed first and migrated inward. Saturn formed more slowly, migrated inward and caught up to Jupiter. The two planets became locked in resonance and migrated outward together until either the

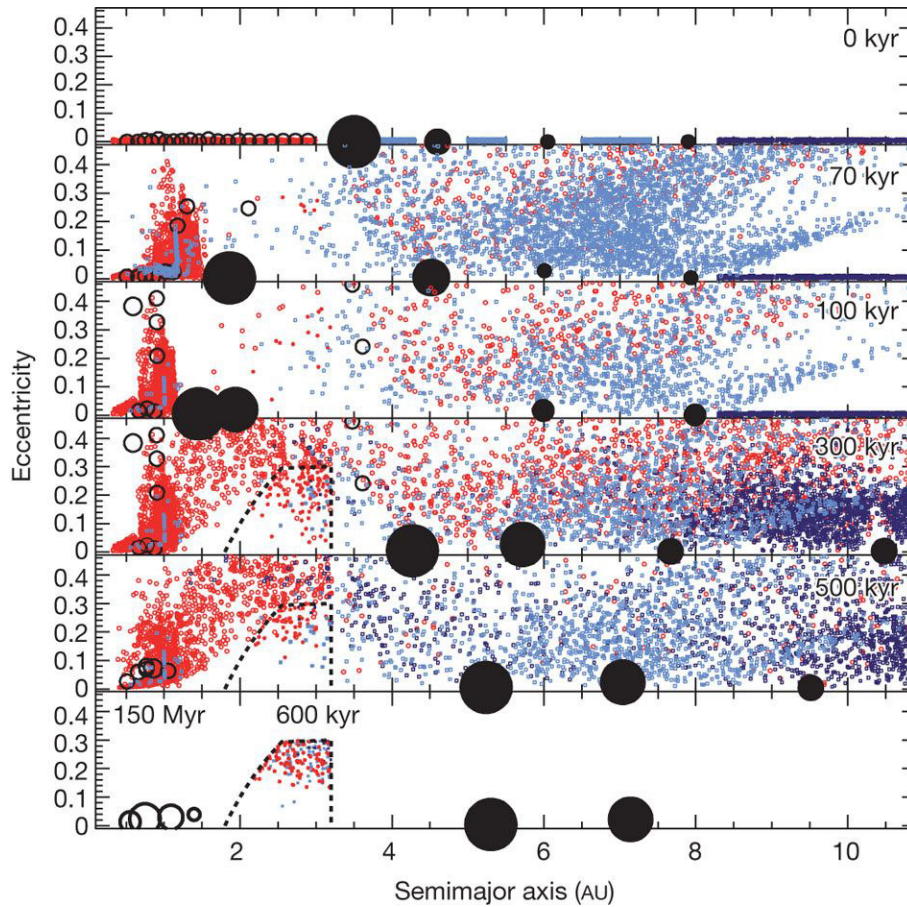


Fig. 22 Evolution of the Grand Tack model, from [488]. The giant planets' migration (black symbols) sculpts the distribution of rocky bodies in the inner Solar System. Here Jupiter migrated inward, then Saturn migrated inward, and then the two planets migrated back out. The red dots indicate presumably dry, S-type planetesimals that formed interior to Jupiter's orbit, whereas the blue dots represent planetesimals originally between and beyond the giant planets' orbits. Rocky planetary embryos are shown as empty circles. The bottom three panels include dashed contours of the present-day main asteroid belt.

disk dissipated or certain conditions slowed their migration (e.g., if the disk was flared such that Saturn dropped below the gap-opening limit in the outer disk).

The evolution of the Grand Tack model is shown in Figure 22. If Jupiter's inward migration reached 1.5-2 au then the inner disk would have been truncated at ~1 au, depleting Mars' feeding zone but not Earth's [488, 69]. The terrestrial planets in simulations provide a good match to the real ones [488, 217, 69].

The asteroid belt is severely depleted by Jupiter's migration but is not completely emptied [488, 489]. The S-types were scattered outward by Jupiter's inward

migration, then back inward by Jupiter's outward migration, with an efficiency of implantation of $\sim 0.1\%$. The C-types were scattered inward by Jupiter and Saturn's outward migration. The final belt provides a reasonable match to the real one – particularly when evolved over Gyr timescales [123]. It is worth noting, however, that the initial conditions in Fig. 22 neglect additional (possibly much more important) phases of implantation that took place during Jupiter and Saturn's rapid gas accretion [420].

The Grand Tack's potential Achilles heel is the mechanism of outward migration itself (see discussion in [425]). The most stringent constraint on outward migration is that it requires a relatively limited range of mass ratios between Jupiter and Saturn (roughly between a ratio of 2:1 and 4:1; [309]). It remains to be seen whether long-range outward migration remains viable when gas accretion is consistently taken into account, as the gas giants' mass ratio should be continuously changing during this phase. There may also be geochemical constraints related to the speed of accretion in the Grand Tack model [524].

3.3.3 The Low-mass Asteroid belt model

The Low-Mass Asteroid belt model makes the assumption that Mars' small mass is a consequence of a primordial mass deficit between Earth and Jupiter's present-day orbits. Gas disks are generally expected to have smooth radial distributions, but this is not the case for dust. Dust drifts within disks and ALMA images show that dust rings are common in protoplanetary disks [14, 16]. Given that planetesimal formation via the streaming instability is sensitive to the local conditions [456, 517], dust rings may be expected to produce rings of planetesimals. One model of dust drift and coagulation, combined with the conditions needed to trigger the streaming instability, showed that planetesimals may indeed form rings [135].

Since the 1990s it was known that if an edge existed in the initial distribution of planetary embryos or planetesimals, any planet that formed beyond that edge would be much less massive than the planets that formed within the main disk [502, 503, 89, 6, 88]. However, it was Hansen in 2009 [182] who proposed that such an edge might really have existed in the early Solar System. Indeed, he showed that the terrestrial planets can be matched if they formed from a narrow annulus of rocky material between the orbits of Venus and Earth (see Fig. 23). In this model the large Earth/Mars mass ratio is a simple consequence of the depletion of material past Earth's orbit, and the small Mercury/Venus mass ratio is a consequence of the analogous depletion interior to Venus' orbit.

The most extreme incarnation of the Low-mass asteroid belt model proposes that no planetesimals formed between the orbits of Earth and Jupiter [182, 421], but the model is also consistent with planetesimal forming in the belt, just at a reduced efficiency. Yet even an empty primordial asteroid belt would have been dynamically re-filled with objects originating across the Solar System. Rapid gas accretion onto Jupiter and later Saturn destabilizes the orbits of nearby planetesimals, many of which are gravitationally scattered in all directions. Under the action of gas drag, a

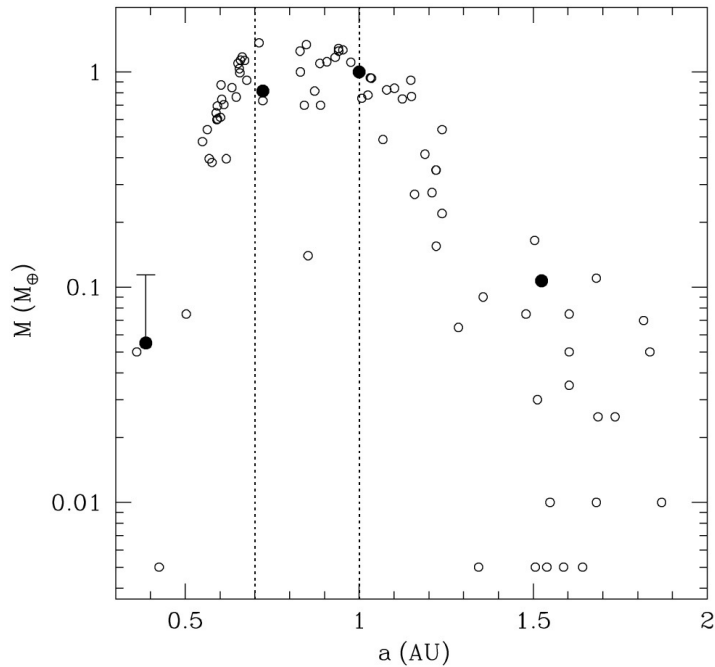


Fig. 23 Distribution of simulated terrestrial planets formed assuming that all of the terrestrial planets' mass was initially found in a narrow annulus between the orbits of Venus and Earth (denoted by the dashed vertical lines). The open circles show simulated planets and the solid ones are the real planets. From [182].

fraction of planetesimals are trapped on stable, low-eccentricity orbits, preferentially in the asteroid belt [420], and some are scattered past the asteroid belt to the terrestrial planet region itself (see Fig. 27 and Section 3.4). On a longer timescale, the growing terrestrial planets scatter remnant planetesimals outward, a small fraction of which are trapped in the main belt, preferentially in the inner parts [421].

The main uncertainty in the Low-mass asteroid belt are the initial conditions. When disk models, dust growth and drift, disk observations and interpretation (including studies of ALMA-detected disks), and meteorite constraints (including the broad age distribution of noncarbonaceous chondrites, which indicate many different planetesimal formation events; [250]) are all accounted for, will it be a reasonable assumption that the terrestrial planets could have formed from a narrow ring of planetesimals?

3.3.4 The Early Instability model

It has been demonstrated numerically that dynamical instabilities among giant planets cause severe damage to the small bodies in their same systems (see Fig. 19). The Solar System's giant planets are thought to have undergone an instability, albeit a much less violent one than the typical instability incurred by giant exoplanet systems. Nonetheless, the Solar System's instability is violent enough that, if they were fully-formed at the time, the terrestrial planets would have had a very low probability of survival [230]. Yet the timing of the instability is uncertain, and it could have happened anytime in the first 100 million years of Solar System evolution [338, 328]. One may then wonder whether a very early instability could have played a role in shaping the distribution of the terrestrial planets.

The Early Instability model, conceived and developed by Clement et al. [104, 103, 105], is built on the premise that the giant planets' instability took place within roughly 10 Myr of the dissipation of the gaseous disk. The evolution of one realization of the model is shown in Figure 24. The early evolution of the Early Instability model is identical to that in the classical model. The giant planets' dynamical instability – triggered after 10 Myr in the simulation from Fig. 24 – strongly excites the orbits of inner Solar System objects extending through the asteroid belt in to Mars' feeding zone [124, 105]. The belt is strongly depleted and dynamically excited, and Mars' growth is effectively stunted. In a fraction of simulations no Mars forms at all [104]! The growth of Earth and Venus are largely unperturbed and qualitatively similar to the classical model.

The instability itself is stochastic in nature. Matching the instability statistically requires a large number of numerical realizations, which produce a spectrum of Solar Systems with different properties. Such simulations have more constraints than many because they include all of the planets and not just the terrestrial planets. One remarkable feature of the Early Instability model is that systems that provide the best match to the outer Solar System are the same ones that provide the best match to the terrestrial planets [104, 103, 105].

The main uncertainty in the Early Instability model is simply the timing of the instability. Mars' formation was largely complete within 5-10 Myr [368, 117], shortly after the disappearance of the gaseous disk. To affect terrestrial planet formation the giant planets must therefore have gone unstable within perhaps 5 Myr of the disk's dispersal. This would also imply a cometary bombardment in the inner Solar System that was coincident with the late phases of terrestrial planet growth. While such a bombardment would deliver only a very small amount of mass to Earth [334, 167], it would provide a large component of Earth's noble gases [305]. The Xe isotopic compositions of the mantle and atmosphere are different [350, 78], and it has been suggested that a comet-delivered component contributed to the atmospheric Xe budget but not to the mantle Xe [304]. It remains to be understood whether or not this implies that the bulk of Earth accreted with little cometary influx, which would constrain the timing of cometary delivery and presumably of the instability itself.

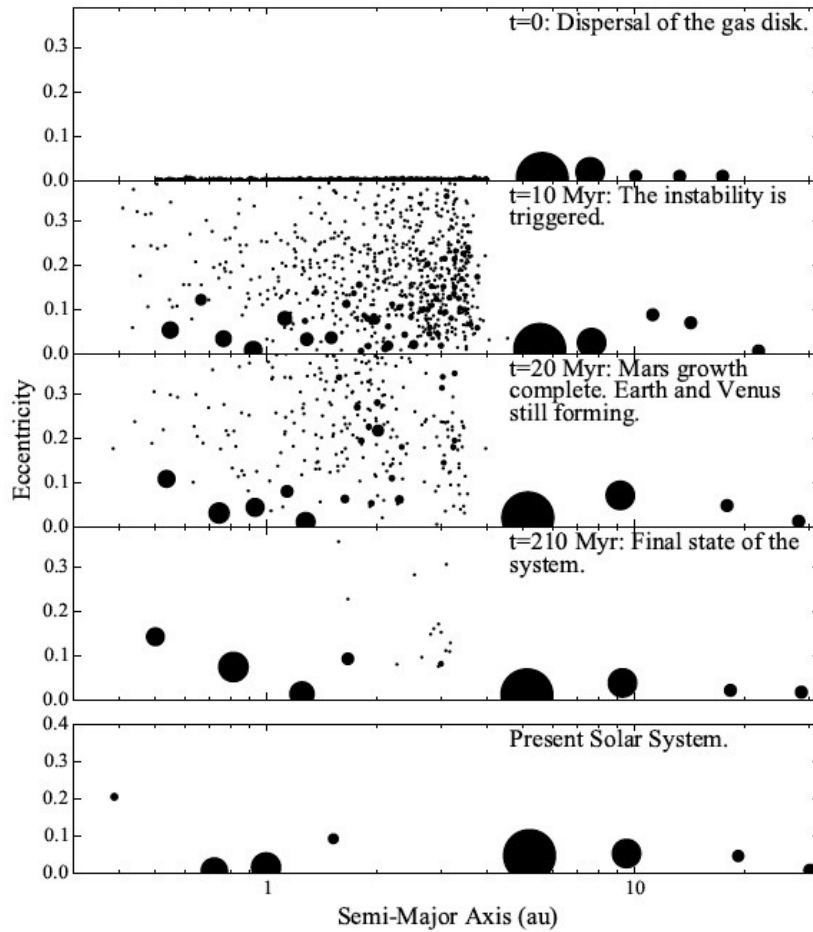


Fig. 24 Evolution of the Early Instability model (from [104]). In this case the giant planets' instability was triggered 10 Myr after the dissipation of the disk. The instability strongly excited the orbits of growing planetesimals and planetary embryos in the asteroid belt and Mars' feeding zone. Mars' growth was stunted but Earth and Venus continued to accrete for ~ 100 Myr. The final system has a large Earth/Mars mass ratio and an overall planetary system architecture similar to the actual Solar System (shown at bottom for comparison).

3.3.5 Other models

It is worth noting that the three scenarios outlined above as alternatives to the classical model are not the only ones that have been proposed. For example, it was suggested that sweeping secular resonances during the dissipation of the gaseous disk could have depleted and excited the asteroid belt and generated an edge in the terrestrial planets' mass distribution [356, 472, 71]. The main uncertainty in that

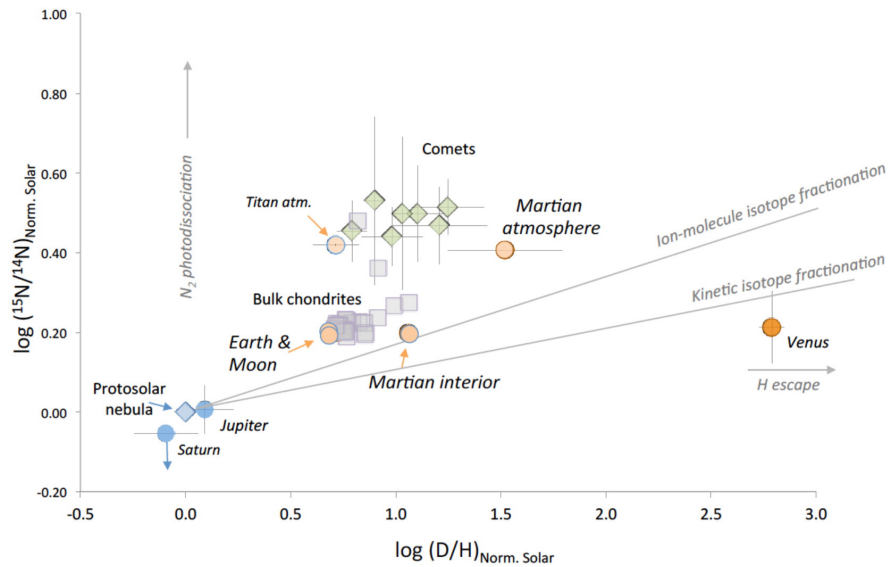


Fig. 25 Measured $^{15}\text{N}/^{14}\text{N}$ isotope ratios vs. D/H ratios of Solar System objects. Arrows indicate how different processes would affect an object's evolution in this isotope space. From Marty et al. [305].

model is whether a non-zero eccentricity of Jupiter can realistically be maintained during the gas dissipation phase.

It has also been suggested that pebble accretion may have played a role in terrestrial planet formation [269, 90]. Isotopic analyses of meteorites may help to constrain the degree to which carbonaceous pebbles from the outer Solar System contributed to the growth of the terrestrial planets [447, 76]. In general, the formation of Earth-mass planets within the disk lifetime poses a problem because, given that the gas disk is required for pebble accretion, such planets should grow fast enough to migrate inward and become super-Earths [258].

3.4 Origin of water on Earth and rocky exoplanets

We now turn our attention to the origin of planets' water. Cosmochemical tracers such as isotopic ratios can be used to constrain the potential sources of Earth's water (see, e.g., [334, 303]). While bulk density measurements of solid exoplanets can in principle be used to trace water contents [483, 460, 156, 451], in practice it is extremely challenging [3, 452, 132]. There have been a few recent reviews on the origins of Earth's water in dynamical and cosmochemical context [372, 319, 322].

Earth is our benchmark for water. While it appears blue from space, all of Earth's oceans only add up to $\sim 2.5 \times 10^{-4} M_{\oplus}$ of water. This is generally referred to as one "ocean" of water. The water budget of Earth's interior is quite uncertain. Different studies infer different quantities of water trapped in hydrated silicates, with overall budgets between roughly one and ten oceans [193, 349, 303, 180]. Earth's core may be very dry [28] or may contain fifty or more oceans of water [370]. While papers often quote Earth as being roughly one part in a thousand water by mass, it is important to be aware of the uncertainty.

Figure 25 shows the D/H ratios for a number of Solar System objects (for a compilation of references to the D/H measurements, see [334, 306, 9, 10]). The Sun and gas-dominated planets have D/H ratios roughly six times lower than Earth's. This is interpreted as the isotopic composition of the gaseous protoplanetary disk. Carbonaceous chondrite meteorites have similar D/H values to Earth. Most measured comets have higher D/H values than Earth, although two recently-measured Jupiter-family comets [187, 279] and one Oort cloud comet [56] have Earth-like D/H ratios. In contrast, ESA's Rosetta mission measured the D/H ratio of comet 67P/C-G to be more than three times the terrestrial value. A recent result [459, 280] found that very active comets tended to have Earth-like D/H whereas less active ones have higher D/H. One interpretation is that comets' original water was Earth-like and loss processes during outgassing have fractionated the surviving D/H. If true, that would mean render the D/H ratio useless as a discriminant between comets and carbonaceous sources of water. One must then resort to dynamical constraints or perhaps to other isotopic systems.

Fig. 25 naively would suggest carbonaceous chondrite-like objects as the source of Earth's water and Nitrogen. Yet even if Earth's water were delivered by carbonaceous objects, that is only a part of the story. A complete model must explain the full evolution of our planetary system and, in the context of Earth's water, ask: where did the water-bearing objects themselves originate?

We can break down the various models for water delivery into six rough scenarios that we outline below. Two of these models invoke local sources of water whereas the others propose that Earth's water was delivered from farther out in the disk. For a comprehensive review of these models, see Meech & Raymond (2019) [322].

Adsorption of water vapor onto silicate grains

In a simple picture of the structure of disks, water should exist as a solid past the snow line and as a vapor closer-in. If water vapor was indeed present where silicate grains were coalescing to form the terrestrial planets, then "in-gassing" may have attached hydrogen molecules to silicate grains [461, 354, 27, 455, 115]. This process is called adsorption. The mechanism can in principle have seeded Earth with a few oceans of water, albeit without taking any water loss processes into account (such as ^{26}Al -driven heating [175, 330] or impact-related losses [160, 466]). Yet at face value it should have seeded Earth with nebular water, which has a D/H ratio six times smaller than Earth's. It also cannot explain the abundance of other volatiles such as C,

N and the noble gases, which would then require an alternate source containing little hydrogen. Finally, it begs the question of why the Enstatite chondrites – meteorites that provide the closest chemical match to Earth’s bulk composition [116] – appear to have formed without any water.

Oxidation of H-rich primordial envelope

As planetary embryos grow they gravitationally accrete H-rich envelopes if they are more massive than a few tenths of Earth’s mass [209, 256]. This hydrogen could have chemically reacted with Earth’s surface magma ocean and generated water by hydrating silicates [208]. Given that the D/H ratio of nebular gas was many times smaller than Earth’s water, this model, like the previous one, predicts that Earth’s initial D/H ratio was small. In this case, however, it is possible to envision that Earth’s D/H changed in time. The loss of a thick hydrogen envelope would certainly entail mass fractionation, and for a certain range of parameters Earth’s final D/H ratio can be matched even though its water was acquired from gas [161]. However, the collateral effects of this presumed atmospheric loss have not been quantified, and appear to be at odds with other constraints, such as the abundance of ^{129}Xe from the decay of ^{129}I [305]. In addition, it seems quite a coincidence for Earth to match carbonaceous chondrites in multiple isotopic systems as a result of such loss processes, which would affect different molecules differently.

Pebble “snow”

Planets beyond the snow line accrete water as a solid. It is simply a building block. Yet the snow line is a moving target. As the disk evolves and cools the snow line generally moves inward [444, 262, 301]. A planet on a static orbit would see the snow line sweep past it. Such a planet would start off in the rocky part of the disk but, once the snow line passed interior to its orbit, would find itself outside the snow line, in the presumably icy part of the disk.

As the snow line sweeps inward, new ice does not come from the condensation of water vapor. This is because the speed at which gas moves through the disk is far faster than the motion of the snow line itself [333]. Thus, the gas just interior to the snow line is dry. Rather, ice at the snow line comes from pebbles and dust that drift inward through the disk. The source of these drifting pebbles is thought to move outward as an analogous wave of dust coagulation and growth sweeps radially out through the disk [48, 255, 47, 202]. If anything blocks the inward flow of pebbles – such as a growing giant planet core [254, 53] – the snow line will continue to move inward but it will not bring any ice along with it [333]. The source of water will also drop if the outward-sweeping growth front producing pebbles reaches the outer edge of the disk [207].

In the Solar System there is evidence that the pebble-sized building blocks carbonaceous and noncarbonaceous were segregated as of 1-1.5 Myr after CAIs

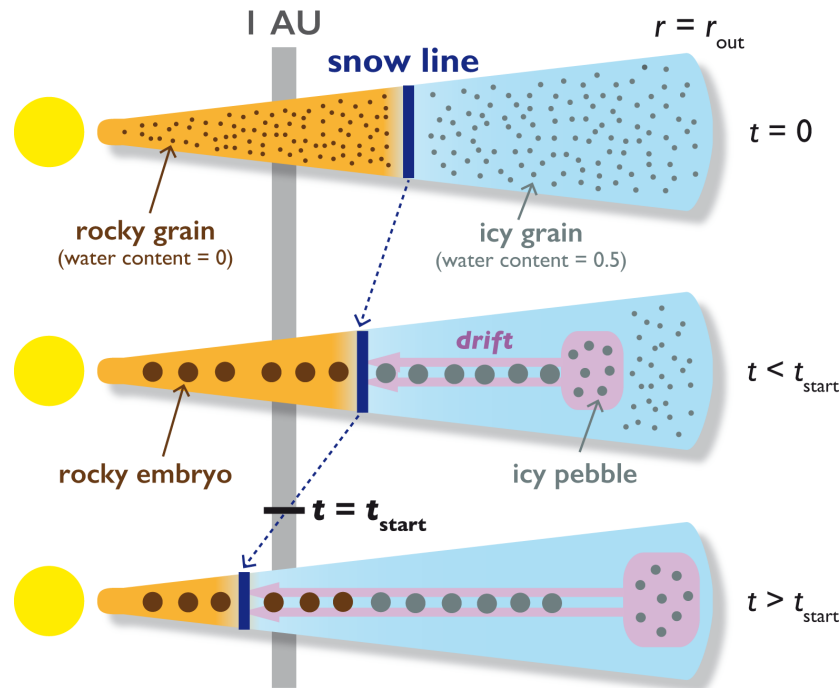


Fig. 26 The *pebble snow* model [379, 445, 207]. Rocky planetary embryos grow from rocky grains interior to the snow line. As the disk cools, the snow line sweeps inward and ice-rich pebbles from the outer parts of the disk deliver water to the terrestrial planet region. From [445].

[75, 250]. This would suggest that carbonaceous pebbles did not deliver Earth's water, as their widespread presence in the inner Solar System would presumably have produced a category of meteorites intermediate in isotopic composition between the carbonaceous and noncarbonaceous. The Enstatite chondrites, which formed near the end of the disk's lifetime and are the closest chemical match to Earth, are dry [10].

Nonetheless, pebble snow may be a key mechanism in delivering water to rocky exoplanets (see below).

Wide feeding zone

A planet's feeding zone is simply the radial distribution of its constituents. In the classical model the terrestrial planets formed from a broad disk of planetary embryos extending from Venus' orbit out to Jupiter's. For example, in the simulation from Fig. 21, each of the three surviving terrestrial planets accreted material from a broad swath of the disk. Given that the constituent planetesimals should have a radial gradient in composition based on the local temperature [130], this implies that

volatiles are naturally incorporated into growing planets if the planets' feeding zones extend out far enough [334, 427, 429].

The planets' broad feeding zones – in concert with the isotopic match between Earth's water and that of carbonaceous chondrites – led to the scenario that Earth's water was delivered by primordial carbonaceous planetesimals or planetary embryos [334, 427, 429]. However, this idea was built on the classical model. As the classical model crumbled under the weight of the small Mars problem (see Section 3.3) the idea that Earth's water was a result of its broad feeding zone no longer made sense. The Early Instability model [104, 103, 105] starts from essentially the same initial conditions as the classical model and presents a viable solution to the small Mars problem all the while delivering water to Earth by the same mechanism. However, like the classical model [426], the Early Instability may only adequately deliver water to Earth in simulations that fail to match Mars' small mass (Clement and Rubie, personal communication). The Early Instability model acknowledges that in order to understand in the first place the existence of water-rich asteroids intermixed with water-poor asteroids in the asteroid belt, which may have been the result of the growth and/or migration of the giant planets. That leads us to the next scenario.

External pollution

The orbits of leftover planetesimals are strongly perturbed by the growth and migration of the giant planets. The phase of rapid gas accretion is particularly dramatic. The mass of the giant planets can increase from $\sim 10\text{--}20 M_{\oplus}$ up to hundreds of Earth masses on a $\sim 10^5$ year timescale [404, 203]. This rapid gas accretion destabilizes the orbits of any nearby planetesimals that managed to avoid being accreted. Many planetesimals undergo close gravitational encounters with the growing planet and are scattered in all directions. Under the action of gas drag, many planetesimals are trapped interior to the giant planet's orbit [420, 438]. This happens when a planetesimal on an eccentric orbit that crosses the giant planet's orbit at apocenter undergoes sufficient orbital energy loss due to gas drag to drop its apocenter away from the giant planet, releasing it from the gas giant's dynamical clutches.

Figure 27 shows this process in action. Jupiter's growth triggers a pulse of planetesimal scattering, and a second is triggered when Saturn forms. The outcomes of these pulses can vary because the disk itself changes in time as it both slowly dissipates and, more importantly, is sculpted by the giant planets.

The relative number of planetesimals that are trapped in the main asteroid belt (providing an orbital match to the C-types) vs. those that are scattered *past* the asteroid belt to the terrestrial planets (to deliver water) varies as a function of the strength of gas drag [420]. When gas drag is strong – i.e., for a massive inner gas disk or smaller planetesimals – scattered planetesimals are rapidly decoupled from Jupiter and are generally trapped in the outer parts of the main belt. When gas drag is weak – for a low-density inner disk or large planetesimals – it takes a large number of orbits for gas drag to decouple planetesimals' orbits from Jupiter. Planetesimals

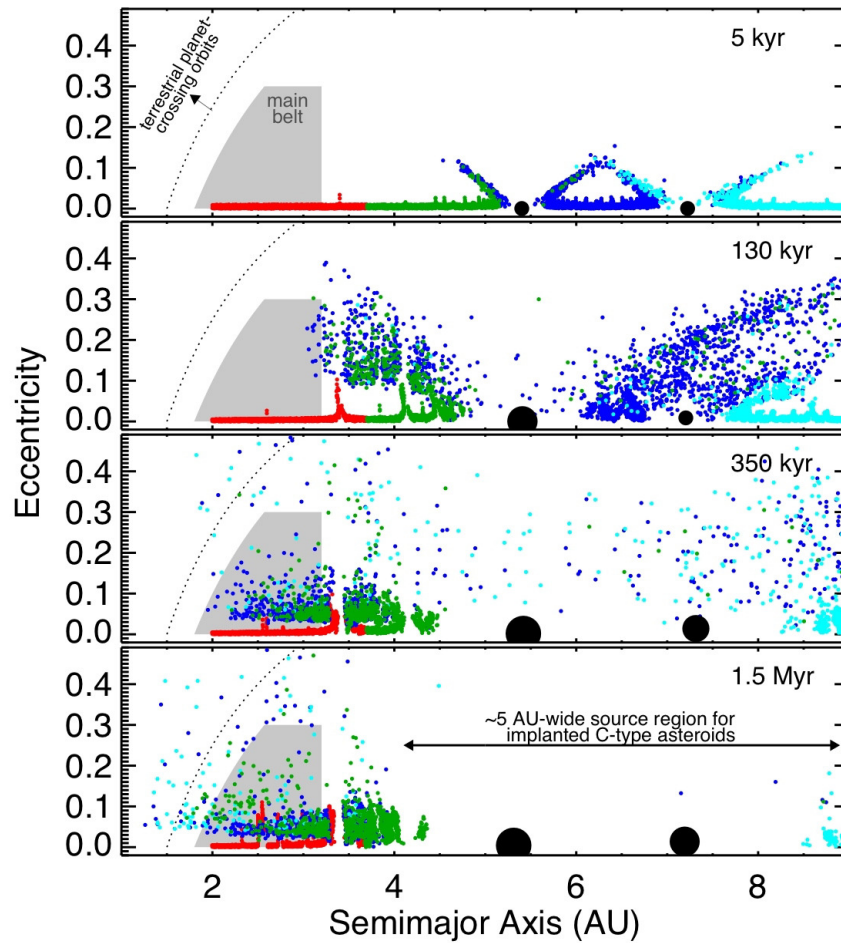


Fig. 27 Scattering of ten thousand planetesimals driven by the growth of Jupiter (from 100-200 kyr) and Saturn (from 300-400 kyr). Planetesimals from the Jupiter-Saturn region end up polluting the inner Solar System *en masse*. Some are trapped in the outer parts of the main asteroid belt (shaded) and some are scattered past the belt to the terrestrial planet region (above the dashed line). And even so, this example shows the minimum expected impact of the giant planets' growth, as it assumed the giant planets to have formed on low-eccentricity, non-migrating orbits in 3:2 resonance. Planetesimal colors correspond simply to each object's starting location. There is an underlying gaseous disk in the simulation, whose structure and overall density evolve in time in a consistent way. In this example planetesimals were assumed to be 100km in diameter for the gas drag calculation. From [420].

are more frequently scattered farther inward to pollute the terrestrial planet-forming region and to deliver water.

A similar mechanism is driven by giant planet migration. In the Grand Tack model, Jupiter and Saturn's outward migration scatters a large number of planetesimals inward ([488, 489]; see Fig. 22). Given that the giant planets are migrating away, scattered planetesimals are more easily decoupled from the giant planets. The distribution of scattered planetesimals that survive on orbits interior to the giant planets' have a much weaker size dependence than for those that were scattered during the giant planets' growth and for which gas drag played a central role. The dependence on the gas surface density is also much weaker.

Both migration and growth can thus generate populations of terrestrial planet-crossing planetesimals that originated beyond Jupiter. Given their distant origins these planetesimals tend to have high-eccentricity orbits, but simulations show that they are nonetheless accreted by the terrestrial planets on a geochemically consistent timescale and in sufficient quantity to easily deliver Earth's water budget [374]. In addition, they naturally match the compositions of carbonaceous meteorites.

In the wide feeding zone model, the C-type asteroids represented the distant, mother source of Earth's water. In the pollution model, Earth's water was delivered from the same parent population as the objects that were implanted into the asteroid belt as C-types. Thus, Earth's water and C-type asteroids are brother and sister.

At present, the pollution scenario is the leading model to explain the origin of Earth's water. It matches the amount and chemical signature of Earth's water, and naturally fits within different models of Solar System formation.

Inward migration

Earth-mass planets migrate relatively rapidly in protplanetary disks (see Sections 2.2 and 3.1). Given that large embryos are thought to form fastest past the snow line [254, 335], this implies that many inward-migrating planets or cores should be water-rich [55]. Indeed, the migration model for super-Earth formation predicts that most should be water-rich [418, 211]. Inward-migrating gas giants can shepherd material interior to their orbits and trigger the formation of very water-rich terrestrial planets [424, 296].

A number of lines of evidence point to the terrestrial planets having formed from ~Mars-mass planetary embryos [337]. This is below the mass threshold for large-scale migration [491], and so we do not think that Earth accreted any water from inward-migrating embryos.

However, migration may prove a central water delivery mechanism in other systems (see below).

Extrapolation to exoplanets

Let us now very simply extrapolate these six water delivery (or water production) mechanisms to exoplanet systems. Most of these mechanisms can account for Earth's water budget with perhaps an order of magnitude variation.

We propose that the water contents of rocky planets are likely to have a bimodal distribution. Migration is the key player. If embryos grew large enough and underwent long-range migration then they must invariably pollute the terrestrial planet-forming region [212]. This should lead to elevated water contents of $\sim 10\%$ by mass. However, if migration was not involved, then the other mechanisms discussed can still deliver an Earth-like or higher water budget. Gas giants are rare enough around Sun-like and low-mass stars that they probably do not play the central role in water delivery in general terms (although they likely dominate in their own systems). Pebble snow can in principle deliver tens to hundreds of oceans, but requires a clear path between the outward-sweeping icy pebble front and the rocky planet zone that is unencumbered by pressure bumps, including those produced by growing planets (which are themselves growing by consuming icy pebbles).

If migration is indeed the key, then one might predict an observational marker between the action of migration and the planets' water and other volatile contents. Such an observational test is beyond current capabilities but may be imaginable in the coming decade or two.

4 The future of planet formation studies

We conclude this broad-sweeping review with our vision for the future of planet formation. We cannot pretend to have a coherent view of all of the theoretical and empirical challenges that will push the field forward. Nonetheless, we proceed by highlighting three action items: a key bottleneck for planet formation models, one particularly promising path forward, and a call for connection.

A key bottleneck for planet formation

We consider the central bottleneck in planet formation to be understanding the underlying structure of protoplanetary disks (see Section 2.1 and discussion in [339]). Disks are the birthplace of planets. Their underlying structure controls how dust grows and drifts, where dust or pebbles pile up to become sufficiently concentrated to form planetesimals, as well as how fast and in what direction planets migrate. Simple viscous disk models do not match observations and have been supplanted by models that include effects such as ambipolar diffusion and wind-driven angular momentum loss. ALMA observations of disks [16] provide ever more stringent constraints on such models, yet to date there is no underlying model that matches the population of disk observations. Of course, interactions with other stars during the embedded cluster phase leads to a diversity of disk properties but with statistically described distributions [39]. We encourage future work to develop comprehensive, trustworthy disk models.

Coupling dynamical and chemical models

One key path forward for understanding the early evolution of the Solar System is coupling dynamical and accretion models with cosmochemical constraints. Some constraints are already being used by current models. For example, the D/H ratio – especially when combined with the $^{15/14}\text{N}$ ratio [306, 305] – appears to be a powerful tracer of Earth’s water. Isotope systems such as Hf/W already provide strong constraints on the timing of planetary accretion. Some formation models also incorporate simple chemical models [441]. Yet there remain many connections to be made between dynamical models and cosmochemistry.

A call to connect different constraints and models

We conclude this chapter with a call to create as many connections as possible. This is a large variety of disciplines linked together to create the field of planet formation. These include observations of protoplanetary disks and debris disks, exoplanet studies, meteorite analysis, planetary surfaces (e.g., crater modeling), orbital dynamics, gasdynamics, small body studies, and a variety of different types of numerical modeling. We encourage the reader to strive to make connections between their specialty and others. Many of the most interesting dynamical models come from connections between subdisciplines. For example, the idea of the Solar System’s instability (the *Nice model* [479, 167, 361]) was born from a dynamical model to explain the now-defunct terminal lunar cataclysm. The *Grand Tack* model of Solar System formation [488] was inspired by numerical studies of planet migration designed to explain the origin of hot Jupiters [275]. Giant exoplanets orbiting stars with wide companions have more eccentric orbits than giant exoplanets around single stars; this is a result of Oort cloud comet-like oscillations in the orbits of wide binary stars [232].

Connecting the dots in new ways is essential to moving the field of planet formation forward.

Acknowledgements We are grateful to the Agence Nationale pour la Recherche, who sponsored our research from 2014-2018 (project *MOJO*). We encourage the interested reader to check out the *MOJO* videos, which we made to explain some key concepts in planet formation as well as results from the project. The videos are (poetically) introduced at this URL: <https://wp.me/p3BSYQ-1Ys>.

References

1. Abod, C.P., Simon, J.B., Li, R., Armitage, P.J., Youdin, A.N., Kretke, K.A.: The Mass and Size Distribution of Planetesimals Formed by the Streaming Instability. II. The Effect of the Radial Gas Pressure Gradient. *Astrophysical Journal* **883**(2), 192 (2019). DOI 10.3847/1538-4357/ab40a3
2. Absil, O., Defrère, D., Coudé du Foresto, V., Di Folco, E., Mérand, A., Augereau, J.C., Ertel, S., Hanot, C., Kervella, P., Mollier, B., Scott, N., Che, X., Monnier, J.D., Thureau, N., Tuthill, P.G., ten Brummelaar, T.A., McAlister, H.A., Sturmman, J., Sturmman, L., Turner, N.: A near-infrared interferometric survey of debris-disc stars. III. First statistics based on 42 stars observed with CHARA/FLUOR. *Astronomy & Astrophysics* **555**, A104 (2013). DOI 10.1051/0004-6361/201321673
3. Adams, E.R., Seager, S., Elkins-Tanton, L.: Ocean Planet or Thick Atmosphere: On the Mass-Radius Relationship for Solid Exoplanets with Massive Atmospheres. *Astrophysical Journal* **673**, 1160–1164 (2008). DOI 10.1086/524925
4. Adams, F.C., Hollenbach, D., Laughlin, G., Gorti, U.: Photoevaporation of Circumstellar Disks Due to External Far-Ultraviolet Radiation in Stellar Aggregates. *Astrophysical Journal* **611**, 360–379 (2004). DOI 10.1086/421989
5. Adams, F.C., Laughlin, G.: Migration and dynamical relaxation in crowded systems of giant planets. *Icarus* **163**, 290–306 (2003). DOI 10.1016/S0019-1035(03)00081-2
6. Agnor, C.B., Canup, R.M., Levison, H.F.: On the Character and Consequences of Large Impacts in the Late Stage of Terrestrial Planet Formation. *Icarus* **142**, 219–237 (1999). DOI 10.1006/icar.1999.6201
7. Alexander, C.M.O.: Quantitative models for the elemental and isotopic fractionations in chondrites: The carbonaceous chondrites. *Geochemica and Cosmochemica Acta* **254**, 277–309 (2019). DOI 10.1016/j.gca.2019.02.008
8. Alexander, C.M.O.: Quantitative models for the elemental and isotopic fractionations in the chondrites: The non-carbonaceous chondrites. *Geochemica and Cosmochemica Acta* **254**, 246–276 (2019). DOI 10.1016/j.gca.2019.01.026
9. Alexander, C.M.O., Bowden, R., Fogel, M.L., Howard, K.T., Herd, C.D.K., Nittler, L.R.: The Provenances of Asteroids, and Their Contributions to the Volatile Inventories of the Terrestrial Planets. *Science* **337**, 721 (2012). DOI 10.1126/science.1223474
10. Alexander, C.M.O., McKeegan, K.D., Altwegg, K.: Water Reservoirs in Small Planetary Bodies: Meteorites, Asteroids, and Comets. *Space Science Reviews* **214**, 36 (2018). DOI 10.1007/s11214-018-0474-9
11. Alexander, R., Pascucci, I., Andrews, S., Armitage, P., Cieza, L.: The Dispersal of Protoplanetary Disks. *Protostars and Planets VI* pp. 475–496 (2014)
12. Alexander, R.D., Armitage, P.J.: The Stellar Mass-Accretion Rate Relation in T Tauri Stars and Brown Dwarfs. *Astrophysical Journal Letters* **639**, L83–L86 (2006). DOI 10.1086/503030
13. Alexander, R.D., Pascucci, I.: Deserts and pile-ups in the distribution of exoplanets due to photoevaporative disc clearing. *Monthly Notices of the Royal Astronomical Society* **422**, L82–L86 (2012). DOI 10.1111/j.1745-3933.2012.01243.x
14. ALMA Partnership, Brogan, C.L., Pérez, L.M., Hunter, T.R., Dent, W.R.F., Hales, A.S., Hills, R.E., Corder, S., Fomalont, E.B., Vlahakis, C., Asaki, Y., Barkats, D., Hirota, A., Hodge, J.A., Impellizzeri, C.M.V., Kneissl, R., Liuzzo, E., Lucas, R., Marcelino, N., Matsushita, S., Nakanishi, K., Phillips, N., Richards, A.M.S., Toledo, I., Aladro, R., Brogiere, D., Cortes, J.R., Cortes, P.C., Espada, D., Galarza, F., Garcia-Appadoo, D., Guzman-Ramirez, L., Humphreys, E.M., Jung, T., Kamenoi, S., Laing, R.A., Leon, S., Marconi, G., Mignano, A., Nikolic, B., Nyman, L.A., Radiszcz, M., Remijan, A., Rodón, J.A., Sawada, T., Takahashi, S., Tilanus, R.P.J., Vila Vilaro, B., Watson, L.C., Wiklind, T., Akiyama, E., Chapillon, E., de Gregorio-Monsalvo, I., Di Francesco, J., Gueth, F., Kawamura, A., Lee, C.F., Nguyen Luong, Q., Mangum, J., Pietu, V., Sanhueza, P., Saigo, K., Takakuwa, S., Ubach, C., van Kempen, T., Wootten, A., Castro-Carrizo, A., Francke, H., Gallardo, J., Garcia, J., Gonzalez, S., Hill, T., Kaminski, T., Kurono, Y., Liu, H.Y., Lopez, C., Morales, F., Plarre, K., Schieven, G., Testi,

- L., Videla, L., Villard, E., Andreani, P., Hibbard, J.E., Tatematsu, K.: The 2014 ALMA Long Baseline Campaign: First Results from High Angular Resolution Observations toward the HL Tau Region. *Astrophysical Journal Letters* **808**, L3 (2015). DOI 10.1088/2041-8205/808/1/L3
15. Amelin, Y., Krot, A.N., Hutcheon, I.D., Ulyanov, A.A.: Lead Isotopic Ages of Chondrules and Calcium-Aluminum-Rich Inclusions. *Science* **297**(5587), 1678–1683 (2002). DOI 10.1126/science.1073950
 16. Andrews, S.M., Huang, J., Pérez, L.M., Isella, A., Dullemond, C.P., Kurtovic, N.T., Guzmán, V.V., Carpenter, J.M., Wilner, D.J., Zhang, S., Zhu, Z., Birnstiel, T., Bai, X.N., Benisty, M., Hughes, A.M., Öberg, K.I., Ricci, L.: The Disk Substructures at High Angular Resolution Project (DSHARP). I. Motivation, Sample, Calibration, and Overview. *Astrophysical Journal Letters* **869**(2), L41 (2018). DOI 10.3847/2041-8213/aaf741
 17. Andrews, S.M., Williams, J.P.: Circumstellar Dust Disks in Taurus-Auriga: The Submillimeter Perspective. *Astrophysical Journal* **631**, 1134–1160 (2005). DOI 10.1086/432712
 18. Andrews, S.M., Williams, J.P.: A Submillimeter View of Circumstellar Dust Disks in ρ Ophiuchi. *Astrophysical Journal* **671**, 1800–1812 (2007). DOI 10.1086/522885
 19. Andrews, S.M., Williams, J.P.: High-Resolution Submillimeter Constraints on Circumstellar Disk Structure. *Astrophysical Journal* **659**, 705–728 (2007). DOI 10.1086/511741
 20. Andrews, S.M., Wilner, D.J., Hughes, A.M., Qi, C., Dullemond, C.P.: Protoplanetary Disk Structures in Ophiuchus. *Astrophysical Journal* **700**, 1502–1523 (2009). DOI 10.1088/0004-637X/700/2/1502
 21. Andrews, S.M., Wilner, D.J., Hughes, A.M., Qi, C., Dullemond, C.P.: Protoplanetary Disk Structures in Ophiuchus. II. Extension to Fainter Sources. *Astrophysical Journal* **723**, 1241–1254 (2010). DOI 10.1088/0004-637X/723/2/1241
 22. Andrews, S.M., Wilner, D.J., Zhu, Z., Birnstiel, T., Carpenter, J.M., Pérez, L.M., Bai, X.N., Öberg, K.I., Hughes, A.M., Isella, A., Ricci, L.: Ringed Substructure and a Gap at 1 au in the Nearest Protoplanetary Disk. *Astrophysical Journal Letters* **820**, L40 (2016). DOI 10.3847/2041-8205/820/2/L40
 23. Anglada-Escudé, G., López-Morales, M., Chambers, J.E.: How Eccentric Orbital Solutions Can Hide Planetary Systems in 2:1 Resonant Orbits. *Astrophysical Journal* **709**(1), 168–178 (2010). DOI 10.1088/0004-637X/709/1/168
 24. Anglada-Escudé, G., Tuomi, M., Gerlach, E., Barnes, R., Heller, R., Jenkins, J.S., Wende, S., Vogt, S.S., Butler, R.P., Reiners, A., Jones, H.R.A.: A dynamically-packed planetary system around GJ 667C with three super-Earths in its habitable zone. *Astronomy & Astrophysics* **556**, A126 (2013). DOI 10.1051/0004-6361/201321331
 25. Armitage, P.J.: Dynamics of Protoplanetary Disks. *Annual Reviews of Astronomy and Astrophysics* **49**, 195–236 (2011). DOI 10.1146/annurev-astro-081710-102521
 26. Armitage, P.J., Eisner, J.A., Simon, J.B.: Prompt Planetesimal Formation beyond the Snow Line. *Astrophysical Journal Letters* **828**, L2 (2016). DOI 10.3847/2041-8205/828/1/L2
 27. Asaduzzaman, A.M., Zega, T.J., Laref, S., Runge, K., Deymier, P.A., Muralidharan, K.: A computational investigation of adsorption of organics on mineral surfaces: Implications for organics delivery in the early solar system. *Earth and Planetary Science Letters* **408**, 355–361 (2014). DOI 10.1016/j.epsl.2014.10.029
 28. Badro, J., Cote, A., Brodholt, J.: A seismologically consistent compositional model of Earth's core. *PNAS* **132**, 94 (2014)
 29. Bae, J., Zhu, Z., Baruteau, C., Benisty, M., Dullemond, C.P., Facchini, S., Isella, A., Keppler, M., Pérez, L.M., Teague, R.: An Ideal Testbed for Planet-Disk Interaction: Two Giant Protoplanets in Resonance Shaping the PDS 70 Protoplanetary Disk. *Astrophysical Journal Letters* **884**(2), L41 (2019). DOI 10.3847/2041-8213/ab46b0
 30. Bai, X.N.: Towards a Global Evolutionary Model of Protoplanetary Disks. *Astrophysical Journal* **821**, 80 (2016). DOI 10.3847/0004-637X/821/2/80
 31. Bai, X.N.: Global Simulations of the Inner Regions of Protoplanetary Disks with Comprehensive Disk Microphysics. *Astrophysical Journal* **845**(1), 75 (2017). DOI 10.3847/1538-4357/aa7dda

32. Bai, X.N., Stone, J.M.: Wind-driven Accretion in Protoplanetary Disks. I. Suppression of the Magnetorotational Instability and Launching of the Magnetocentrifugal Wind. *Astrophysical Journal* **769**(1), 76 (2013). DOI 10.1088/0004-637X/769/1/76
33. Baillié, K., Charnoz, S., Pantin, E.: Time evolution of snow regions and planet traps in an evolving protoplanetary disk. *Astronomy & Astrophysics* **577**, A65 (2015). DOI 10.1051/0004-6361/201424987
34. Balbus, S.A., Hawley, J.F.: Instability, turbulence, and enhanced transport in accretion disks. *Reviews of Modern Physics* **70**, 1–53 (1998). DOI 10.1103/RevModPhys.70.1
35. Barbato, D., Sozzetti, A., Desidera, S., Damasso, M., Bonomo, A.S., Giacobbe, P., Colombo, L.S., Lazzoni, C., Claudi, R., Gratton, R., LoCurto, G., Marzari, F., Mordasini, C.: Exploring the realm of scaled solar system analogues with HARPS. *Astronomy & Astrophysics* **615**, A175 (2018). DOI 10.1051/0004-6361/201832791
36. Barenfeld, S.A., Carpenter, J.M., Sargent, A.I., Isella, A., Ricci, L.: Measurement of Circumstellar Disk Sizes in the Upper Scorpius OB Association with ALMA. *Astrophysical Journal* **851**(2), 85 (2017). DOI 10.3847/1538-4357/aa989d
37. Baruteau, C., Meru, F., Paardekooper, S.J.: Rapid inward migration of planets formed by gravitational instability. *Monthly Notices of the Royal Astronomical Society* **416**(3), 1971–1982 (2011). DOI 10.1111/j.1365-2966.2011.19172.x
38. Batalha, N.M., Rowe, J.F., Bryson, S.T., Barclay, T., Burke, C.J., Caldwell, D.A., Christiansen, J.L., Mullally, F., Thompson, S.E., Brown, T.M., Dupree, A.K., Fabrycky, D.C., Ford, E.B., Fortney, J.J., Gilliland, R.L., Isaacson, H., Latham, D.W., Marcy, G.W., Quinn, S.N., Ragozzine, D., Shporer, A., Borucki, W.J., Ciardi, D.R., Gautier III, T.N., Haas, M.R., Jenkins, J.M., Koch, D.G., Lissauer, J.J., Rapin, W., Basri, G.S., Boss, A.P., Buchhave, L.A., Carter, J.A., Charbonneau, D., Christensen-Dalsgaard, J., Clarke, B.D., Cochran, W.D., Demory, B.O., Desert, J.M., Devore, E., Doyle, L.R., Esquerdo, G.A., Everett, M., Fressin, F., Geary, J.C., Girouard, F.R., Gould, A., Hall, J.R., Holman, M.J., Howard, A.W., Howell, S.B., Ibrahim, K.A., Kinemuchi, K., Kjeldsen, H., Klaus, T.C., Li, J., Lucas, P.W., Meibom, S., Morris, R.L., Prša, A., Quintana, E., Sanderfer, D.T., Sasselov, D., Seader, S.E., Smith, J.C., Steffen, J.H., Still, M., Stumpe, M.C., Tarter, J.C., Tenenbaum, P., Torres, G., Twicken, J.D., Uddin, K., Van Cleve, J., Walkowicz, L., Welsh, W.F.: Planetary Candidates Observed by Kepler. III. Analysis of the First 16 Months of Data. *Astrophysical Journal Supplement Series* **204**, 24 (2013). DOI 10.1088/0067-0049/204/2/24
39. Bate, M.R.: On the diversity and statistical properties of protostellar discs. *Monthly Notices of the Royal Astronomical Society* **475**, 5618–5658 (2018). DOI 10.1093/mnras/sty169
40. Batygin, K., Morbidelli, A.: Analytical treatment of planetary resonances. *Astronomy & Astrophysics* **556**, A28 (2013). DOI 10.1051/0004-6361/201220907
41. Batygin, K., Morbidelli, A., Holman, M.J.: Chaotic Disintegration of the Inner Solar System. *Astrophysical Journal* **799**, 120 (2015). DOI 10.1088/0004-637X/799/2/120
42. Beaugé, C., Nesvorný, D.: Multiple-planet Scattering and the Origin of Hot Jupiters. *Astrophysical Journal* **751**, 119 (2012). DOI 10.1088/0004-637X/751/2/119
43. Bell, K.R., Lin, D.N.C.: Using FU Orionis Outbursts to Constrain Self-regulated Protostellar Disk Models. *Astrophysical Journal* **427**, 987 (1994). DOI 10.1086/174206
44. Benítez-Llambay, P., Masset, F., Koenigsberger, G., Szulágyi, J.: Planet heating prevents inward migration of planetary cores. *Nature* **520**, 63–65 (2015). DOI 10.1038/nature14277
45. Benítez-Llambay, P., Pessah, M.E.: Torques Induced by Scattered Pebble-flow in Protoplanetary Disks. *Astrophysical Journal Letters* **855**(2), L28 (2018). DOI 10.3847/2041-8213/aab2ae
46. Béthune, W., Lesur, G., Ferreira, J.: Global simulations of protoplanetary disks with net magnetic flux. I. Non-ideal MHD case. *Astronomy & Astrophysics* **600**, A75 (2017). DOI 10.1051/0004-6361/201630056
47. Birnstiel, T., Fang, M., Johansen, A.: Dust Evolution and the Formation of Planetesimals. *Space Science Reviews* **205**, 41–75 (2016). DOI 10.1007/s11214-016-0256-1
48. Birnstiel, T., Klahr, H., Ercolano, B.: A simple model for the evolution of the dust population in protoplanetary disks. *Astronomy & Astrophysics* **539**, A148 (2012). DOI 10.1051/0004-6361/201118136

49. Bitsch, B., Crida, A., Morbidelli, A., Kley, W., Dobbs-Dixon, I.: Stellar irradiated discs and implications on migration of embedded planets. I. Equilibrium discs. *Astronomy & Astrophysics* **549**, A124 (2013). DOI 10.1051/0004-6361/201220159
50. Bitsch, B., Izidoro, A., Johansen, A., Raymond, S.N., Morbidelli, A., Lambrechts, M., Jacobson, S.A.: Formation of planetary systems by pebble accretion and migration: growth of gas giants. *Astronomy & Astrophysics* **623**, A88 (2019). DOI 10.1051/0004-6361/201834489
51. Bitsch, B., Johansen, A., Lambrechts, M., Morbidelli, A.: The structure of protoplanetary discs around evolving young stars. *Astronomy & Astrophysics* **575**, A28 (2015). DOI 10.1051/0004-6361/201424964
52. Bitsch, B., Lambrechts, M., Johansen, A.: The growth of planets by pebble accretion in evolving protoplanetary discs. *Astronomy & Astrophysics* **582**, A112 (2015). DOI 10.1051/0004-6361/201526463
53. Bitsch, B., Morbidelli, A., Johansen, A., Lega, E., Lambrechts, M., Crida, A.: Pebble-isolation mass: Scaling law and implications for the formation of super-Earths and gas giants. *Astronomy & Astrophysics* **612**, A30 (2018). DOI 10.1051/0004-6361/201731931
54. Bitsch, B., Morbidelli, A., Lega, E., Crida, A.: Stellar irradiated discs and implications on migration of embedded planets. II. Accreting-discs. *Astronomy & Astrophysics* **564**, A135 (2014). DOI 10.1051/0004-6361/201323007
55. Bitsch, B., Raymond, S.N., Izidoro, A.: Rocky super-Earths or waterworlds: the interplay of planet migration, pebble accretion, and disc evolution. *Astronomy & Astrophysics* **624**, A109 (2019). DOI 10.1051/0004-6361/201935007
56. Biver, N., Moreno, R., Bockelée-Morvan, D., Sandqvist, A., Colom, P., Crovisier, J., Lis, D.C., Boissier, J., Debout, V., Paubert, G., Milam, S., Hjalmarson, A., Lundin, S., Karlsson, T., Battelino, M., Frisk, U., Murtagh, D., Odin Team: Isotopic ratios of H, C, N, O, and S in comets C/2012 F6 (Lemmon) and C/2014 Q2 (Lovejoy). *Astronomy & Astrophysics* **589**, A78 (2016). DOI 10.1051/0004-6361/201528041
57. Blum, J., Wurm, G.: The Growth Mechanisms of Macroscopic Bodies in Protoplanetary Disks. *Annual Reviews of Astronomy and Astrophysics* **46**, 21–56 (2008). DOI 10.1146/annurev.astro.46.060407.145152
58. Boehnke, P., Harrison, T.M.: Illusory Late Heavy Bombardments. *Proceedings of the National Academy of Science* **113**, 10802–10806 (2016). DOI 10.1073/pnas.1611535113
59. Boisvert, J.H., Nelson, B.E., Steffen, J.H.: Systematic mischaracterization of exoplanetary system dynamical histories from a model degeneracy near mean-motion resonance. *Monthly Notices of the Royal Astronomical Society* **480**, 2846–2852 (2018). DOI 10.1093/mnras/sty2023
60. Boley, A.C.: The Two Modes of Gas Giant Planet Formation. *Astrophysical Journal Letters* **695**(1), L53–L57 (2009). DOI 10.1088/0004-637X/695/1/L53
61. Boley, A.C., Ford, E.B.: The Formation of Systems with Tightly-packed Inner Planets (STIPs) via Aerodynamic Drift. arXiv:1306.0566 (2013)
62. Boley, A.C., Hayfield, T., Mayer, L., Durisen, R.H.: Clumps in the outer disk by disk instability: Why they are initially gas giants and the legacy of disruption. *Icarus* **207**(2), 509–516 (2010). DOI 10.1016/j.icarus.2010.01.015
63. Bonomo, A.S., Desidera, S., Benatti, S., Borsa, F., Crespi, S., Damasso, M., Lanza, A.F., Sozzetti, A., Lodato, G., Marzari, F., Boccato, C., Claudi, R.U., Cosentino, R., Covino, E., Gratton, R., Maggio, A., Micela, G., Molinari, E., Pagano, I., Piotto, G., Poretti, E., Smareglia, R., Affer, L., Biazzo, K., Bignamini, A., Esposito, M., Giacobbe, P., Hébrard, G., Malavolta, L., Maldonado, J., Mancini, L., Martinez Fiorenzano, A., Masiero, S., Nascimbeni, V., Pedani, M., Rainer, M., Scandariato, G.: The GAPS Programme with HARPS-N at TNG . XIV. Investigating giant planet migration history via improved eccentricity and mass determination for 231 transiting planets. *Astronomy & Astrophysics* **602**, A107 (2017). DOI 10.1051/0004-6361/201629882
64. Boss, A.P.: Giant planet formation by gravitational instability. *Science* **276**, 1836–1839 (1997). DOI 10.1126/science.276.5320.1836
65. Boss, A.P.: Evolution of the Solar Nebula. IV. Giant Gaseous Protoplanet Formation. *Astrophysical Journal* **503**(2), 923–937 (1998). DOI 10.1086/306036

66. Boss, A.P.: Possible Rapid Gas Giant Planet Formation in the Solar Nebula and Other Protoplanetary Disks. *Astrophysical Journal Letters* **536**(2), L101–L104 (2000). DOI 10.1086/312737
67. Bouvier, A., Wadhwa, M.: The age of the Solar System redefined by the oldest Pb–Pb age of a meteoritic inclusion. *Nature Geoscience* **3**, 637–641 (2010). DOI 10.1038/ngeo941
68. Bowler, B.P., Nielsen, E.L.: Occurrence Rates from Direct Imaging Surveys. ArXiv e-prints (2018)
69. Brasser, R., Matsumura, S., Ida, S., Mojzsis, S.J., Werner, S.C.: Analysis of Terrestrial Planet Formation by the Grand Tack Model: System Architecture and Tack Location. *Astrophysical Journal* **821**, 75 (2016). DOI 10.3847/0004-637X/821/2/75
70. Briceño, C., Vivas, A.K., Calvet, N., Hartmann, L., Pacheco, R., Herrera, D., Romero, L., Berlind, P., Sánchez, G., Snyder, J.A., Andrews, P.: The CIDA-QUEST Large-Scale Survey of Orion OB1: Evidence for Rapid Disk Dissipation in a Dispersed Stellar Population. *Science* **291**, 93–97 (2001). DOI 10.1126/science.291.5501.93
71. Bromley, B.C., Kenyon, S.J.: Terrestrial Planet Formation: Dynamical Shake-up and the Low Mass of Mars. *Astronomical Journal* **153**, 216 (2017). DOI 10.3847/1538-3881/aa6aaa
72. Bryan, M.L., Knutson, H.A., Lee, E.J., Fulton, B.J., Batygin, K., Ngo, H., Meshkat, T.: An Excess of Jupiter Analogs in Super-Earth Systems. *Astronomical Journal* **157**(2), 52 (2019). DOI 10.3847/1538-3881/aaf57f
73. Bryden, G., Beichman, C.A., Carpenter, J.M., Rieke, G.H., Stapelfeldt, K.R., Werner, M.W., Tanner, A.M., Lawler, S.M., Wyatt, M.C., Trilling, D.E., Su, K.Y.L., Blaylock, M., Stansberry, J.A.: Planets and Debris Disks: Results from a Spitzer/MIPS Search for Infrared Excess. *Astrophysical Journal* **705**(2), 1226–1236 (2009). DOI 10.1088/0004-637X/705/2/1226
74. Bryden, G., Beichman, C.A., Trilling, D.E., Rieke, G.H., Holmes, E.K., Lawler, S.M., Stapelfeldt, K.R., Werner, M.W., Gautier, T.N., Blaylock, M., Gordon, K.D., Stansberry, J.A., Su, K.Y.L.: Frequency of Debris Disks around Solar-Type Stars: First Results from a Spitzer MIPS Survey. *Astrophysical Journal* **636**, 1098–1113 (2006). DOI 10.1086/498093
75. Budde, G., Burkhardt, C., Brenneka, G.A., Fischer-Gödde, M., Kruijer, T.S., Kleine, T.: Molybdenum isotopic evidence for the origin of chondrules and a distinct genetic heritage of carbonaceous and non-carbonaceous meteorites. *Earth and Planetary Science Letters* **454**, 293–303 (2016). DOI 10.1016/j.epsl.2016.09.020
76. Budde, G., Burkhardt, C., Kleine, T.: Molybdenum isotopic evidence for the late accretion of outer Solar System material to Earth. *Nature Astronomy* **3**, 736–741 (2019). DOI 10.1038/s41550-019-0779-y
77. Butler, R.P., Wright, J.T., Marcy, G.W., Fischer, D.A., Vogt, S.S., Tinney, C.G., Jones, H.R.A., Carter, B.D., Johnson, J.A., McCarthy, C., Penny, A.J.: Catalog of Nearby Exoplanets. *Astrophysical Journal* **646**, 505–522 (2006). DOI 10.1086/504701
78. Caracausi, A., Avice, G., Burnard, P.G., Füre, E., Marty, B.: Chondritic xenon in the Earth’s mantle. *Nature* **533**, 82–85 (2016). DOI 10.1038/nature17434
79. Carpenter, J.M., Bouwman, J., Mamajek, E.E., Meyer, M.R., Hillenbrand, L.A., Backman, D.E., Henning, T., Hines, D.C., Hollenbach, D., Kim, J.S., Moro-Martin, A., Pascucci, I., Silverstone, M.D., Stauffer, J.R., Wolf, S.: Formation and Evolution of Planetary Systems: Properties of Debris Dust Around Solar-Type Stars. *Astrophysical Journal Supplement Series* **181**, 197–226 (2009). DOI 10.1088/0067-0049/181/1/197
80. Carrera, D., Davies, M.B., Johansen, A.: Survival of habitable planets in unstable planetary systems. *Monthly Notices of the Royal Astronomical Society* **463**, 3226–3238 (2016). DOI 10.1093/mnras/stw2218
81. Carrera, D., Ford, E.B., Izidoro, A., Jontof-Hutter, D., Raymond, S.N., Wolfgang, A.: Identifying Inflated Super-Earths and Photo-evaporated Cores. *Astrophysical Journal* **866**, 104 (2018). DOI 10.3847/1538-4357/aadf8a
82. Carrera, D., Gorti, U., Johansen, A., Davies, M.B.: Planetesimal Formation by the Streaming Instability in a Photoevaporating Disk. *Astrophysical Journal* **839**, 16 (2017). DOI 10.3847/1538-4357/aa6932

83. Carrera, D., Johansen, A., Davies, M.B.: How to form planetesimals from mm-sized chondrules and chondrule aggregates. *Astronomy & Astrophysics* **579**, A43 (2015). DOI 10.1051/0004-6361/201425120
84. Carrera, D., Raymond, S.N., Davies, M.B.: Planet-planet scattering as the source of the highest eccentricity exoplanets. *Astronomy & Astrophysics* **629**, L7 (2019). DOI 10.1051/0004-6361/201935744
85. Cassan, A., Kubas, D., Beaulieu, J.P., Dominik, M., Horne, K., Greenhill, J., Wambsgans, J., Menzies, J., Williams, A., Jørgensen, U.G., Udalski, A., Bennett, D.P., Albrow, M.D., Batista, V., Brilliant, S., Caldwell, J.A.R., Cole, A., Coutures, C., Cook, K.H., Dieters, S., Dominis Prester, D., Donatowicz, J., Fouqué, P., Hill, K., Kains, N., Kane, S., Marquette, J.B., Martin, R., Pollard, K.R., Sahu, K.C., Vinter, C., Warren, D., Watson, B., Zub, M., Sumi, T., Szymański, M.K., Kubiak, M., Poleski, R., Soszynski, I., Ulaczyk, K., Pietrzyński, G., Wyrzykowski, Ł.: One or more bound planets per Milky Way star from microlensing observations. *Nature* **481**, 167–169 (2012). DOI 10.1038/nature10684
86. Chambers, J.: A semi-analytic model for oligarchic growth. *Icarus* **180**, 496–513 (2006). DOI 10.1016/j.icarus.2005.10.017
87. Chambers, J.: An Analytic Model for an Evolving Protoplanetary Disk with a Disk Wind. *Astrophysical Journal* **879**(2), 98 (2019). DOI 10.3847/1538-4357/ab2537
88. Chambers, J.E.: Making More Terrestrial Planets. *Icarus* **152**, 205–224 (2001). DOI 10.1006/icar.2001.6639
89. Chambers, J.E., Wetherill, G.W.: Making the Terrestrial Planets: N-Body Integrations of Planetary Embryos in Three Dimensions. *Icarus* **136**, 304–327 (1998). DOI 10.1006/icar.1998.6007
90. Chambers, K.C., Magnier, E.A., Metcalfe, N., Flewelling, H.A., Huber, M.E., Waters, C.Z., Denneau, L., Draper, P.W., Farrow, D., Finkbeiner, D.P., Holmberg, C., Koppenhoefer, J., Price, P.A., Saglia, R.P., Schlafly, E.F., Smartt, S.J., Sweeney, W., Wainscoat, R.J., Burgett, W.S., Grav, T., Heasley, J.N., Hodapp, K.W., Jedicke, R., Kaiser, N., Kudritzki, R.P., Luppino, G.A., Lupton, R.H., Monet, D.G., Morgan, J.S., Onaka, P.M., Stubbs, C.W., Tonry, J.L., Banados, E., Bell, E.F., Bender, R., Bernard, E.J., Botticella, M.T., Casertano, S., Chastel, S., Chen, W.P., Chen, X., Cole, S., Deacon, N., Frenk, C., Fitzsimmons, A., Gezari, S., Goessl, C., Goggia, T., Goldman, B., Grebel, E.K., Hambly, N.C., Hasinger, G., Heavens, A.F., Heckman, T.M., Henderson, R., Henning, T., Holman, M., Hopp, U., Ip, W.H., Isani, S., Keyes, C.D., Koekemoer, A., Kotak, R., Long, K.S., Lucey, J.R., Liu, M., Martin, N.F., McLean, B., Morganson, E., Murphy, D.N.A., Nieto-Santisteban, M.A., Norberg, P., Peacock, J.A., Pier, E.A., Postman, M., Primak, N., Rae, C., Rest, A., Riess, A., Riffeser, A., Rix, H.W., Roser, S., Schilbach, E., Schultz, A.S.B., Scolnic, D., Szalay, A., Seitz, S., Shiao, B., Small, E., Smith, K.W., Soderblom, D., Taylor, A.N., Thakar, A.R., Thiel, J., Thilker, D., Urata, Y., Valenti, J., Walter, F., Watters, S.P., Werner, S., White, R., Wood-Vasey, W.M., Wyse, R.: The Pan-STARRS1 Surveys. arxiv:1612.05560 (2016)
91. Chandrasekhar, S.: Dynamical Friction. I. General Considerations: the Coefficient of Dynamical Friction. *Astrophysical Journal* **97**, 255 (1943). DOI 10.1086/144517
92. Chang, S.H., Gu, P.G., Bodenheimer, P.H.: Tidal and Magnetic Interactions Between a Hot Jupiter and its Host Star in the Magnetospheric Cavity of a Protoplanetary Disk. *Astrophysical Journal* **708**(2), 1692–1702 (2010). DOI 10.1088/0004-637X/708/2/1692
93. Chapman, C.R., Cohen, B.A., Grinspoon, D.H.: What are the real constraints on the existence and magnitude of the late heavy bombardment? *Icarus* **189**, 233–245 (2007). DOI 10.1016/j.icarus.2006.12.020
94. Chatterjee, S., Ford, E.B., Matsumura, S., Rasio, F.A.: Dynamical Outcomes of Planet-Planet Scattering. *Astrophysical Journal* **686**, 580–602 (2008). DOI 10.1086/590227
95. Chatterjee, S., Tan, J.C.: Inside-out Planet Formation. *Astrophysical Journal* **780**, 53 (2014). DOI 10.1088/0004-637X/780/1/53
96. Chatterjee, S., Tan, J.C.: Vulcan Planets: Inside-out Formation of the Innermost Super-Earths. *Astrophysical Journal Letters* **798**, L32 (2015). DOI 10.1088/2041-8205/798/2/L32
97. Chen, J., Kipping, D.: Probabilistic Forecasting of the Masses and Radii of Other Worlds. *Astrophysical Journal* **834**, 17 (2017). DOI 10.3847/1538-4357/834/1/17

98. Chiang, E., Laughlin, G.: The minimum-mass extrasolar nebula: in situ formation of close-in super-Earths. *Monthly Notices of the Royal Astronomical Society* **431**, 3444–3455 (2013). DOI 10.1093/mnras/stt424
99. Chiang, E., Youdin, A.N.: Forming Planetesimals in Solar and Extrasolar Nebulae. *Annual Review of Earth and Planetary Sciences* **38**, 493–522 (2010). DOI 10.1146/annurev-earth-040809-152513
100. Chiang, E.I., Goldreich, P.: Spectral Energy Distributions of T Tauri Stars with Passive Circumstellar Disks. *Astrophysical Journal* **490**, 368 (1997). DOI 10.1086/304869
101. Clanton, C., Gaudi, B.S.: Synthesizing Exoplanet Demographics from Radial Velocity and Microlensing Surveys. II. The Frequency of Planets Orbiting M Dwarfs. *Astrophysical Journal* **791**, 91 (2014). DOI 10.1088/0004-637X/791/2/91
102. Clanton, C., Gaudi, B.S.: Synthesizing Exoplanet Demographics: A Single Population of Long-period Planetary Companions to M Dwarfs Consistent with Microlensing, Radial Velocity, and Direct Imaging Surveys. *Astrophysical Journal* **819**, 125 (2016). DOI 10.3847/0004-637X/819/2/125
103. Clement, M.S., Kaib, N.A., Raymond, S.N., Chambers, J.E., Walsh, K.J.: The early instability scenario: Terrestrial planet formation during the giant planet instability, and the effect of collisional fragmentation. *Icarus* **321**, 778–790 (2019). DOI 10.1016/j.icarus.2018.12.033
104. Clement, M.S., Kaib, N.A., Raymond, S.N., Walsh, K.J.: Mars' growth stunted by an early giant planet instability. *Icarus* **311**, 340–356 (2018). DOI 10.1016/j.icarus.2018.04.008
105. Clement, M.S., Raymond, S.N., Kaib, N.A.: Excitation and Depletion of the Asteroid Belt in the Early Instability Scenario. *Astronomical Journal* **157**(1), 38 (2019). DOI 10.3847/1538-3881/aaf21e
106. Coleman, G.A.L., Papaloizou, J.C.B., Nelson, R.P.: In situ accretion of gaseous envelopes on to planetary cores embedded in evolving protoplanetary discs. *Monthly Notices of the Royal Astronomical Society* **470**(3), 3206–3219 (2017). DOI 10.1093/mnras/stx1297
107. Connelly, J.N., Amelin, Y., Krot, A.N., Bizzarro, M.: Chronology of the Solar System's Oldest Solids. *Astrophysical Journal Letters* **675**, L121 (2008). DOI 10.1086/533586
108. Connelly, J.N., Bizzarro, M., Krot, A.N., Nordlund, Å., Wielandt, D., Ivanova, M.A.: The Absolute Chronology and Thermal Processing of Solids in the Solar Protoplanetary Disk. *Science* **338**, 651 (2012). DOI 10.1126/science.1226919
109. Cossou, C., Raymond, S.N., Hersant, F., Pierens, A.: Hot super-Earths and giant planet cores from different migration histories. *Astronomy & Astrophysics* **569**, A56 (2014). DOI 10.1051/0004-6361/201424157
110. Cossou, C., Raymond, S.N., Pierens, A.: Convergence zones for Type I migration: an inward shift for multiple planet systems. *Astronomy & Astrophysics* **553**, L2 (2013). DOI 10.1051/0004-6361/201220853
111. Cresswell, P., Dirksen, G., Kley, W., Nelson, R.P.: On the evolution of eccentric and inclined protoplanets embedded in protoplanetary disks. *Astronomy & Astrophysics* **473**, 329–342 (2007). DOI 10.1051/0004-6361:20077666
112. Crida, A., Morbidelli, A., Masset, F.: On the width and shape of gaps in protoplanetary disks. *Icarus* **181**, 587–604 (2006). DOI 10.1016/j.icarus.2005.10.007
113. Cumming, A., Butler, R.P., Marcy, G.W., Vogt, S.S., Wright, J.T., Fischer, D.A.: The Keck Planet Search: Detectability and the Minimum Mass and Orbital Period Distribution of Extrasolar Planets. *Proceedings of the Astronomical Society of the Pacific* **120**, 531–554 (2008). DOI 10.1086/588487
114. D'Angelo, G., Kley, W., Henning, T.: Orbital Migration and Mass Accretion of Protoplanets in Three-dimensional Global Computations with Nested Grids. *Astrophysical Journal* **586**(1), 540–561 (2003). DOI 10.1086/367555
115. D'Angelo, M., Cazaux, S., Kamp, I., Thi, W.F., Woitke, P.: Water delivery in the inner solar nebula. Monte Carlo simulations of forsterite hydration. *Astronomy & Astrophysics* **622**, A208 (2019). DOI 10.1051/0004-6361/201833715
116. Dauphas, N.: The isotopic nature of the Earth's accreting material through time. *Nature* **541**, 521–524 (2017). DOI 10.1038/nature20830

117. Dauphas, N., Pourmand, A.: Hf-W-Th evidence for rapid growth of Mars and its status as a planetary embryo. *Nature* **473**, 489–492 (2011). DOI 10.1038/nature10077
118. Davis, S.S.: The Surface Density Distribution in the Solar Nebula. *Astrophysical Journal Letters* **627**, L153–L155 (2005). DOI 10.1086/432464
119. Dawson, R.I., Chiang, E., Lee, E.J.: A metallicity recipe for rocky planets. *Monthly Notices of the Royal Astronomical Society* **453**, 1471–1483 (2015). DOI 10.1093/mnras/stv1639
120. Dawson, R.I., Lee, E.J., Chiang, E.: Correlations between Compositions and Orbits Established by the Giant Impact Era of Planet Formation. *Astrophysical Journal* **822**, 54 (2016). DOI 10.3847/0004-637X/822/1/54
121. Dawson, R.I., Murray-Clay, R.A.: Giant Planets Orbiting Metal-rich Stars Show Signatures of Planet-Planet Interactions. *Astrophysical Journal Letters* **767**, L24 (2013). DOI 10.1088/2041-8205/767/2/L24
122. Deck, K.M., Batygin, K.: Migration of Two Massive Planets into (and out of) First Order Mean Motion Resonances. *Astrophysical Journal* **810**(2), 119 (2015). DOI 10.1088/0004-637X/810/2/119
123. Deienno, R., Gomes, R.S., Walsh, K.J., Morbidelli, A., Nesvorný, D.: Is the Grand Tack model compatible with the orbital distribution of main belt asteroids? *Icarus* **272**, 114–124 (2016). DOI 10.1016/j.icarus.2016.02.043
124. Deienno, R., Izidoro, A., Morbidelli, A., Gomes, R.S., Nesvorný, D., Raymond, S.N.: Excitation of a Primordial Cold Asteroid Belt as an Outcome of Planetary Instability. *Astrophysical Journal* **864**, 50 (2018). DOI 10.3847/1538-4357/aad55d
125. DeMeo, F.E., Carry, B.: The taxonomic distribution of asteroids from multi-filter all-sky photometric surveys. *Icarus* **226**, 723–741 (2013). DOI 10.1016/j.icarus.2013.06.027
126. DeMeo, F.E., Carry, B.: Solar System evolution from compositional mapping of the asteroid belt. *Nature* **505**, 629–634 (2014). DOI 10.1038/nature12908
127. Demory, B.O., Gillon, M., Deming, D., Valencia, D., Seager, S., Benneke, B., Lovis, C., Cubillos, P., Harrington, J., Stevenson, K.B., Mayor, M., Pepe, F., Queloz, D., Ségransan, D., Udry, S.: Detection of a transit of the super-Earth 55 Cancri e with warm Spitzer. *Astronomy & Astrophysics* **533**, A114 (2011). DOI 10.1051/0004-6361/201117178
128. Desch, S.J., Turner, N.J.: High-temperature Ionization in Protoplanetary Disks. *Astrophysical Journal* **811**(2), 156 (2015). DOI 10.1088/0004-637X/811/2/156
129. Dodson-Robinson, S.E., Salyk, C.: Transitional Disks as Signposts of Young, Multiplanet Systems. *Astrophysical Journal* **738**(2), 131 (2011). DOI 10.1088/0004-637X/738/2/131
130. Dodson-Robinson, S.E., Willacy, K., Bodenheimer, P., Turner, N.J., Beichman, C.A.: Ice lines, planetesimal composition and solid surface density in the solar nebula. *Icarus* **200**(2), 672–693 (2009). DOI 10.1016/j.icarus.2008.11.023
131. Dong, S., Zhu, Z.: Fast Rise of “Neptune-size” Planets (4–8 R_{\oplus}) from $P \sim 10$ to ~ 250 Days – Statistics of Kepler Planet Candidates up to ~ 0.75 AU. *Astrophysical Journal* **778**, 53 (2013). DOI 10.1088/0004-637X/778/1/53
132. Dorn, C., Khan, A., Heng, K., Connolly, J.A.D., Alibert, Y., Benz, W., Tackley, P.: Can we constrain the interior structure of rocky exoplanets from mass and radius measurements? *Astronomy & Astrophysics* **577**, A83 (2015). DOI 10.1051/0004-6361/201424915
133. Dorn, C., Mosegaard, K., Grimm, S.L., Alibert, Y.: Interior Characterization in Multiplanetary Systems: TRAPPIST-1. *Astrophysical Journal* **865**(1), 20 (2018). DOI 10.3847/1538-4357/aad95d
134. Drażkowska, J., Alibert, Y.: Planetesimal formation starts at the snow line. *Astronomy & Astrophysics* **608**, A92 (2017). DOI 10.1051/0004-6361/201731491
135. Drażkowska, J., Alibert, Y., Moore, B.: Close-in planetesimal formation by pile-up of drifting pebbles. *Astronomy & Astrophysics* **594**, A105 (2016). DOI 10.1051/0004-6361/201628983
136. Drażkowska, J., Dullemond, C.P.: Planetesimal formation during protoplanetary disk buildup. *Astronomy & Astrophysics* **614**, A62 (2018). DOI 10.1051/0004-6361/201732221
137. Duffell, P.C., Haiman, Z., MacFadyen, A.I., D’Orazio, D.J., Farris, B.D.: The Migration of Gap-opening Planets is Not Locked to Viscous Disk Evolution. *Astrophysical Journal Letters* **792**(1), L10 (2014). DOI 10.1088/2041-8205/792/1/L10

138. Dullemond, C.P., Birnstiel, T., Huang, J., Kurtovic, N.T., Andrews, S.M., Guzmán, V.V., Pérez, L.M., Isella, A., Zhu, Z., Benisty, M., Wilner, D.J., Bai, X.N., Carpenter, J.M., Zhang, S., Ricci, L.: The Disk Substructures at High Angular Resolution Project (DSHARP). VI. Dust Trapping in Thin-ringed Protoplanetary Disks. *Astrophysical Journal Letters* **869**(2), L46 (2018). DOI 10.3847/2041-8213/aaf742
139. Dürmann, C., Kley, W.: Migration of massive planets in accreting disks. *Astronomy & Astrophysics* **574**, A52 (2015). DOI 10.1051/0004-6361/201424837
140. Eisner, J.A., Carpenter, J.M.: Distribution of Circumstellar Disk Masses in the Young Cluster NGC 2024. *Astrophysical Journal* **598**, 1341–1349 (2003). DOI 10.1086/379102
141. Eklund, H., Masset, F.S.: Evolution of eccentricity and inclination of hot protoplanets embedded in radiative discs. *Monthly Notices of the Royal Astronomical Society* **469**(1), 206–217 (2017). DOI 10.1093/mnras/stx856
142. Ertel, S., Absil, O., Defrère, D., Le Bouquin, J.B., Augereau, J.C., Marion, L., Blind, N., Bonsor, A., Bryden, G., Lebreton, J., Milli, J.: A near-infrared interferometric survey of debris-disk stars. IV. An unbiased sample of 92 southern stars observed in H band with VLTI/PIONIER. *Astronomy & Astrophysics* **570**, A128 (2014). DOI 10.1051/0004-6361/201424438
143. Fabrycky, D.C., Lissauer, J.J., Ragozzine, D., Rowe, J.F., Steffen, J.H., Agol, E., Barclay, T., Batalha, N., Borucki, W., Ciardi, D.R., Ford, E.B., Gautier, T.N., Geary, J.C., Holman, M.J., Jenkins, J.M., Li, J., Morehead, R.C., Morris, R.L., Shporer, A., Smith, J.C., Still, M., Van Cleve, J.: Architecture of Kepler’s Multi-transiting Systems. II. New Investigations with Twice as Many Candidates. *Astrophysical Journal* **790**, 146 (2014). DOI 10.1088/0004-637X/790/2/146
144. Fang, J., Margot, J.L.: Architecture of Planetary Systems Based on Kepler Data: Number of Planets and Coplanarity. *Astrophysical Journal* **761**, 92 (2012). DOI 10.1088/0004-637X/761/2/92
145. Fernandes, R.B., Mulders, G.D., Pascucci, I., Mordasini, C., Emsenhuber, A.: Hints for a Turnover at the Snow Line in the Giant Planet Occurrence Rate. *Astrophysical Journal* **874**(1), 81 (2019). DOI 10.3847/1538-4357/ab0300
146. Fischer, D.A., Marcy, G.W., Butler, R.P., Vogt, S.S., Laughlin, G., Henry, G.W., Abouav, D., Peek, K.M.G., Wright, J.T., Johnson, J.A., McCarthy, C., Isaacson, H.: Five Planets Orbiting 55 Cancri. *Astrophysical Journal* **675**, 790–801 (2008). DOI 10.1086/525512
147. Fischer, D.A., Valenti, J.: The Planet-Metallicity Correlation. *Astrophysical Journal* **622**, 1102–1117 (2005). DOI 10.1086/428383
148. Fischer, R.A., Ciesla, F.J.: Dynamics of the terrestrial planets from a large number of N-body simulations. *Earth and Planetary Science Letters* **392**, 28–38 (2014). DOI 10.1016/j.epsl.2014.02.011
149. Fischer, R.A., Nimmo, F.: Effects of core formation on the Hf-W isotopic composition of the Earth and dating of the Moon-forming impact. *Earth and Planetary Science Letters* **499**, 257–265 (2018). DOI 10.1016/j.epsl.2018.07.030
150. Flock, M., Fromang, S., Turner, N.J., Benisty, M.: 3D Radiation Nonideal Magnetohydrodynamical Simulations of the Inner Rim in Protoplanetary Disks. *Astrophysical Journal* **835**, 230 (2017). DOI 10.3847/1538-4357/835/2/230
151. Flock, M., Turner, N.J., Mulders, G.D., Hasegawa, Y., Nelson, R.P., Bitsch, B.: Planet formation and migration near the silicate sublimation front in protoplanetary disks. *Astronomy & Astrophysics* **630**, A147 (2019). DOI 10.1051/0004-6361/201935806
152. Fogg, M.J., Nelson, R.P.: Oligarchic and giant impact growth of terrestrial planets in the presence of gas giant planet migration. *Astronomy & Astrophysics* **441**, 791–806 (2005). DOI 10.1051/0004-6361:20053453
153. Fogg, M.J., Nelson, R.P.: On the formation of terrestrial planets in hot-Jupiter systems. *Astronomy & Astrophysics* **461**, 1195–1208 (2007). DOI 10.1051/0004-6361:20066171
154. Ford, E.B., Rasio, F.A.: Origins of Eccentric Extrasolar Planets: Testing the Planet-Planet Scattering Model. *Astrophysical Journal* **686**, 621–636 (2008). DOI 10.1086/590926

155. Foreman-Mackey, D., Morton, T.D., Hogg, D.W., Agol, E., Schölkopf, B.: The Population of Long-period Transiting Exoplanets. *Astronomical Journal* **152**, 206 (2016). DOI 10.3847/0004-6256/152/6/206
156. Fortney, J.J., Marley, M.S., Barnes, J.W.: Planetary Radii across Five Orders of Magnitude in Mass and Stellar Insolation: Application to Transits. *Astrophysical Journal* **659**, 1661–1672 (2007). DOI 10.1086/512120
157. Fressin, F., Torres, G., Charbonneau, D., Bryson, S.T., Christiansen, J., Dressing, C.D., Jenkins, J.M., Walkowicz, L.M., Batalha, N.M.: The False Positive Rate of Kepler and the Occurrence of Planets. *Astrophysical Journal* **766**, 81 (2013). DOI 10.1088/0004-637X/766/2/81
158. Fulton, B.J., Petigura, E.A.: The California Kepler Survey VII. Precise Planet Radii Leveraging Gaia DR2 Reveal the Stellar Mass Dependence of the Planet Radius Gap. ArXiv e-prints (2018)
159. Fulton, B.J., Petigura, E.A., Howard, A.W., Isaacson, H., Marcy, G.W., Cargile, P.A., Hebb, L., Weiss, L.M., Johnson, J.A., Morton, T.D., Sinukoff, E., Crossfield, I.J.M., Hirsch, L.A.: The California-Kepler Survey. III. A Gap in the Radius Distribution of Small Planets. *Astronomical Journal* **154**, 109 (2017). DOI 10.3847/1538-3881/aa80eb
160. Genda, H., Abe, Y.: Enhanced atmospheric loss on protoplanets at the giant impact phase in the presence of oceans. *Nature* **433**, 842–844 (2005). DOI 10.1038/nature03360
161. Genda, H., Ikoma, M.: Origin of the ocean on the Earth: Early evolution of water D/H in a hydrogen-rich atmosphere. *Icarus* **194**(1), 42–52 (2008). DOI 10.1016/j.icarus.2007.09.007
162. Gillon, M., Triaud, A.H.M.J., Demory, B.O., Jehin, E., Agol, E., Deck, K.M., Lederer, S.M., de Wit, J., Burdanov, A., Ingalls, J.G., Bolmont, E., Leconte, J., Raymond, S.N., Selsis, F., Turbet, M., Barkaoui, K., Burgasser, A., Burleigh, M.R., Carey, S.J., Chaushev, A., Copperwheat, C.M., Delrez, L., Fernandes, C.S., Holdsworth, D.L., Kotze, E.J., Van Grootel, V., Almléay, Y., Benkhaldoun, Z., Magain, P., Queloz, D.: Seven temperate terrestrial planets around the nearby ultracool dwarf star TRAPPIST-1. *Nature* **542**, 456–460 (2017). DOI 10.1038/nature21360
163. Ginzburg, S., Schlichting, H.E., Sari, R.: Super-Earth Atmospheres: Self-consistent Gas Accretion and Retention. *Astrophysical Journal* **825**, 29 (2016). DOI 10.3847/0004-637X/825/1/29
164. Goldreich, P., Schlichting, H.E.: Overstable Librations can Account for the Paucity of Mean Motion Resonances among Exoplanet Pairs. *Astronomical Journal* **147**(2), 32 (2014). DOI 10.1088/0004-6256/147/2/32
165. Goldreich, P., Tremaine, S.: The excitation of density waves at the Lindblad and corotation resonances by an external potential. *Astrophysical Journal* **233**, 857–871 (1979). DOI 10.1086/157448
166. Goldreich, P., Tremaine, S.: Disk-satellite interactions. *Astrophysical Journal* **241**, 425–441 (1980). DOI 10.1086/158356
167. Gomes, R., Levison, H.F., Tsiganis, K., Morbidelli, A.: Origin of the cataclysmic Late Heavy Bombardment period of the terrestrial planets. *Nature* **435**, 466–469 (2005). DOI 10.1038/nature03676
168. Gomes, R.S., Morbidelli, A., Levison, H.F.: Planetary migration in a planetesimal disk: why did Neptune stop at 30 AU? *Icarus* **170**, 492–507 (2004). DOI 10.1016/j.icarus.2004.03.011
169. Gonzalez, G.: The stellar metallicity-giant planet connection. *Monthly Notices of the Royal Astronomical Society* **285**, 403–412 (1997)
170. Gould, A., Dong, S., Gaudi, B.S., Udalski, A., Bond, I.A., Greenhill, J., Street, R.A., Dominik, M., Sumi, T., Szymański, M.K., Han, C., Allen, W., Bolt, G., Bos, M., Christie, G.W., DePoy, D.L., Drummond, J., Eastman, J.D., Gal-Yam, A., Higgins, D., Janczak, J., Kaspi, S., Kozłowski, S., Lee, C., Mallia, F., Maury, A., Maoz, D., McCormick, J., Monard, L.A.G., Moorhouse, D., Morgan, N., Natusch, T., Ofek, E.O., Park, B., Pogge, R.W., Polishook, D., Santaló, R., Shporer, A., Spector, O., Thornley, G., Yee, J.C., μ FUN Collaboration, Kubiak, M., Pietrzyński, G., Soszyński, I., Szewczyk, O., Wyrzykowski, Ł., Ulaczyk, K., Poleski, R., OGLE Collaboration, Abe, F., Bennett, D.P., Botzler, C.S., Douchin, D., Freeman, M.,

- Fukui, A., Furusawa, K., Hearnshaw, J.B., Hosaka, S., Itow, Y., Kamiya, K., Kilmartin, P.M., Korpela, A., Lin, W., Ling, C.H., Makita, S., Masuda, K., Matsubara, Y., Miyake, N., Muraki, Y., Nagaya, M., Nishimoto, K., Ohnishi, K., Okumura, T., Perrott, Y.C., Philpott, L., Rattenbury, N., Saito, T., Sako, T., Sullivan, D.J., Sweatman, W.L., Tristram, P.J., von Seggern, E., Yock, P.C.M., MOA Collaboration, Albrow, M., Batista, V., Beaulieu, J.P., Brilliant, S., Caldwell, J., Calitz, J.J., Cassan, A., Cole, A., Cook, K., Coutures, C., Dieters, S., Dominis Prester, D., Donatowicz, J., Fouqué, P., Hill, K., Hoffman, M., Jablonski, F., Kane, S.R., Kains, N., Kubas, D., Marquette, J., Martin, R., Martioli, E., Meintjes, P., Menzies, J., Pedretti, E., Pollard, K., Sahu, K.C., Vinter, C., Wambsganss, J., Watson, R., Williams, A., Zub, M., PLANET Collaboration, Allan, A., Bode, M.F., Bramich, D.M., Burgdorf, M.J., Clay, N., Fraser, S., Hawkins, E., Horne, K., Kerins, E., Lister, T.A., Mottram, C., Saunders, E.S., Snodgrass, C., Steele, I.A., Tsapras, Y., RoboNet Collaboration, Jørgensen, U.G., Anguita, T., Bozza, V., Calchi Novati, S., Harpsøe, K., Hinse, T.C., Hundertmark, M., Kjærgaard, P., Liebig, C., Mancini, L., Masi, G., Mathiasen, M., Rahvar, S., Ricci, D., Scarpetta, G., Southworth, J., Surdej, J., Thöne, C.C., MiNDSTEp Consortium: Frequency of Solar-like Systems and of Ice and Gas Giants Beyond the Snow Line from High-magnification Microlensing Events in 2005-2008. *Astrophysical Journal* **720**, 1073–1089 (2010). DOI 10.1088/0004-637X/720/2/1073
171. Gradie, J., Tedesco, E.: Compositional structure of the asteroid belt. *Science* **216**, 1405–1407 (1982). DOI 10.1126/science.216.4553.1405
 172. Greaves, J.S., Rice, W.K.M.: Do all Sun-like stars have planets? Inferences from the disc mass reservoirs of Class 0 protostars. *Monthly Notices of the Royal Astronomical Society* **412**(1), L88–L92 (2011). DOI 10.1111/j.1745-3933.2011.01011.x
 173. Greenberg, R., Hartmann, W.K., Chapman, C.R., Wacker, J.F.: Planetesimals to planets - Numerical simulation of collisional evolution. *Icarus* **35**, 1–26 (1978). DOI 10.1016/0019-1035(78)90057-X
 174. Gressel, O., Turner, N.J., Nelson, R.P., McNally, C.P.: Global Simulations of Protoplanetary Disks With Ohmic Resistivity and Ambipolar Diffusion. *Astrophysical Journal* **801**(2), 84 (2015). DOI 10.1088/0004-637X/801/2/84
 175. Grimm, R.E., McSween, H.Y.: Heliocentric zoning of the asteroid belt by aluminum-26 heating. *Science* **259**, 653–655 (1993)
 176. Grishin, E., Perets, H.B.: Application of Gas Dynamical Friction for Planetesimals. I. Evolution of Single Planetesimals. *Astrophysical Journal* **811**(1), 54 (2015). DOI 10.1088/0004-637X/811/1/54
 177. Gupta, A., Schlichting, H.E.: Sculpting the valley in the radius distribution of small exoplanets as a by-product of planet formation: the core-powered mass-loss mechanism. *Monthly Notices of the Royal Astronomical Society* **487**(1), 24–33 (2019). DOI 10.1093/mnras/stz1230
 178. Hahn, J.M.: The Dynamics of Planetary Systems and Astrophysical Disks. WILEY-VCH (2009)
 179. Haisch Jr., K.E., Lada, E.A., Lada, C.J.: Disk Frequencies and Lifetimes in Young Clusters. *Astrophysical Journal Letters* **553**, L153–L156 (2001). DOI 10.1086/320685
 180. Halliday, A.N.: The origins of volatiles in the terrestrial planets. *Geochemica and Cosmochemica Acta* **105**, 146–171 (2013). DOI 10.1016/j.gca.2012.11.015
 181. Halliday, A.N., Kleine, T.: Meteorites and the Timing, Mechanisms, and Conditions of Terrestrial Planet Accretion and Early Differentiation, pp. 775–801 (2006)
 182. Hansen, B.M.S.: Formation of the Terrestrial Planets from a Narrow Annulus. *Astrophysical Journal* **703**, 1131–1140 (2009). DOI 10.1088/0004-637X/703/1/1131
 183. Hansen, B.M.S., Murray, N.: Migration Then Assembly: Formation of Neptune-mass Planets inside 1 AU. *Astrophysical Journal* **751**, 158 (2012). DOI 10.1088/0004-637X/751/2/158
 184. Hansen, B.M.S., Murray, N.: Testing in Situ Assembly with the Kepler Planet Candidate Sample. *Astrophysical Journal* **775**, 53 (2013). DOI 10.1088/0004-637X/775/1/53
 185. Hartmann, L., Calvet, N., Gullbring, E., D'Alessio, P.: Accretion and the Evolution of T Tauri Disks. *Astrophysical Journal* **495**, 385–400 (1998). DOI 10.1086/305277

186. Hartmann, W.K.: The Collapse of the Terminal Cataclysm Paradigm...and Where We Go from Here. In: Lunar and Planetary Science Conference, Lunar and Planetary Science Conference, p. 1064 (2019)
187. Hartogh, P., Lis, D.C., Bockelée-Morvan, D., de Val-Borro, M., Biver, N., Küppers, M., Emprechtinger, M., Bergin, E.A., Crovisier, J., Rengel, M., Moreno, R., Szutowicz, S., Blake, G.A.: Ocean-like water in the Jupiter-family comet 103P/Hartley 2. *Nature* **478**, 218–220 (2011). DOI 10.1038/nature10519
188. Hasegawa, Y., Pudritz, R.E.: Evolutionary Tracks of Trapped, Accreting Protoplanets: The Origin of the Observed Mass-Period Relation. *Astrophysical Journal* **760**, 117 (2012). DOI 10.1088/0004-637X/760/2/117
189. Hayashi, C.: Structure of the Solar Nebula, Growth and Decay of Magnetic Fields and Effects of Magnetic and Turbulent Viscosities on the Nebula. *Progress of Theoretical Physics Supplement* **70**, 35–53 (1981). DOI 10.1143/PTPS.70.35
190. Helled, R., Bodenheimer, P., Podolak, M., Boley, A., Meru, F., Nayakshin, S., Fortney, J.J., Mayer, L., Alibert, Y., Boss, A.P.: Giant Planet Formation, Evolution, and Internal Structure. *Protostars and Planets VI* pp. 643–665 (2014)
191. Henon, M., Heiles, C.: The applicability of the third integral of motion: Some numerical experiments. *Astronomical Journal* **69**, 73 (1964). DOI 10.1086/109234
192. Hillenbrand, L.A., Carpenter, J.M., Kim, J.S., Meyer, M.R., Backman, D.E., Moro-Martín, A., Hollenbach, D.J., Hines, D.C., Pascucci, I., Bouwman, J.: The Complete Census of 70 μm -bright Debris Disks within “the Formation and Evolution of Planetary Systems” Spitzer Legacy Survey of Sun-like Stars. *Astrophysical Journal* **677**, 630–656 (2008). DOI 10.1086/529027
193. Hirschmann, M.M.: Water, Melting, and the Deep Earth H₂O Cycle. *Annual Review of Earth and Planetary Sciences* **34**, 629–653 (2006). DOI 10.1146/annurev.earth.34.031405.125211
194. Hollenbach, D., Johnstone, D., Lizano, S., Shu, F.: Photoevaporation of disks around massive stars and application to ultracompact H II regions. *Astrophysical Journal* **428**, 654–669 (1994). DOI 10.1086/174276
195. Howard, A.W., Marcy, G.W., Bryson, S.T., Jenkins, J.M., Rowe, J.F., Batalha, N.M., Borucki, W.J., Koch, D.G., Dunham, E.W., Gautier III, T.N., Van Cleve, J., Cochran, W.D., Latham, D.W., Lissauer, J.J., Torres, G., Brown, T.M., Gilliland, R.L., Buchhave, L.A., Caldwell, D.A., Christensen-Dalsgaard, J., Ciardi, D., Fressin, F., Haas, M.R., Howell, S.B., Kjeldsen, H., Seager, S., Rogers, L., Sasselov, D.D., Steffen, J.H., Basri, G.S., Charbonneau, D., Christiansen, J., Clarke, B., Dupree, A., Fabrycky, D.C., Fischer, D.A., Ford, E.B., Fortney, J.J., Tarter, J., Girouard, F.R., Holman, M.J., Johnson, J.A., Klaus, T.C., Machalek, P., Moorhead, A.V., Morehead, R.C., Ragozzine, D., Tenenbaum, P., Twicken, J.D., Quinn, S.N., Isaacson, H., Shporer, A., Lucas, P.W., Walkowicz, L.M., Welsh, W.F., Boss, A., Devore, E., Gould, A., Smith, J.C., Morris, R.L., Prsa, A., Morton, T.D., Still, M., Thompson, S.E., Mullally, F., Endl, M., MacQueen, P.J.: Planet Occurrence within 0.25 AU of Solar-type Stars from Kepler. *Astrophysical Journal Supplement Series* **201**, 15 (2012). DOI 10.1088/0067-0049/201/2/15
196. Howard, A.W., Marcy, G.W., Johnson, J.A., Fischer, D.A., Wright, J.T., Isaacson, H., Valenti, J.A., Anderson, J., Lin, D.N.C., Ida, S.: The Occurrence and Mass Distribution of Close-in Super-Earths, Neptunes, and Jupiters. *Science* **330**, 653– (2010). DOI 10.1126/science.1194854
197. Hu, X., Tan, J.C., Zhu, Z., Chatterjee, S., Birnstiel, T., Youdin, A.N., Mohanty, S.: Inside-Out Planet Formation. IV. Pebble Evolution and Planet Formation Timescales. *ArXiv e-prints* (2017)
198. Hu, X., Zhu, Z., Tan, J.C., Chatterjee, S.: Inside-out Planet Formation. III. Planet-Disk Interaction at the Dead Zone Inner Boundary. *Astrophysical Journal* **816**, 19 (2016). DOI 10.3847/0004-637X/816/1/19
199. Hubickyj, O., Bodenheimer, P., Lissauer, J.J.: Accretion of the gaseous envelope of Jupiter around a 5–10 Earth-mass core. *Icarus* **179**, 415–431 (2005). DOI 10.1016/j.icarus.2005.06.021

200. Hughes, A.M., Duchêne, G., Matthews, B.C.: Debris Disks: Structure, Composition, and Variability. *Annual Reviews of Astronomy and Astrophysics* **56**, 541–591 (2018). DOI 10.1146/annurev-astro-081817-052035
201. Ida, S., Guillot, T.: Formation of dust-rich planetesimals from sublimated pebbles inside of the snow line. *Astronomy & Astrophysics* **596**, L3 (2016). DOI 10.1051/0004-6361/201629680
202. Ida, S., Guillot, T., Morbidelli, A.: The radial dependence of pebble accretion rates: A source of diversity in planetary systems. I. Analytical formulation. *Astronomy & Astrophysics* **591**, A72 (2016). DOI 10.1051/0004-6361/201628099
203. Ida, S., Lin, D.N.C.: Toward a Deterministic Model of Planetary Formation. I. A Desert in the Mass and Semimajor Axis Distributions of Extrasolar Planets. *Astrophysical Journal* **604**, 388–413 (2004). DOI 10.1086/381724
204. Ida, S., Lin, D.N.C.: Toward a Deterministic Model of Planetary Formation. IV. Effects of Type I Migration. *Astrophysical Journal* **673**, 487–501 (2008). DOI 10.1086/523754
205. Ida, S., Lin, D.N.C.: Toward a Deterministic Model of Planetary Formation. VI. Dynamical Interaction and Coagulation of Multiple Rocky Embryos and Super-Earth Systems around Solar-type Stars. *Astrophysical Journal* **719**, 810–830 (2010). DOI 10.1088/0004-637X/719/1/810
206. Ida, S., Lin, D.N.C., Nagasawa, M.: Toward a Deterministic Model of Planetary Formation. VII. Eccentricity Distribution of Gas Giants. *Astrophysical Journal* **775**, 42 (2013). DOI 10.1088/0004-637X/775/1/42
207. Ida, S., Yamamura, T., Okuzumi, S.: Water delivery by pebble accretion to rocky planets in habitable zones in evolving disks. *Astronomy & Astrophysics* **624**, A28 (2019). DOI 10.1051/0004-6361/201834556
208. Ikoma, M., Genda, H.: Constraints on the Mass of a Habitable Planet with Water of Nebular Origin. *Astrophysical Journal* **648**(1), 696–706 (2006). DOI 10.1086/505780
209. Ikoma, M., Nakazawa, K., Emori, H.: Formation of Giant Planets: Dependences on Core Accretion Rate and Grain Opacity. *Astrophysical Journal* **537**, 1013–1025 (2000). DOI 10.1086/309050
210. Inamdar, N.K., Schlichting, H.E.: The formation of super-Earths and mini-Neptunes with giant impacts. *Monthly Notices of the Royal Astronomical Society* **448**, 1751–1760 (2015). DOI 10.1093/mnras/stv030
211. Izidoro, A., Bitsch, B., Raymond, S.N., Johansen, A., Morbidelli, A., Lambrechts, M., Jacobson, S.A.: Formation of planetary systems by pebble accretion and migration: Hot super-Earth systems from breaking compact resonant chains. arXiv e-prints arXiv:1902.08772 (2019)
212. Izidoro, A., Morbidelli, A., Raymond, S.N.: Terrestrial Planet Formation in the Presence of Migrating Super-Earths. *Astrophysical Journal* **794**, 11 (2014). DOI 10.1088/0004-637X/794/1/11
213. Izidoro, A., Morbidelli, A., Raymond, S.N., Hersant, F., Pierens, A.: Accretion of Uranus and Neptune from inward-migrating planetary embryos blocked by Jupiter and Saturn. *Astronomy & Astrophysics* **582**, A99 (2015). DOI 10.1051/0004-6361/201425525
214. Izidoro, A., Ogihara, M., Raymond, S.N., Morbidelli, A., Pierens, A., Bitsch, B., Cossou, C., Hersant, F.: Breaking the chains: hot super-Earth systems from migration and disruption of compact resonant chains. *Monthly Notices of the Royal Astronomical Society* **470**, 1750–1770 (2017). DOI 10.1093/mnras/stx1232
215. Izidoro, A., Raymond, S.N., Morbidelli, A., Hersant, F., Pierens, A.: Gas Giant Planets as Dynamical Barriers to Inward-Migrating Super-Earths. *Astrophysical Journal Letters* **800**, L22 (2015). DOI 10.1088/2041-8205/800/2/L22
216. Izidoro, A., Raymond, S.N., Morbidelli, A., Winter, O.C.: Terrestrial planet formation constrained by Mars and the structure of the asteroid belt. *Monthly Notices of the Royal Astronomical Society* **453**, 3619–3634 (2015). DOI 10.1093/mnras/stv1835
217. Jacobson, S.A., Morbidelli, A.: Lunar and terrestrial planet formation in the Grand Tack scenario. *Philosophical Transactions of the Royal Society of London Series A* **372**, 0174 (2014). DOI 10.1098/rsta.2013.0174

218. Jacobson, S.A., Morbidelli, A., Raymond, S.N., O'Brien, D.P., Walsh, K.J., Rubie, D.C.: Highly siderophile elements in Earth's mantle as a clock for the Moon-forming impact. *Nature* **508**, 84–87 (2014). DOI 10.1038/nature13172
219. Jacquet, E., Balbus, S., Latter, H.: On linear dust-gas streaming instabilities in protoplanetary discs. *Monthly Notices of the Royal Astronomical Society* **415**(4), 3591–3598 (2011). DOI 10.1111/j.1365-2966.2011.18971.x
220. Jin, S., Mordasini, C.: Compositional Imprints in Density–Distance–Time: A Rocky Composition for Close-in Low-mass Exoplanets from the Location of the Valley of Evaporation. *Astrophysical Journal* **853**, 163 (2018). DOI 10.3847/1538-4357/aa9f1e
221. Johansen, A., Blum, J., Tanaka, H., Ormel, C., Bizzarro, M., Rickman, H.: The Multifaceted Planetesimal Formation Process. Protostars and Planets VI pp. 547–570 (2014)
222. Johansen, A., Davies, M.B., Church, R.P., Holmelin, V.: Can Planetary Instability Explain the Kepler Dichotomy? *Astrophysical Journal* **758**, 39 (2012). DOI 10.1088/0004-637X/758/1/39
223. Johansen, A., Lambrechts, M.: Forming Planets via Pebble Accretion. Annual Review of Earth and Planetary Sciences **45**, 359–387 (2017). DOI 10.1146/annurev-earth-063016-020226
224. Johansen, A., Mac Low, M.M., Lacerda, P., Bizzarro, M.: Growth of asteroids, planetary embryos, and Kuiper belt objects by chondrule accretion. *Science Advances* **1**, 1500109 (2015). DOI 10.1126/sciadv.1500109
225. Johansen, A., Youdin, A., Klahr, H.: Zonal Flows and Long-lived Axisymmetric Pressure Bumps in Magnetorotational Turbulence. *Astrophysical Journal* **697**, 1269–1289 (2009). DOI 10.1088/0004-637X/697/2/1269
226. Johnson, B.C., Walsh, K.J., Minton, D.A., Krot, A.N., Levison, H.F.: Timing of the formation and migration of giant planets as constrained by cb chondrites. *Science Advances* **2**(12) (2016). DOI 10.1126/sciadv.1601658. URL <http://advances.sciencemag.org/content/2/12/e1601658>
227. Johnson, J.A., Butler, R.P., Marcy, G.W., Fischer, D.A., Vogt, S.S., Wright, J.T., Peek, K.M.G.: A New Planet around an M Dwarf: Revealing a Correlation between Exoplanets and Stellar Mass. *Astrophysical Journal* **670**, 833–840 (2007). DOI 10.1086/521720
228. Jones, H.R.A., Butler, R.P., Tinney, C.G., Marcy, G.W., Carter, B.D., Penny, A.J., McCarthy, C., Bailey, J.: High-eccentricity planets from the Anglo-Australian Planet Search. *Monthly Notices of the Royal Astronomical Society* **369**, 249–256 (2006). DOI 10.1111/j.1365-2966.2006.10298.x
229. Jurić, M., Tremaine, S.: Dynamical Origin of Extrasolar Planet Eccentricity Distribution. *Astrophysical Journal* **686**, 603–620 (2008). DOI 10.1086/590047
230. Kaib, N.A., Chambers, J.E.: The fragility of the terrestrial planets during a giant-planet instability. *Monthly Notices of the Royal Astronomical Society* **455**, 3561–3569 (2016). DOI 10.1093/mnras/stv2554
231. Kaib, N.A., Cowan, N.B.: The feeding zones of terrestrial planets and insights into Moon formation. *Icarus* **252**, 161–174 (2015). DOI 10.1016/j.icarus.2015.01.013
232. Kaib, N.A., Raymond, S.N., Duncan, M.: Planetary system disruption by Galactic perturbations to wide binary stars. *Nature* **493**, 381–384 (2013). DOI 10.1038/nature11780
233. Kanagawa, K.D., Tanaka, H., Muto, T., Tanigawa, T., Takeuchi, T.: Formation of a disc gap induced by a planet: effect of the deviation from Keplerian disc rotation. *Monthly Notices of the Royal Astronomical Society* **448**(1), 994–1006 (2015). DOI 10.1093/mnras/stv025
234. Kanagawa, K.D., Tanaka, H., Szuszkiewicz, E.: Radial Migration of Gap-opening Planets in Protoplanetary Disks. I. The Case of a Single Planet. *Astrophysical Journal* **861**(2), 140 (2018). DOI 10.3847/1538-4357/aac8d9
235. Kataoka, A., Tanaka, H., Okuzumi, S., Wada, K.: Fluffy dust forms icy planetesimals by static compression. *Astronomy & Astrophysics* **557**, L4 (2013). DOI 10.1051/0004-6361/201322151
236. Kerridge, J.F.: Carbon, hydrogen and nitrogen in carbonaceous chondrites Abundances and isotopic compositions in bulk samples. *Geochemica and Cosmochemica Acta* **49**, 1707–1714 (1985). DOI 10.1016/0016-7037(85)90141-3

237. Kimura, K., Lewis, R.S., Anders, E.: Distribution of gold and rhenium between nickel-iron and silicate melts: implications for the abundance of siderophile elements on the Earth and Moon. *Geochemica and Cosmochemica Acta* **38**, 683–701 (1974). DOI 10.1016/0016-7037(74)90144-6
238. Kimura, S.S., Tsuribe, T.: Conditions of Gravitational Instability in Protoplanetary Disks. *Proceedings of the Astronomical Society of Japan* **64**, 116 (2012). DOI 10.1093/pasj/64.5.116
239. Kita, N.T., Huss, G.R., Tachibana, S., Amelin, Y., Nyquist, L.E., Hutcheon, I.D.: Constraints on the Origin of Chondrules and CAIs from Short-lived and Long-Lived Radionuclides. In: A.N. Krot, E.R.D. Scott, B. Reipurth (eds.) *Chondrites and the Protoplanetary Disk, Astronomical Society of the Pacific Conference Series*, vol. 341, p. 558 (2005)
240. Kleine, T., Touboul, M., Bourdon, B., Nimmo, F., Mezger, K., Palme, H., Jacobsen, S.B., Yin, Q.Z., Halliday, A.N.: Hf-W chronology of the accretion and early evolution of asteroids and terrestrial planets. *Geochemica and Cosmochemica Acta* **73**, 5150–5188 (2009)
241. Kokubo, E., Ida, S.: On Runaway Growth of Planetesimals. *Icarus* **123**, 180–191 (1996). DOI 10.1006/icar.1996.0148
242. Kokubo, E., Ida, S.: Oligarchic Growth of Protoplanets. *Icarus* **131**, 171–178 (1998). DOI 10.1006/icar.1997.5840
243. Kokubo, E., Ida, S.: Formation of Protoplanets from Planetesimals in the Solar Nebula. *Icarus* **143**, 15–27 (2000). DOI 10.1006/icar.1999.6237
244. Kokubo, E., Ida, S.: Formation of Terrestrial Planets from Protoplanets. II. Statistics of Planetary Spin. *Astrophysical Journal* **671**, 2082–2090 (2007). DOI 10.1086/522364
245. Kral, Q., Krivov, A.V., Defrère, D., van Lieshout, R., Bonsor, A., Augereau, J.C., Thébault, P., Ertel, S., Lebreton, J., Absil, O.: Exozodiacal clouds: hot and warm dust around main sequence stars. *The Astronomical Review* **13**(2), 69–111 (2017). DOI 10.1080/21672857.2017.1353202
246. Krasinsky, G.A., Pitjeva, E.V., Vasilyev, M.V., Yagudina, E.I.: Hidden Mass in the Asteroid Belt. *Icarus* **158**, 98–105 (2002). DOI 10.1006/icar.2002.6837
247. Kretke, K.A., Lin, D.N.C.: The Importance of Disk Structure in Stalling Type I Migration. *Astrophysical Journal* **755**, 74 (2012). DOI 10.1088/0004-637X/755/1/74
248. Krivov, A.V.: Debris disks: seeing dust, thinking of planetesimals and planets. *Research in Astronomy and Astrophysics* **10**, 383–414 (2010). DOI 10.1088/1674-4527/10/5/001
249. Krot, A.N., Amelin, Y., Cassen, P., Meibom, A.: Young chondrules in CB chondrites from a giant impact in the early Solar System. *Nature* **436**, 989–992 (2005). DOI 10.1038/nature03830
250. Kruijjer, T.S., Burkhardt, C., Budde, C., Kleine, T.: Age of Jupiter inferred from the distinct genetics and formation times of meteorites. *PNAS* (2017)
251. Kruijjer, T.S., Touboul, M., Fischer-Gödde, M., Bermingham, K.R., Walker, R.J., Kleine, T.: Protracted core formation and rapid accretion of protoplanets. *Science* **344**, 1150–1154 (2014). DOI 10.1126/science.1251766
252. Kuchynka, P., Folkner, W.M.: A new approach to determining asteroid masses from planetary range measurements. *Icarus* **222**, 243–253 (2013). DOI 10.1016/j.icarus.2012.11.003
253. Lambrechts, M., Johansen, A.: Rapid growth of gas-giant cores by pebble accretion. *Astronomy & Astrophysics* **544**, A32 (2012). DOI 10.1051/0004-6361/201219127
254. Lambrechts, M., Johansen, A.: Forming the cores of giant planets from the radial pebble flux in protoplanetary discs. *Astronomy & Astrophysics* **572**, A107 (2014). DOI 10.1051/0004-6361/201424343
255. Lambrechts, M., Johansen, A., Morbidelli, A.: Separating gas-giant and ice-giant planets by halting pebble accretion. *Astronomy & Astrophysics* **572**, A35 (2014). DOI 10.1051/0004-6361/201423814
256. Lambrechts, M., Lega, E.: Reduced gas accretion on super-Earths and ice giants. *Astronomy & Astrophysics* **606**, A146 (2017). DOI 10.1051/0004-6361/201731014
257. Lambrechts, M., Lega, E., Nelson, R.P., Crida, A., Morbidelli, A.: Quasi-static contraction during runaway gas accretion onto giant planets. *Astronomy & Astrophysics* **630**, A82 (2019). DOI 10.1051/0004-6361/201834413

258. Lambrechts, M., Morbidelli, A., Jacobson, S.A., Johansen, A., Bitsch, B., Izidoro, A., Raymond, S.N.: Formation of planetary systems by pebble accretion and migration. How the radial pebble flux determines a terrestrial-planet or super-Earth growth mode. *Astronomy & Astrophysics* **627**, A83 (2019). DOI 10.1051/0004-6361/201834229
259. Laplace, P.S., Bowditch, N., Bowditch, N.I.: *Mécanique céleste* (1829)
260. Laskar, J.: Large scale chaos and the spacing of the inner planets. *Astronomy & Astrophysics* **317**, L75–L78 (1997)
261. Laws, C., Gonzalez, G., Walker, K.M., Tyagi, S., Dodsworth, J., Snider, K., Suntzeff, N.B.: Parent Stars of Extrasolar Planets. VII. New Abundance Analyses of 30 Systems. *Astronomical Journal* **125**, 2664–2677 (2003). DOI 10.1086/374626
262. Lecar, M., Podolak, M., Sasselov, D., Chiang, E.: On the Location of the Snow Line in a Protoplanetary Disk. *Astrophysical Journal* **640**, 1115–1118 (2006). DOI 10.1086/500287
263. Lee, E.J., Chiang, E.: Breeding Super-Earths and Birthing Super-puffs in Transitional Disks. *Astrophysical Journal* **817**, 90 (2016). DOI 10.3847/0004-637X/817/2/90
264. Lee, E.J., Chiang, E.: Magnetospheric Truncation, Tidal Inspiral, and the Creation of Short-period and Ultra-short-period Planets. *Astrophysical Journal* **842**, 40 (2017). DOI 10.3847/1538-4357/aa6fb3
265. Lee, E.J., Chiang, E., Ormel, C.W.: Make Super-Earths, Not Jupiters: Accreting Nebular Gas onto Solid Cores at 0.1 AU and Beyond. *Astrophysical Journal* **797**, 95 (2014). DOI 10.1088/0004-637X/797/2/95
266. Lee, M.H., Peale, S.J.: Dynamics and Origin of the 2:1 Orbital Resonances of the GJ 876 Planets. *Astrophysical Journal* **567**, 596–609 (2002). DOI 10.1086/338504
267. Lega, E., Crida, A., Bitsch, B., Morbidelli, A.: Migration of Earth-sized planets in 3D radiative discs. *Monthly Notices of the Royal Astronomical Society* **440**, 683–695 (2014). DOI 10.1093/mnras/stu304
268. Lestrade, J.F., Matthews, B.C., Sibthorpe, B., Kennedy, G.M., Wyatt, M.C., Bryden, G., Greaves, J.S., Thilliez, E., Moro-Martín, A., Booth, M., Dent, W.R.F., Duchêne, G., Harvey, P.M., Horner, J., Kalas, P., Kavelaars, J.J., Phillips, N.M., Rodriguez, D.R., Su, K.Y.L., Wilner, D.J.: A DEBRIS disk around the planet hosting M-star GJ 581 spatially resolved with Herschel. *Astronomy & Astrophysics* **548**, A86 (2012). DOI 10.1051/0004-6361/201220325
269. Levison, H.F., Kretke, K.A., Walsh, K.J., Bottke, W.F.: Growing the terrestrial planets from the gradual accumulation of sub-meter sized objects. *Proceedings of the National Academy of Science* **112**, 14180–14185 (2015). DOI 10.1073/pnas.1513364112
270. Levison, H.F., Morbidelli, A., Tsiganis, K., Nesvorný, D., Gomes, R.: Late Orbital Instabilities in the Outer Planets Induced by Interaction with a Self-gravitating Planetesimal Disk. *Astronomical Journal* **142**, 152 (2011). DOI 10.1088/0004-6256/142/5/152
271. Levison, H.F., Morbidelli, A., Vanlaerhoven, C., Gomes, R., Tsiganis, K.: Origin of the structure of the Kuiper belt during a dynamical instability in the orbits of Uranus and Neptune. *Icarus* **196**, 258–273 (2008). DOI 10.1016/j.icarus.2007.11.035
272. Levison, H.F., Stewart, G.R.: Remarks on Modeling the Formation of Uranus and Neptune. *Icarus* **153**, 224–228 (2001). DOI 10.1006/icar.2001.6672
273. Levison, H.F., Thommes, E., Duncan, M.J.: Modeling the Formation of Giant Planet Cores. I. Evaluating Key Processes. *Astronomical Journal* **139**, 1297–1314 (2010). DOI 10.1088/0004-6256/139/4/1297
274. Lichtenberg, T., Golabek, G.J., Burn, R., Meyer, M.R., Alibert, Y., Gerya, T.V., Mordasini, C.: A water budget dichotomy of rocky protoplanets from ^{26}Al -heating. *Nature Astronomy* **3**, 307–313 (2019). DOI 10.1038/s41550-018-0688-5
275. Lin, D.N.C., Bodenheimer, P., Richardson, D.C.: Orbital migration of the planetary companion of 51 Pegasi to its present location. *Nature* **380**, 606–607 (1996). DOI 10.1038/380606a0
276. Lin, D.N.C., Ida, S.: On the Origin of Massive Eccentric Planets. *Astrophysical Journal* **477**, 781–+ (1997). DOI 10.1086/303738
277. Lin, D.N.C., Papaloizou, J.: Tidal torques on accretion discs in binary systems with extreme mass ratios. *Monthly Notices of the Royal Astronomical Society* **186**, 799–812 (1979). DOI 10.1093/mnras/186.4.799

278. Lin, D.N.C., Papaloizou, J.: On the tidal interaction between protoplanets and the protoplanetary disk. III - Orbital migration of protoplanets. *Astrophysical Journal* **309**, 846–857 (1986). DOI 10.1086/164653
279. Lis, D.C., Biver, N., Bockelée-Morvan, D., Hartogh, P., Bergin, E.A., Blake, G.A., Crovisier, J., de Val-Borro, M., Jehin, E., Küppers, M., Manfroid, J., Moreno, R., Rengel, M., Szutowicz, S.: A Herschel Study of D/H in Water in the Jupiter-family Comet 45P/Honda-Mrkos-Pajdušáková and Prospects for D/H Measurements with CCAT. *Astrophysical Journal Letters* **774**, L3 (2013). DOI 10.1088/2041-8205/774/1/L3
280. Lis, D.C., Bockelée-Morvan, D., Güsten, R., Biver, N., Stutzki, J., Delorme, Y., Durán, C., Wiesemeyer, H., Okada, Y.: Terrestrial deuterium-to-hydrogen ratio in water in hyperactive comets. *Astronomy & Astrophysics* **625**, L5 (2019). DOI 10.1051/0004-6361/201935554
281. Lissauer, J.J.: Timescales for planetary accretion and the structure of the protoplanetary disk. *Icarus* **69**, 249–265 (1987). DOI 10.1016/0019-1035(87)90104-7
282. Lissauer, J.J.: Planet formation. *Annual Reviews of Astronomy and Astrophysics* **31**, 129–174 (1993). DOI 10.1146/annurev.aa.31.090193.001021
283. Lissauer, J.J., Hubickyj, O., D'Angelo, G., Bodenheimer, P.: Models of Jupiter's growth incorporating thermal and hydrodynamic constraints. *Icarus* **199**, 338–350 (2009). DOI 10.1016/j.icarus.2008.10.004
284. Lissauer, J.J., Ragozzine, D., Fabrycky, D.C., Steffen, J.H., Ford, E.B., Jenkins, J.M., Shporer, A., Holman, M.J., Rowe, J.F., Quintana, E.V., Batalha, N.M., Borucki, W.J., Bryson, S.T., Caldwell, D.A., Carter, J.A., Ciardi, D., Dunham, E.W., Fortney, J.J., Gautier III, T.N., Howell, S.B., Koch, D.G., Latham, D.W., Marcy, G.W., Morehead, R.C., Sasselov, D.: Architecture and Dynamics of Kepler's Candidate Multiple Transiting Planet Systems. *Astrophysical Journal Supplement Series* **197**, 8 (2011). DOI 10.1088/0067-0049/197/1/8
285. Lissauer, J.J., Stevenson, D.J.: Formation of Giant Planets. *Protostars and Planets V* pp. 591–606 (2007)
286. Lodders, K.: Solar System Abundances and Condensation Temperatures of the Elements. *Astrophysical Journal* **591**, 1220–1247 (2003). DOI 10.1086/375492
287. Looney, L.W., Mundy, L.G., Welch, W.J.: Envelope Emission in Young Stellar Systems: A Subarcsecond Survey of Circumstellar Structure. *Astrophysical Journal* **592**, 255–265 (2003). DOI 10.1086/375582
288. Lopez, E.D.: Born dry in the photoevaporation desert: Kepler's ultra-short-period planets formed water-poor. *Monthly Notices of the Royal Astronomical Society* **472**, 245–253 (2017). DOI 10.1093/mnras/stx1558
289. Lovis, C., Mayor, M.: Planets around evolved intermediate-mass stars. I. Two substellar companions in the open clusters NGC 2423 and NGC 4349. *Astronomy & Astrophysics* **472**, 657–664 (2007). DOI 10.1051/0004-6361:20077375
290. Luger, R., Sestovic, M., Kruse, E., Grimm, S.L., Demory, B.O., Agol, E., Bolmont, E., Fabrycky, D., Fernandes, C.S., Van Grootel, V., Burgasser, A., Gillon, M., Ingalls, J.G., Jehin, E., Raymond, S.N., Selsis, F., Triaud, A.H.M.J., Barclay, T., Barentsen, G., Howell, S.B., Delrez, L., de Wit, J., Foreman-Mackey, D., Holdsworth, D.L., Leconte, J., Lederer, S., Turbet, M., Almeida, Y., Benkhaldoun, Z., Magain, P., Morris, B.M., Heng, K., Queloz, D.: A seven-planet resonant chain in TRAPPIST-1. *Nature Astronomy* **1**, 0129 (2017). DOI 10.1038/s41550-017-0129
291. Lykawka, P.S., Ito, T.: Constraining the Formation of the Four Terrestrial Planets in the Solar System. arXiv e-prints arXiv:1908.04934 (2019)
292. Lynden-Bell, D., Pringle, J.E.: The evolution of viscous discs and the origin of the nebular variables. *Monthly Notices of the Royal Astronomical Society* **168**, 603–637 (1974)
293. Lyra, W., Paardekooper, S.J., Mac Low, M.M.: Orbital Migration of Low-mass Planets in Evolutionary Radiative Models: Avoiding Catastrophic Infall. *Astrophysical Journal Letters* **715**, L68–L73 (2010). DOI 10.1088/2041-8205/715/2/L68
294. Mamajek, E.E.: Initial Conditions of Planet Formation: Lifetimes of Primordial Disks. In: T. Usuda, M. Tamura, M. Ishii (eds.) American Institute of Physics Conference Series, *American Institute of Physics Conference Series*, vol. 1158, pp. 3–10 (2009). DOI 10.1063/1.3215910

295. Manara, C.F., Morbidelli, A., Guillot, T.: Why do protoplanetary disks appear not massive enough to form the known exoplanet population? *Astronomy & Astrophysics* **618**, L3 (2018). DOI 10.1051/0004-6361/201834076
296. Mandell, A.M., Raymond, S.N., Sigurdsson, S.: Formation of Earth-like Planets During and After Giant Planet Migration. *Astrophysical Journal* **660**, 823–844 (2007). DOI 10.1086/512759
297. Marcy, G.W., Isaacson, H., Howard, A.W., Rowe, J.F., Jenkins, J.M., Bryson, S.T., Latham, D.W., Howell, S.B., Gautier III, T.N., Batalha, N.M., Rogers, L., Ciardi, D., Fischer, D.A., Gilliland, R.L., Kjeldsen, H., Christensen-Dalsgaard, J., Huber, D., Chaplin, W.J., Basu, S., Buchhave, L.A., Quinn, S.N., Borucki, W.J., Koch, D.G., Hunter, R., Caldwell, D.A., Van Cleve, J., Kolbl, R., Weiss, L.M., Petigura, E., Seager, S., Morton, T., Johnson, J.A., Ballard, S., Burke, C., Cochran, W.D., Endl, M., MacQueen, P., Everett, M.E., Lissauer, J.J., Ford, E.B., Torres, G., Fressin, F., Brown, T.M., Steffen, J.H., Charbonneau, D., Basri, G.S., Sasselov, D.D., Winn, J., Sanchis-Ojeda, R., Christiansen, J., Adams, E., Henze, C., Dupree, A., Fabrycky, D.C., Fortney, J.J., Tarter, J., Holman, M.J., Tenenbaum, P., Shporer, A., Lucas, P.W., Welsh, W.F., Orosz, J.A., Bedding, T.R., Campante, T.L., Davies, G.R., Elsworth, Y., Handberg, R., Hekker, S., Karoff, C., Kawaler, S.D., Lund, M.N., Lundkvist, M., Metcalfe, T.S., Miglio, A., Silva Aguirre, V., Stello, D., White, T.R., Boss, A., Devore, E., Gould, A., Prsa, A., Agol, E., Barclay, T., Coughlin, J., Brugamyer, E., Mullally, F., Quintana, E.V., Still, M., Thompson, S.E., Morrison, D., Twicken, J.D., Désert, J.M., Carter, J., Crepp, J.R., Hébrard, G., Santerne, A., Moutou, C., Sobeck, C., Hudgins, D., Haas, M.R., Robertson, P., Lillo-Box, J., Barrado, D.: Masses, Radii, and Orbits of Small Kepler Planets: The Transition from Gaseous to Rocky Planets. *Astrophysical Journal Supplement Series* **210**, 20 (2014). DOI 10.1088/0067-0049/210/2/20
298. Marois, C., Macintosh, B., Barman, T., Zuckerman, B., Song, I., Patience, J., Lafrenière, D., Doyon, R.: Direct Imaging of Multiple Planets Orbiting the Star HR 8799. *Science* **322**, 1348– (2008). DOI 10.1126/science.1166585
299. Marois, C., Zuckerman, B., Konopacky, Q.M., Macintosh, B., Barman, T.: Images of a fourth planet orbiting HR 8799. *Nature* **468**, 1080–1083 (2010). DOI 10.1038/nature09684
300. Marshall, J.P., Moro-Martín, A., Eiroa, C., Kennedy, G., Mora, A., Sibthorpe, B., Lestrade, J.F., Maldonado, J., Sanz-Forcada, J., Wyatt, M.C., Matthews, B., Horner, J., Montesinos, B., Bryden, G., del Burgo, C., Greaves, J.S., Ivison, R.J., Meeus, G., Olofsson, G., Pilbratt, G.L., White, G.J.: Correlations between the stellar, planetary, and debris components of exoplanet systems observed by Herschel. *Astronomy & Astrophysics* **565**, A15 (2014). DOI 10.1051/0004-6361/201323058
301. Martin, R.G., Livio, M.: On the evolution of the snow line in protoplanetary discs. *Monthly Notices of the Royal Astronomical Society* **425**, L6–L9 (2012). DOI 10.1111/j.1745-3933.2012.01290.x
302. Martin, R.G., Livio, M.: The Solar System as an Exoplanetary System. *Astrophysical Journal* **810**, 105 (2015). DOI 10.1088/0004-637X/810/2/105
303. Marty, B.: The origins and concentrations of water, carbon, nitrogen and noble gases on Earth. *Earth and Planetary Science Letters* **313**, 56–66 (2012). DOI 10.1016/j.epsl.2011.10.040
304. Marty, B., Altwegg, K., Balsiger, H., Bar-Nun, A., Bekaert, D.V., Berthelier, J.J., Bieler, A., Briois, C., Calmonte, U., Combi, M., De Keyser, J., Fiethe, B., Fuselier, S.A., Gasc, S., Gombosi, T.I., Hansen, K.C., Hässig, M., Jäckel, A., Kopp, E., Korth, A., Le Roy, L., Mall, U., Mousis, O., Owen, T., Rème, H., Rubin, M., Sémon, T., Tzou, C.Y., Waite, J.H., Wurz, P.: Xenon isotopes in 67P/Churyumov-Gerasimenko show that comets contributed to Earth's atmosphere. *Science* **356**, 1069–1072 (2017). DOI 10.1126/science.aal3496
305. Marty, B., Avice, G., Sano, Y., Altwegg, K., Balsiger, H., Hässig, M., Morbidelli, A., Mousis, O., Rubin, M.: Origins of volatile elements (H, C, N, noble gases) on Earth and Mars in light of recent results from the ROSETTA cometary mission. *Earth and Planetary Science Letters* **441**, 91–102 (2016). DOI 10.1016/j.epsl.2016.02.031
306. Marty, B., Yokochi, R.: Water in the Early Earth. *Rev. Mineral Geophys.* **62**, 421–450 (2006)

307. Marzari, F.: Impact of planet-planet scattering on the formation and survival of debris discs. *Monthly Notices of the Royal Astronomical Society* **444**, 1419–1424 (2014). DOI 10.1093/mnras/stu1544
308. Marzari, F., Weidenschilling, S.J.: Eccentric Extrasolar Planets: The Jumping Jupiter Model. *Icarus* **156**, 570–579 (2002). DOI 10.1006/icar.2001.6786
309. Masset, F., Snellgrove, M.: Reversing type II migration: resonance trapping of a lighter giant protoplanet. *Monthly Notices of the Royal Astronomical Society* **320**, L55–L59 (2001). DOI 10.1046/j.1365-8711.2001.04159.x
310. Masset, F.S.: Coorbital thermal torques on low-mass protoplanets. *Monthly Notices of the Royal Astronomical Society* **472**(4), 4204–4219 (2017). DOI 10.1093/mnras/stx2271
311. Masset, F.S., Morbidelli, A., Crida, A., Ferreira, J.: Disk Surface Density Transitions as Protoplanet Traps. *Astrophysical Journal* **642**, 478–487 (2006). DOI 10.1086/500967
312. Matsumoto, Y., Nagasawa, M., Ida, S.: The orbital stability of planets trapped in the first-order mean-motion resonances. *Icarus* **221**(2), 624–631 (2012). DOI 10.1016/j.icarus.2012.08.032
313. Matsumura, S., Ida, S., Nagasawa, M.: Effects of Dynamical Evolution of Giant Planets on Survival of Terrestrial Planets. *Astrophysical Journal* **767**, 129 (2013). DOI 10.1088/0004-637X/767/2/129
314. Matsumura, S., Thommes, E.W., Chatterjee, S., Rasio, F.A.: Unstable Planetary Systems Emerging Out of Gas Disks. *Astrophysical Journal* **714**, 194–206 (2010). DOI 10.1088/0004-637X/714/1/194
315. Matthews, B.C., Krivov, A.V., Wyatt, M.C., Bryden, G., Eiroa, C.: Observations, Modeling, and Theory of Debris Disks. In: H. Beuther, R.S. Klessen, C.P. Dullemond, T. Henning (eds.) *Protostars and Planets VI*, p. 521 (2014)
316. Mayer, L., Lufkin, G., Quinn, T., Wadsley, J.: Fragmentation of Gravitationally Unstable Gaseous Protoplanetary Disks with Radiative Transfer. *Astrophysical Journal Letters* **661**(1), L77–L80 (2007). DOI 10.1086/518433
317. Mayer, L., Quinn, T., Wadsley, J., Stadel, J.: Formation of Giant Planets by Fragmentation of Protoplanetary Disks. *Science* **298**(5599), 1756–1759 (2002). DOI 10.1126/science.1077635
318. Mayor, M., Marmier, M., Lovis, C., Udry, S., Ségransan, D., Pepe, F., Benz, W., Bertaux, J., Bouchy, F., Dumusque, X., Lo Curto, G., Mordasini, C., Queloz, D., Santos, N.C.: The HARPS search for southern extra-solar planets XXXIV. Occurrence, mass distribution and orbital properties of super-Earths and Neptune-mass planets. arXiv:1109.2497 (2011)
319. McCubbin, F.M., Barnes, J.J.: Origin and abundances of H₂O in the terrestrial planets, Moon, and asteroids. *Earth and Planetary Science Letters* **526**, 115771 (2019). DOI 10.1016/j.epsl.2019.115771
320. McNally, C.P., Nelson, R.P., Paardekooper, S.J., Benítez-Llambay, P.: Migrating super-Earths in low-viscosity discs: unveiling the roles of feedback, vortices, and laminar accretion flows. *Monthly Notices of the Royal Astronomical Society* **484**(1), 728–748 (2019). DOI 10.1093/mnras/stz023
321. McNeil, D.S., Nelson, R.P.: On the formation of hot Neptunes and super-Earths. *Monthly Notices of the Royal Astronomical Society* **401**, 1691–1708 (2010). DOI 10.1111/j.1365-2966.2009.15805.x
322. Meech, K., Raymond, S.N.: Origin of Earth's water: sources and constraints. arXiv e-prints arXiv:1912.04361 (2019)
323. Meru, F., Bate, M.R.: On the fragmentation criteria of self-gravitating protoplanetary discs. *Monthly Notices of the Royal Astronomical Society* **410**(1), 559–572 (2011). DOI 10.1111/j.1365-2966.2010.17465.x
324. Meyer, M.R., Carpenter, J.M., Mamajek, E.E., Hillenbrand, L.A., Hollenbach, D., Moro-Martín, A., Kim, J.S., Silverstone, M.D., Najita, J., Hines, D.C., Pascucci, I., Stauffer, J.R., Bouwman, J., Backman, D.E.: Evolution of Mid-Infrared Excess around Sun-like Stars: Constraints on Models of Terrestrial Planet Formation. *Astrophysical Journal Letters* **673**, L181–L184 (2008). DOI 10.1086/527470
325. Millholland, S., Wang, S., Laughlin, G.: Kepler Multi-planet Systems Exhibit Unexpected Intra-system Uniformity in Mass and Radius. *Astrophysical Journal Letters* **849**(2), L33 (2017). DOI 10.3847/2041-8213/aa9714

326. Mills, S.M., Fabrycky, D.C., Migaszewski, C., Ford, E.B., Petigura, E., Isaacson, H.: A resonant chain of four transiting, sub-Neptune planets. *Nature* **533**, 509–512 (2016). DOI 10.1038/nature17445
327. Moeckel, N., Throop, H.B.: Bondi-Hoyle-Lyttleton Accretion Onto a Protoplanetary Disk. *Astrophysical Journal* **707**(1), 268–277 (2009). DOI 10.1088/0004-637X/707/1/268
328. Mojzsis, S.J., Brasser, R., Kelly, N.M., Abramov, O., Werner, S.C.: Onset of Giant Planet Migration before 4480 Million Years Ago. *Astrophysical Journal* **881**(1), 44 (2019). DOI 10.3847/1538-4357/ab2c03
329. Montesinos, B., Eiroa, C., Krivov, A.V., Marshall, J.P., Pilbratt, G.L., Liseau, R., Mora, A., Maldonado, J., Wolf, S., Ertel, S., Bayo, A., Augereau, J.C., Heras, A.M., Fridlund, M., Danchi, W.C., Solano, E., Kirchschrager, F., del Burgo, C., Montes, D.: Incidence of debris discs around FGK stars in the solar neighbourhood. *Astronomy & Astrophysics* **593**, A51 (2016). DOI 10.1051/0004-6361/201628329
330. Monteux, J., Golabek, G.J., Rubie, D.C., Tobie, G., Young, E.D.: Water and the Interior Structure of Terrestrial Planets and Icy Bodies. *Space Science Reviews* **214**(1), 39 (2018). DOI 10.1007/s11214-018-0473-x
331. Moorhead, A.V., Adams, F.C.: Giant planet migration through the action of disk torques and planet planet scattering. *Icarus* **178**, 517–539 (2005). DOI 10.1016/j.icarus.2005.05.005
332. Morales, J.C., Mustill, A.J., Ribas, I., Davies, M.B., Reiners, A., Bauer, F.F., Kossakowski, D., Herrero, E., Rodríguez, E., López-González, M.J., Rodríguez-López, C., Béjar, V.J.S., González-Cuesta, L., Luque, R., Pallé, E., Perger, M., Baroch, D., Johansen, A., Klahr, H., Mordasini, C., Anglada-Escudé, G., Caballero, J.A., Cortés-Contreras, M., Dreizler, S., Lafarga, M., Nagel, E., Passegger, V.M., Reffert, S., Rosich, A., Schweitzer, A., Tal-Or, L., Trifonov, T., Zechmeister, M., Quirrenbach, A., Amado, P.J., Guenther, E.W., Hagen, H.J., Henning, T., Jeffers, S.V., Kaminski, A., Kürster, M., Montes, D., Seifert, W., Abellán, F.J., Abril, M., Aceituno, J., Aceituno, F.J., Alonso-Floriano, F.J., Ammler-von Eiff, M., Antona, R., Arroyo-Torres, B., Azzaro, M., Barrado, D., Becerril-Jarque, S., Benítez, D., Berdiñas, Z.M., Bergond, G., Brinkmüller, M., del Burgo, C., Burn, R., Calvo-Ortega, R., Cano, J., Cárdenas, M.C., Guillén, C.C., Carro, J., Casal, E., Casanova, V., Casasayas-Barris, N., Chaturvedi, P., Cifuentes, C., Claret, A., Colomé, J., Czesla, S., Díez-Alonso, E., Dorda, R., Emsenhuber, A., Fernández, M., Fernández-Martín, A., Ferro, I.M., Fuhrmeister, B., Galadí-Enríquez, D., Cava, I.G., Vargas, M.L.G., García-Piquer, A., Gesa, L., González-Álvarez, E., Hernández, J.I.G., González-Peinado, R., Guàrdia, J., Guijarro, A., de Guindos, E., Hatzes, A.P., Hauschildt, P.H., Hedrosa, R.P., Hermelo, I., Arabi, R.H., Otero, F.H., Hintz, D., Holgado, G., Huber, A., Huke, P., Johnson, E.N., de Juan, E., Kehr, M., Kemmer, J., Kim, M., Klüter, J., Klutsch, A., Labarga, F., Labiche, N., Lalitha, S., Lampón, M., Lara, L.M., Launhardt, R., Lázaro, F.J., Lizon, J.L., Llamas, M., Lodieu, N., López del Fresno, M., Salas, J.F.L., López-Santiago, J., Madinabeitia, H.M., Mall, U., Mancini, L., Mand el, H., Marfil, E., Molina, J.A.M., Martín, E.L., Martín-Fernández, P., Martín-Ruiz, S., Martínez-Rodríguez, H., Marvin, C.J., Mirabet, E., Moya, A., Naranjo, V., Nelson, R.P., Nortmann, L., Nowak, G., Ofir, A., Pascual, J., Pavlov, A., Pedraz, S., Medialdea, D.P., Pérez-Calpena, A., Perryman, M.A.C., Rabaza, O., Ballesta, A.R., Rebolo, R., Redondo, P., Rix, H.W., Rodler, F., Trinidad, A.R., Sabotta, S., Sadegi, S., Salz, M., Sánchez-Blanco, E., Carrasco, M.A.S., Sánchez-López, A., Sanz-Forcada, J., Sarkis, P., Sarmiento, L.F., Schäfer, S., Schlecker, M., Schmitt, J.H.M.M., Schöfer, P., Solano, E., Sota, A., Stahl, O., Stock, S., Stuber, T., Stürmer, J., Suárez, J.C., Taberner, H.M., Tulloch, S.M., Veredas, G., Vico-Linares, J.I., Vilardell, F., Wagner, K., Winkler, J., Wolthoff, V., Yan, F., Osorio, M.R.Z.: A giant exoplanet orbiting a very-low-mass star challenges planet formation models. *Science* **365**(6460), 1441–1445 (2019). DOI 10.1126/science.aax3198
333. Morbidelli, A., Bitsch, B., Crida, A., Gounelle, M., Guillot, T., Jacobson, S., Johansen, A., Lambrechts, M., Lega, E.: Fossilized condensation lines in the Solar System protoplanetary disk. *Icarus* **267**, 368–376 (2016). DOI 10.1016/j.icarus.2015.11.027
334. Morbidelli, A., Chambers, J., Lunine, J.I., Petit, J.M., Robert, F., Valsecchi, G.B., Cyr, K.E.: Source regions and time scales for the delivery of water to Earth. *Meteoritics and Planetary Science* **35**, 1309–1320 (2000). DOI 10.1111/j.1945-5100.2000.tb01518.x

335. Morbidelli, A., Lambrechts, M., Jacobson, S., Bitsch, B.: The great dichotomy of the Solar System: Small terrestrial embryos and massive giant planet cores. *Icarus* **258**, 418–429 (2015). DOI 10.1016/j.icarus.2015.06.003
336. Morbidelli, A., Levison, H.F., Tsiganis, K., Gomes, R.: Chaotic capture of Jupiter's Trojan asteroids in the early Solar System. *Nature* **435**, 462–465 (2005). DOI 10.1038/nature03540
337. Morbidelli, A., Nesvorný, D.: Dynamics of pebbles in the vicinity of a growing planetary embryo: hydro-dynamical simulations. *Astronomy & Astrophysics* **546**, A18 (2012). DOI 10.1051/0004-6361/201219824
338. Morbidelli, A., Nesvorný, D., Laurenz, V., Marchi, S., Rubie, D.C., Elkins-Tanton, L., Wieczorek, M., Jacobson, S.: The timeline of the lunar bombardment: Revisited. *Icarus* **305**, 262–276 (2018). DOI 10.1016/j.icarus.2017.12.046
339. Morbidelli, A., Raymond, S.N.: Challenges in planet formation. *Journal of Geophysical Research (Planets)* **121**, 1962–1980 (2016). DOI 10.1002/2016JE005088
340. Morbidelli, A., Tsiganis, K., Crida, A., Levison, H.F., Gomes, R.: Dynamics of the Giant Planets of the Solar System in the Gaseous Protoplanetary Disk and Their Relationship to the Current Orbital Architecture. *Astronomical Journal* **134**, 1790–1798 (2007). DOI 10.1086/521705
341. Morbidelli, A., Wood, B.J.: Late Accretion and the Late Veneer. Washington DC American Geophysical Union Geophysical Monograph Series **212**, 71–82 (2015). DOI 10.1002/9781118860359.ch4
342. Mordasini, C., Alibert, Y., Benz, W.: Extrasolar planet population synthesis. I. Method, formation tracks, and mass-distance distribution. *Astronomy & Astrophysics* **501**, 1139–1160 (2009). DOI 10.1051/0004-6361/200810301
343. Mori, S., Bai, X.N., Okuzumi, S.: Temperature Structure in the Inner Regions of Protoplanetary Disks: Inefficient Accretion Heating Controlled by Nonideal Magnetohydrodynamics. *Astrophysical Journal* **872**(1), 98 (2019). DOI 10.3847/1538-4357/ab0022
344. Moriarty, J., Ballard, S.: The Kepler Dichotomy in Planetary Disks: Linking Kepler Observables to Simulations of Late-stage Planet Formation. *Astrophysical Journal* **832**, 34 (2016). DOI 10.3847/0004-637X/832/1/34
345. Morishima, R., Schmidt, M.W., Stadel, J., Moore, B.: Formation and Accretion History of Terrestrial Planets from Runaway Growth through to Late Time: Implications for Orbital Eccentricity. *Astrophysical Journal* **685**, 1247–1261 (2008). DOI 10.1086/590948
346. Morishima, R., Stadel, J., Moore, B.: From planetesimals to terrestrial planets: N-body simulations including the effects of nebular gas and giant planets. *Icarus* **207**, 517–535 (2010). DOI 10.1016/j.icarus.2009.11.038
347. Moro-Martín, A., Carpenter, J.M., Meyer, M.R., Hillenbrand, L.A., Malhotra, R., Hollenbach, D., Najita, J., Henning, T., Kim, J.S., Bouwman, J., Silverstone, M.D., Hines, D.C., Wolf, S., Pascucci, I., Mamajek, E.E., Lunine, J.: Are Debris Disks and Massive Planets Correlated? *Astrophysical Journal* **658**, 1312–1321 (2007). DOI 10.1086/511746
348. Moro-Martín, A., Marshall, J.P., Kennedy, G., Sibthorpe, B., Matthews, B.C., Eiroa, C., Wyatt, M.C., Lestrade, J.F., Maldonado, J., Rodríguez, D., Greaves, J.S., Montesinos, B., Mora, A., Booth, M., Duchêne, G., Wilner, D., Horner, J.: Does the Presence of Planets Affect the Frequency and Properties of Extrasolar Kuiper Belts? Results from the Herschel Debris and Dunes Surveys. *Astrophysical Journal* **801**, 143 (2015). DOI 10.1088/0004-637X/801/2/143
349. Mottl, M., Glazer, B., Kaiser, R., Meech, K.: Water and astrobiology. *Chemie der Erde / Geochemistry* **67**(4), 253–282 (2007). DOI 10.1016/j.chemer.2007.09.002
350. Mukhopadhyay, S.: Early differentiation and volatile accretion recorded in deep-mantle neon and xenon. *Nature* **486**, 101–104 (2012). DOI 10.1038/nature11141
351. Mulders, G.D., Mordasini, C., Pascucci, I., Ciesla, F.J., Emsenhuber, A., Apai, D.: The Exoplanet Population Observation Simulator. II – Population Synthesis in the Era of Kepler. arXiv e-prints arXiv:1905.08804 (2019)
352. Mulders, G.D., Pascucci, I., Apai, D., Ciesla, F.J.: The Exoplanet Population Observation Simulator. I. The Inner Edges of Planetary Systems. *Astronomical Journal* **156**, 24 (2018). DOI 10.3847/1538-3881/aac5ea

353. Mundy, L.G., Looney, L.W., Welch, W.J.: The Structure and Evolution of Envelopes and Disks in Young Stellar Systems. *Protostars and Planets IV* pp. 355–+ (2000)
354. Muralidharan, K., Deymier, P., Stimpfl, M., de Leeuw, N.H., Drake, M.J.: Origin of water in the inner Solar System: A kinetic Monte Carlo study of water adsorption on forsterite. *Icarus* **198**(2), 400–407 (2008). DOI 10.1016/j.icarus.2008.07.017
355. Nagasawa, M., Ida, S., Bessho, T.: Formation of Hot Planets by a Combination of Planet Scattering, Tidal Circularization, and the Kozai Mechanism. *Astrophysical Journal* **678**, 498–508 (2008). DOI 10.1086/529369
356. Nagasawa, M., Lin, D.N.C., Thommes, E.: Dynamical Shake-up of Planetary Systems. I. Embryo Trapping and Induced Collisions by the Sweeping Secular Resonance and Embryo-Disk Tidal Interaction. *Astrophysical Journal* **635**, 578–598 (2005). DOI 10.1086/497386
357. Nayakshin, S.: Tidal downsizing model - I. Numerical methods: saving giant planets from tidal disruptions. *Monthly Notices of the Royal Astronomical Society* **454**(1), 64–82 (2015). DOI 10.1093/mnras/stv1915
358. Ndugu, N., Bitsch, B., Jurua, E.: Planet population synthesis driven by pebble accretion in cluster environments. *Monthly Notices of the Royal Astronomical Society* **474**(1), 886–897 (2018). DOI 10.1093/mnras/stx2815
359. Neishtadt, A.: The separation of motions in systems with rapidly rotating phase. *Journal of Applied Mathematics and Mechanics* **48**(2), 133–139 (1984). DOI 10.1016/0021-8928(84)90078-9
360. Nesvorný, D.: Evidence for Slow Migration of Neptune from the Inclination Distribution of Kuiper Belt Objects. *Astronomical Journal* **150**, 73 (2015). DOI 10.1088/0004-6256/150/3/73
361. Nesvorný, D.: Dynamical Evolution of the Early Solar System. *Annual Reviews of Astronomy and Astrophysics* **56**, 137–174 (2018). DOI 10.1146/annurev-astro-081817-052028
362. Nesvorný, D., Li, R., Youdin, A.N., Simon, J.B., Grundy, W.M.: Trans-Neptunian binaries as evidence for planetesimal formation by the streaming instability. *Nature Astronomy* **3**, 808–812 (2019). DOI 10.1038/s41550-019-0806-z
363. Nesvorný, D., Morbidelli, A.: Statistical Study of the Early Solar System's Instability with Four, Five, and Six Giant Planets. *Astronomical Journal* **144**, 117 (2012). DOI 10.1088/0004-6256/144/4/117
364. Nesvorný, D., Vokrouhlický, D., Bottke, W.F., Levison, H.F.: Evidence for very early migration of the Solar System planets from the Patroclus-Menoetius binary Jupiter Trojan. *Nature Astronomy* **2**, 878–882 (2018). DOI 10.1038/s41550-018-0564-3
365. Nesvorný, D., Vokrouhlický, D., Deienno, R.: Capture of Irregular Satellites at Jupiter. *Astrophysical Journal* **784**(1), 22 (2014). DOI 10.1088/0004-637X/784/1/22
366. Nesvorný, D., Vokrouhlický, D., Morbidelli, A.: Capture of Trojans by Jumping Jupiter. *Astrophysical Journal* **768**, 45 (2013). DOI 10.1088/0004-637X/768/1/45
367. Nesvorný, D., Youdin, A.N., Richardson, D.C.: Formation of Kuiper Belt Binaries by Gravitational Collapse. *Astronomical Journal* **140**(3), 785–793 (2010). DOI 10.1088/0004-6256/140/3/785
368. Nimmo, F., Kleine, T.: How rapidly did Mars accrete? Uncertainties in the Hf/W timing of core formation. *Icarus* **191**, 497–504 (2007). DOI 10.1016/j.icarus.2007.05.002
369. Noll, K.S., Grundy, W.M., Chiang, E.I., Margot, J.L., Kern, S.D.: Binaries in the Kuiper Belt, p. 345 (2008)
370. Nomura, R., Hirose, K., Uesegi, K., Ohishi, Y., Tsuchiyama, A., Miyake, A., Ueno, Y.: Low Core-Mantle Boundary Temperature Inferred from the Solidus of Pyrolyte. *Science* **343**, 522–525 (2014)
371. Nyquist, L.E., Kleine, T., Shih, C.Y., Reese, Y.D.: The distribution of short-lived radioisotopes in the early solar system and the chronology of asteroid accretion, differentiation, and secondary mineralization. *Geochemica and Cosmochemica Acta* **73**, 5115–5136 (2009). DOI 10.1016/j.gca.2008.12.031
372. O'Brien, D.P., Izidoro, A., Jacobson, S.A., Raymond, S.N., Rubie, D.C.: The Delivery of Water During Terrestrial Planet Formation. *Space Science Reviews* **214**(1), 47 (2018). DOI 10.1007/s11214-018-0475-8

373. O'Brien, D.P., Morbidelli, A., Levison, H.F.: Terrestrial planet formation with strong dynamical friction. *Icarus* **184**, 39–58 (2006). DOI 10.1016/j.icarus.2006.04.005
374. O'Brien, D.P., Walsh, K.J., Morbidelli, A., Raymond, S.N., Mandell, A.M.: Water delivery and giant impacts in the Grand Tack scenario. *Icarus* **239**, 74–84 (2014). DOI 10.1016/j.icarus.2014.05.009
375. Ogihara, M., Ida, S.: N-Body Simulations of Planetary Accretion Around M Dwarf Stars. *Astrophysical Journal* **699**, 824–838 (2009). DOI 10.1088/0004-637X/699/1/824
376. Ogihara, M., Kokubo, E., Suzuki, T.K., Morbidelli, A.: Formation of close-in super-Earths in evolving protoplanetary disks due to disk winds. *Astronomy & Astrophysics* **615**, A63 (2018). DOI 10.1051/0004-6361/201832720
377. Ogihara, M., Kokubo, E., Suzuki, T.K., Morbidelli, A.: Formation of the terrestrial planets in the solar system around 1 au via radial concentration of planetesimals. *Astronomy & Astrophysics* **612**, L5 (2018). DOI 10.1051/0004-6361/201832654
378. Ogihara, M., Morbidelli, A., Guillot, T.: A reassessment of the in situ formation of close-in super-Earths. *Astronomy & Astrophysics* **578**, A36 (2015). DOI 10.1051/0004-6361/201525884
379. Oka, A., Nakamoto, T., Ida, S.: Evolution of Snow Line in Optically Thick Protoplanetary Disks: Effects of Water Ice Opacity and Dust Grain Size. *Astrophysical Journal* **738**(2), 141 (2011). DOI 10.1088/0004-637X/738/2/141
380. Okuzumi, S., Tanaka, H., Kobayashi, H., Wada, K.: Rapid Coagulation of Porous Dust Aggregates outside the Snow Line: A Pathway to Successful Icy Planetesimal Formation. *Astrophysical Journal* **752**(2), 106 (2012). DOI 10.1088/0004-637X/752/2/106
381. Ormel, C.W., Klahr, H.H.: The effect of gas drag on the growth of protoplanets. Analytical expressions for the accretion of small bodies in laminar disks. *Astronomy & Astrophysics* **520**, A43 (2010). DOI 10.1051/0004-6361/201014903
382. Owen, J.E., Ercolano, B., Clarke, C.J.: Protoplanetary disc evolution and dispersal: the implications of X-ray photoevaporation. *Monthly Notices of the Royal Astronomical Society* **412**(1), 13–25 (2011). DOI 10.1111/j.1365-2966.2010.17818.x
383. Owen, J.E., Wu, Y.: Kepler Planets: A Tale of Evaporation. *Astrophysical Journal* **775**, 105 (2013). DOI 10.1088/0004-637X/775/2/105
384. Owen, J.E., Wu, Y.: The Evaporation Valley in the Kepler Planets. *Astrophysical Journal* **847**, 29 (2017). DOI 10.3847/1538-4357/aa890a
385. Paardekooper, S.J.: Dynamical corotation torques on low-mass planets. *Monthly Notices of the Royal Astronomical Society* **444**, 2031–2042 (2014). DOI 10.1093/mnras/stu1542
386. Paardekooper, S.J., Baruteau, C., Crida, A., Kley, W.: A torque formula for non-isothermal type I planetary migration - I. Unsaturated horseshoe drag. *Monthly Notices of the Royal Astronomical Society* **401**, 1950–1964 (2010). DOI 10.1111/j.1365-2966.2009.15782.x
387. Paardekooper, S.J., Baruteau, C., Kley, W.: A torque formula for non-isothermal Type I planetary migration - II. Effects of diffusion. *Monthly Notices of the Royal Astronomical Society* **410**, 293–303 (2011). DOI 10.1111/j.1365-2966.2010.17442.x
388. Paardekooper, S.J., Mellema, G.: Halting type I planet migration in non-isothermal disks. *Astronomy & Astrophysics* **459**, L17–L20 (2006). DOI 10.1051/0004-6361:20066304
389. Pätzold, M., Andert, T.P., Hahn, M., Barriot, J.P., Asmar, S.W., Häusler, B., Bird, M.K., Tellmann, S., Oschlisniok, J., Peter, K.: The Nucleus of comet 67P/Churyumov-Gerasimenko - Part I: The global view - nucleus mass, mass-loss, porosity, and implications. *Monthly Notices of the Royal Astronomical Society* **483**(2), 2337–2346 (2019). DOI 10.1093/mnras/sty3171
390. Pecauc, M.J., Mamajek, E.E.: The star formation history and accretion-disc fraction among the K-type members of the Scorpius-Centaurus OB association. *Monthly Notices of the Royal Astronomical Society* **461**(1), 794–815 (2016). DOI 10.1093/mnras/stw1300
391. Petigura, E.A., Howard, A.W., Marcy, G.W.: Prevalence of Earth-size planets orbiting Sun-like stars. *Proceedings of the National Academy of Science* **110**, 19273–19278 (2013)
392. Pfalzner, S., Steinhausen, M., Menten, K.: Short Dissipation Times of Proto-planetary Disks: An Artifact of Selection Effects? *Astrophysical Journal Letters* **793**, L34 (2014). DOI 10.1088/2041-8205/793/2/L34

393. Pichierri, G., Morbidelli, A., Crida, A.: Capture into first-order resonances and long-term stability of pairs of equal-mass planets. *Celestial Mechanics and Dynamical Astronomy* **130**(8), 54 (2018). DOI 10.1007/s10569-018-9848-2
394. Pierens, A.: Fast migration of low-mass planets in radiative discs. *Monthly Notices of the Royal Astronomical Society* **454**, 2003–2014 (2015). DOI 10.1093/mnras/stv2024
395. Pierens, A., Nelson, R.P.: Constraints on resonant-trapping for two planets embedded in a protoplanetary disc. *Astronomy & Astrophysics* **482**, 333–340 (2008). DOI 10.1051/0004-6361/20079062
396. Pierens, A., Raymond, S.N.: Two phase, inward-then-outward migration of Jupiter and Saturn in the gaseous solar nebula. *Astronomy & Astrophysics* **533**, A131 (2011). DOI 10.1051/0004-6361/201117451
397. Pierens, A., Raymond, S.N.: Migration of accreting planets in radiative discs from dynamical torques. *Monthly Notices of the Royal Astronomical Society* **462**(4), 4130–4140 (2016). DOI 10.1093/mnras/stw1904
398. Pierens, A., Raymond, S.N., Nesvornyy, D., Morbidelli, A.: Outward Migration of Jupiter and Saturn in 3:2 or 2:1 Resonance in Radiative Disks: Implications for the Grand Tack and Nice models. *Astrophysical Journal Letters* **795**, L11 (2014). DOI 10.1088/2041-8205/795/1/L11
399. Pinte, C., Dent, W.R.F., Ménard, F., Hales, A., Hill, T., Cortes, P., de Gregorio-Monsalvo, I.: Dust and Gas in the Disk of HL Tauri: Surface Density, Dust Settling, and Dust-to-gas Ratio. *Astrophysical Journal* **816**(1), 25 (2016). DOI 10.3847/0004-637X/816/1/25
400. Pirani, S., Johansen, A., Bitsch, B., Mustill, A.J., Turrini, D.: Consequences of planetary migration on the minor bodies of the early solar system. *Astronomy & Astrophysics* **623**, A169 (2019). DOI 10.1051/0004-6361/201833713
401. Piso, A.M.A., Youdin, A.N.: On the Minimum Core Mass for Giant Planet Formation at Wide Separations. *Astrophysical Journal* **786**(1), 21 (2014). DOI 10.1088/0004-637X/786/1/21
402. Poincare, H.: Les methodes nouvelles de la mecanique celeste (1892)
403. Poincare, H.: Sur une forme Nouvelle des Equations du Probleme des Trois Corps. *Bulletin Astronomique, Serie I* **14**, 53–67 (1897)
404. Pollack, J.B., Hubickyj, O., Bodenheimer, P., Lissauer, J.J., Podolak, M., Greenzweig, Y.: Formation of the Giant Planets by Concurrent Accretion of Solids and Gas. *Icarus* **124**, 62–85 (1996). DOI 10.1006/icar.1996.0190
405. Quarles, B., Kaib, N.: Instabilities in the Early Solar System Due to a Self-gravitating Disk. *Astronomical Journal* **157**(2), 67 (2019). DOI 10.3847/1538-3881/aafa71
406. Quintana, E.V., Barclay, T., Borucki, W.J., Rowe, J.F., Chambers, J.E.: The Frequency of Giant Impacts on Earth-like Worlds. *Astrophysical Journal* **821**, 126 (2016). DOI 10.3847/0004-637X/821/2/126
407. Quintana, E.V., Barclay, T., Raymond, S.N., Rowe, J.F., Bolmont, E., Caldwell, D.A., Howell, S.B., Kane, S.R., Huber, D., Crepp, J.R., Lissauer, J.J., Ciardi, D.R., Coughlin, J.L., Everett, M.E., Henze, C.E., Horch, E., Isaacson, H., Ford, E.B., Adams, F.C., Still, M., Hunter, R.C., Quarles, B., Selsis, F.: An Earth-Sized Planet in the Habitable Zone of a Cool Star. *Science* **344**, 277–280 (2014). DOI 10.1126/science.1249403
408. Rafikov, R.R.: Fast Accretion of Small Planetesimals by Protoplanetary Cores. *Astronomical Journal* **128**, 1348–1363 (2004). DOI 10.1086/423216
409. Rasio, F.A., Ford, E.B.: Dynamical instabilities and the formation of extrasolar planetary systems. *Science* **274**, 954–956 (1996). DOI 10.1126/science.274.5289.954
410. Raymond, S.N., Armitage, P.J., Gorelick, N.: Planet-Planet Scattering in Planetesimal Disks. II. Predictions for Outer Extrasolar Planetary Systems. *Astrophysical Journal* **711**, 772–795 (2010). DOI 10.1088/0004-637X/711/2/772
411. Raymond, S.N., Armitage, P.J., Moro-Martín, A., Booth, M., Wyatt, M.C., Armstrong, J.C., Mandell, A.M., Selsis, F., West, A.A.: Debris disks as signposts of terrestrial planet formation. *Astronomy & Astrophysics* **530**, A62 (2011). DOI 10.1051/0004-6361/201116456
412. Raymond, S.N., Armitage, P.J., Moro-Martín, A., Booth, M., Wyatt, M.C., Armstrong, J.C., Mandell, A.M., Selsis, F., West, A.A.: Debris disks as signposts of terrestrial planet formation. II. Dependence of exoplanet architectures on giant planet and disk properties. *Astronomy & Astrophysics* **541**, A11 (2012). DOI 10.1051/0004-6361/201117049

413. Raymond, S.N., Armitage, P.J., Veras, D.: Interstellar Object 'Oumuamua as an Extinct Fragment of an Ejected Cometary Planetesimal. *Astrophysical Journal Letters* **856**(1), L7 (2018). DOI 10.3847/2041-8213/aab4f6
414. Raymond, S.N., Armitage, P.J., Veras, D., Quintana, E.V., Barclay, T.: Implications of the interstellar object 1I/'Oumuamua for planetary dynamics and planetesimal formation. *Monthly Notices of the Royal Astronomical Society* **476**, 3031–3038 (2018). DOI 10.1093/mnras/sty468
415. Raymond, S.N., Barnes, R., Armitage, P.J., Gorelick, N.: Mean Motion Resonances from Planet-Planet Scattering. *Astrophysical Journal Letters* **687**, L107–L110 (2008). DOI 10.1086/593301
416. Raymond, S.N., Barnes, R., Mandell, A.M.: Observable consequences of planet formation models in systems with close-in terrestrial planets. *Monthly Notices of the Royal Astronomical Society* **384**, 663–674 (2008). DOI 10.1111/j.1365-2966.2007.12712.x
417. Raymond, S.N., Barnes, R., Veras, D., Armitage, P.J., Gorelick, N., Greenberg, R.: Planet-Planet Scattering Leads to Tightly Packed Planetary Systems. *Astrophysical Journal Letters* **696**, L98–L101 (2009). DOI 10.1088/0004-637X/696/1/L98
418. Raymond, S.N., Boulet, T., Izidoro, A., Esteves, L., Bitsch, B.: Migration-driven diversity of super-Earth compositions. *Monthly Notices of the Royal Astronomical Society* **479**, L81–L85 (2018). DOI 10.1093/mnras/sly100
419. Raymond, S.N., Cossou, C.: No universal minimum-mass extrasolar nebula: evidence against in situ accretion of systems of hot super-Earths. *Monthly Notices of the Royal Astronomical Society* **440**, L11–L15 (2014). DOI 10.1093/mnras/slu011
420. Raymond, S.N., Izidoro, A.: Origin of water in the inner Solar System: Planetesimals scattered inward during Jupiter and Saturn's rapid gas accretion. *Icarus* **297**, 134–148 (2017). DOI 10.1016/j.icarus.2017.06.030
421. Raymond, S.N., Izidoro, A.: The empty primordial asteroid belt. *Science Advances* **3**, e1701138 (2017). DOI 10.1126/sciadv.1701138
422. Raymond, S.N., Izidoro, A., Morbidelli, A.: Solar System Formation in the Context of Extra-Solar Planets. arXiv e-prints arXiv:1812.01033 (2018)
423. Raymond, S.N., Kokubo, E., Morbidelli, A., Morishima, R., Walsh, K.J.: Terrestrial Planet Formation at Home and Abroad. *Protostars and Planets VI* pp. 595–618 (2014)
424. Raymond, S.N., Mandell, A.M., Sigurdsson, S.: Exotic Earths: Forming Habitable Worlds with Giant Planet Migration. *Science* **313**, 1413–1416 (2006). DOI 10.1126/science.1130461
425. Raymond, S.N., Morbidelli, A.: The Grand Tack model: a critical review. In: *Complex Planetary Systems, Proceedings of the International Astronomical Union, IAU Symposium*, vol. 310, pp. 194–203 (2014). DOI 10.1017/S1743921314008254
426. Raymond, S.N., O'Brien, D.P., Morbidelli, A., Kaib, N.A.: Building the terrestrial planets: Constrained accretion in the inner Solar System. *Icarus* **203**, 644–662 (2009). DOI 10.1016/j.icarus.2009.05.016
427. Raymond, S.N., Quinn, T., Lunine, J.I.: Making other earths: dynamical simulations of terrestrial planet formation and water delivery. *Icarus* **168**, 1–17 (2004). DOI 10.1016/j.icarus.2003.11.019
428. Raymond, S.N., Quinn, T., Lunine, J.I.: High-resolution simulations of the final assembly of Earth-like planets I. Terrestrial accretion and dynamics. *Icarus* **183**, 265–282 (2006). DOI 10.1016/j.icarus.2006.03.011
429. Raymond, S.N., Quinn, T., Lunine, J.I.: High-Resolution Simulations of The Final Assembly of Earth-Like Planets. 2. Water Delivery And Planetary Habitability. *Astrobiology* **7**, 66–84 (2007). DOI 10.1089/ast.2006.06-0126
430. Raymond, S.N., Scalo, J., Meadows, V.S.: A Decreased Probability of Habitable Planet Formation around Low-Mass Stars. *Astrophysical Journal* **669**, 606–614 (2007). DOI 10.1086/521587
431. Raymond, S.N., Schlichting, H.E., Hersant, F., Selsis, F.: Dynamical and collisional constraints on a stochastic late veneer on the terrestrial planets. *Icarus* **226**(1), 671–681 (2013). DOI 10.1016/j.icarus.2013.06.019

432. Ribas, I., Miralda-Escudé, J.: The eccentricity-mass distribution of exoplanets: signatures of different formation mechanisms? *Astronomy & Astrophysics* **464**, 779–785 (2007). DOI 10.1051/0004-6361:20065726
433. Ribeiro, R., Morbidelli, A., Raymond, S., Izidoro, A., Gomes, R.: Dynamical evidence for an early giant planet instability. Submitted to *Icarus* (2020)
434. Rivera, E.J., Laughlin, G., Butler, R.P., Vogt, S.S., Haghighipour, N., Meschiari, S.: The Lick-Carnegie Exoplanet Survey: a Uranus-Mass Fourth Planet for GJ 876 in an Extrasolar Laplace Configuration. *Astrophysical Journal* **719**, 890–899 (2010). DOI 10.1088/0004-637X/719/1/890
435. Robert, C.M.T., Crida, A., Lega, E., Méheut, H., Morbidelli, A.: Toward a new paradigm for Type II migration. *Astronomy & Astrophysics* **617**, A98 (2018). DOI 10.1051/0004-6361/201833539
436. Robert, F., Merlivat, L., Javoy, M.: Water and Deuterium Content in Eight Chondrites. *Meteoritics* **12**, 349 (1977)
437. Rogers, L.A.: Most 1.6 Earth-radius Planets are Not Rocky. *Astrophysical Journal* **801**, 41 (2015). DOI 10.1088/0004-637X/801/1/41
438. Ronnet, T., Mousis, O., Vernazza, P., Lunine, J.I., Crida, A.: Saturn’s Formation and Early Evolution at the Origin of Jupiter’s Massive Moons. *Astronomical Journal* **155**(5), 224 (2018). DOI 10.3847/1538-3881/aabcc7
439. Rowan, D., Meschiari, S., Laughlin, G., Vogt, S.S., Butler, R.P., Burt, J., Wang, S., Holden, B., Hanson, R., Arriagada, P., Keiser, S., Teske, J., Diaz, M.: The Lick-Carnegie Exoplanet Survey: HD 32963 – A New Jupiter Analog Orbiting a Sun-like Star. *Astrophysical Journal* **817**, 104 (2016). DOI 10.3847/0004-637X/817/2/104
440. Rowe, J.F., Bryson, S.T., Marcy, G.W., Lissauer, J.J., Jontof-Hutter, D., Mullally, F., Gilliland, R.L., Issacson, H., Ford, E., Howell, S.B., Borucki, W.J., Haas, M., Huber, D., Steffen, J.H., Thompson, S.E., Quintana, E., Barclay, T., Still, M., Fortney, J., Gautier III, T.N., Hunter, R., Caldwell, D.A., Ciardi, D.R., Devore, E., Cochran, W., Jenkins, J., Agol, E., Carter, J.A., Geary, J.: Validation of Kepler’s Multiple Planet Candidates. III. Light Curve Analysis and Announcement of Hundreds of New Multi-planet Systems. *Astrophysical Journal* **784**, 45 (2014). DOI 10.1088/0004-637X/784/1/45
441. Rubie, D.C., Jacobson, S.A., Morbidelli, A., O’Brien, D.P., Young, E.D., de Vries, J., Nimmo, F., Palme, H., Frost, D.J.: Accretion and differentiation of the terrestrial planets with implications for the compositions of early-formed Solar System bodies and accretion of water. *Icarus* **248**, 89–108 (2015). DOI 10.1016/j.icarus.2014.10.015
442. Safronov, V.S.: Evolution of the protoplanetary cloud and formation of the earth and planets. (1972)
443. Santos, N.C., Israelian, G., Mayor, M.: The metal-rich nature of stars with planets. *Astronomy & Astrophysics* **373**, 1019–1031 (2001). DOI 10.1051/0004-6361:20010648
444. Sasselov, D.D., Lecar, M.: On the Snow Line in Dusty Protoplanetary Disks. *Astrophysical Journal* **528**, 995–998 (2000). DOI 10.1086/308209
445. Sato, T., Okuzumi, S., Ida, S.: On the water delivery to terrestrial embryos by ice pebble accretion. *Astronomy & Astrophysics* **589**, A15 (2016). DOI 10.1051/0004-6361/201527069
446. Schäfer, U., Yang, C.C., Johansen, A.: Initial mass function of planetesimals formed by the streaming instability. *Astronomy & Astrophysics* **597**, A69 (2017). DOI 10.1051/0004-6361/201629561
447. Schiller, M., Bizzarro, M., Fernandes, V.A.: Isotopic evolution of the protoplanetary disk and the building blocks of Earth and the Moon. *Nature* **555**(7697), 507–510 (2018). DOI 10.1038/nature25990
448. Schiller, M., Connelly, J.N., Glad, A.C., Mikouchi, T., Bizzarro, M.: Early accretion of protoplanets inferred from a reduced inner solar system ^{26}Al inventory. *Earth and Planetary Science Letters* **420**, 45–54 (2015). DOI 10.1016/j.epsl.2015.03.028
449. Schlichting, H.E.: Formation of Close in Super-Earths and Mini-Neptunes: Required Disk Masses and their Implications. *Astrophysical Journal Letters* **795**, L15 (2014). DOI 10.1088/2041-8205/795/1/L15

450. Schoonenberg, D., Ormel, C.W.: Planetesimal formation near the snowline: in or out? *Astronomy & Astrophysics* **602**, A21 (2017). DOI 10.1051/0004-6361/201630013
451. Seager, S., Kuchner, M., Hier-Majumder, C.A., Militzer, B.: Mass-Radius Relationships for Solid Exoplanets. *Astrophysical Journal* **669**(2), 1279–1297 (2007). DOI 10.1086/521346
452. Selsis, F., Chazelas, B., Bordé, P., Ollivier, M., Brachet, F., Decaudin, M., Bouchy, F., Ehrenreich, D., Griefmeier, J.M., Lammer, H., Sotin, C., Grasset, O., Moutou, C., Barge, P., Deleuil, M., Mawet, D., Despois, D., Kasting, J.F., Léger, A.: Could we identify hot ocean-planets with CoRoT, Kepler and Doppler velocimetry? *Icarus* **191**, 453–468 (2007). DOI 10.1016/j.icarus.2007.04.010
453. Sessin, W., Ferraz-Mello, S.: Motion of two planets with periods commensurable in the ratio 2:1 solutions of the hori auxiliary system. *Celestial Mechanics* **32**(4), 307–332 (1984). DOI 10.1007/BF01229087
454. Shakura, N.I., Sunyaev, R.A.: Black holes in binary systems. Observational appearance. *Astronomy & Astrophysics* **24**, 337–355 (1973)
455. Sharp, Z.D.: Nebular ingassing as a source of volatiles to the Terrestrial planets. *Chemical Geology* **448**, 137–150 (2017). DOI 10.1016/j.chemgeo.2016.11.018
456. Simon, J.B., Armitage, P.J., Li, R., Youdin, A.N.: The Mass and Size Distribution of Planetesimals Formed by the Streaming Instability. I. The Role of Self-gravity. *Astrophysical Journal* **822**, 55 (2016). DOI 10.3847/0004-637X/822/1/55
457. Simon, J.B., Armitage, P.J., Youdin, A.N., Li, R.: Evidence for Universality in the Initial Planetesimal Mass Function. *Astrophysical Journal Letters* **847**, L12 (2017). DOI 10.3847/2041-8213/aa8c79
458. Snellgrove, M.D., Papaloizou, J.C.B., Nelson, R.P.: On disc driven inward migration of resonantly coupled planets with application to the system around GJ876. *Astronomy & Astrophysics* **374**, 1092–1099 (2001). DOI 10.1051/0004-6361:20010779
459. Sosa, A., Fernández, J.A.: Masses of long-period comets derived from non-gravitational effects - analysis of the computed results and the consistency and reliability of the non-gravitational parameters. *Monthly Notices of the Royal Astronomical Society* **416**(1), 767–782 (2011). DOI 10.1111/j.1365-2966.2011.19111.x
460. Sotin, C., Grasset, O., Mocquet, A.: Mass radius curve for extrasolar Earth-like planets and ocean planets. *Icarus* **191**(1), 337–351 (2007). DOI 10.1016/j.icarus.2007.04.006
461. Stimpfl, M., Walker, A.M., Drake, M.J., de Leeuw, N.H., Deymier, P.: An ångström-sized window on the origin of water in the inner solar system: Atomistic simulation of adsorption of water on olivine. *Journal of Crystal Growth* **294**(1), 83–95 (2006). DOI 10.1016/j.jcrysgro.2006.05.057
462. Stone, J.M., Ostriker, E.C., Gammie, C.F.: Dissipation in Compressible Magnetohydrodynamic Turbulence. *Astrophysical Journal Letters* **508**(1), L99–L102 (1998). DOI 10.1086/311718
463. Su, K.Y.L., Rieke, G.H., Stansberry, J.A., Bryden, G., Stapelfeldt, K.R., Trilling, D.E., Muzerolle, J., Beichman, C.A., Moro-Martín, A., Hines, D.C., Werner, M.W.: Debris Disk Evolution around A Stars. *Astrophysical Journal* **653**, 675–689 (2006). DOI 10.1086/508649
464. Suzuki, D., Bennett, D.P., Sumi, T., Bond, I.A., Rogers, L.A., Abe, F., Asakura, Y., Bhattacharya, A., Donachie, M., Freeman, M., Fukui, A., Hirao, Y., Itow, Y., Koshimoto, N., Li, M.C.A., Ling, C.H., Masuda, K., Matsubara, Y., Muraki, Y., Nagakane, M., Onishi, K., Oyokawa, H., Rattenbury, N., Saito, T., Sharan, A., Shibai, H., Sullivan, D.J., Tristram, P.J., Yonehara, A., MOA Collaboration: The Exoplanet Mass-ratio Function from the MOA-II Survey: Discovery of a Break and Likely Peak at a Neptune Mass. *Astrophysical Journal* **833**, 145 (2016). DOI 10.3847/1538-4357/833/2/145
465. Suzuki, T.K., Ogihara, M., Morbidelli, A., Crida, A., Guillot, T.: Evolution of protoplanetary discs with magnetically driven disc winds. *Astronomy & Astrophysics* **596**, A74 (2016). DOI 10.1051/0004-6361/201628955
466. Svetsov, V.V.: Atmospheric erosion and replenishment induced by impacts of cosmic bodies upon the Earth and Mars. *Solar System Research* **41**(1), 28–41 (2007). DOI 10.1134/S0038094607010030

467. Tanaka, H., Takeuchi, T., Ward, W.R.: Three-Dimensional Interaction between a Planet and an Isothermal Gaseous Disk. I. Corotation and Lindblad Torques and Planet Migration. *Astrophysical Journal* **565**, 1257–1274 (2002). DOI 10.1086/324713
468. Tanaka, H., Ward, W.R.: Three-dimensional Interaction between a Planet and an Isothermal Gaseous Disk. II. Eccentricity Waves and Bending Waves. *Astrophysical Journal* **602**, 388–395 (2004). DOI 10.1086/380992
469. Tera, F., Papanastassiou, D.A., Wasserburg, G.J.: Isotopic evidence for a terminal lunar cataclysm. *Earth and Planetary Science Letters* **22**, 1 (1974). DOI 10.1016/0012-821X(74)90059-4
470. Terquem, C., Papaloizou, J.C.B.: Migration and the Formation of Systems of Hot Super-Earths and Neptunes. *Astrophysical Journal* **654**, 1110–1120 (2007). DOI 10.1086/509497
471. Thommes, E.W., Duncan, M.J., Levison, H.F.: Oligarchic growth of giant planets. *Icarus* **161**, 431–455 (2003). DOI 10.1016/S0019-1035(02)00043-X
472. Thommes, E.W., Matsumura, S., Rasio, F.A.: Gas Disks to Gas Giants: Simulating the Birth of Planetary Systems. *Science* **321**, 814– (2008). DOI 10.1126/science.1159723
473. Throop, H.B., Bally, J.: Tail-End Bondi-Hoyle Accretion in Young Star Clusters: Implications for Disks, Planets, and Stars. *Astronomical Journal* **135**(6), 2380–2397 (2008). DOI 10.1088/0004-6256/135/6/2380
474. Tominaga, R.T., Takahashi, S.Z., Inutsuka, S.i.: Revised Description of Dust Diffusion and a New Instability Creating Multiple Rings in Protoplanetary Disks. *Astrophysical Journal* **881**(1), 53 (2019). DOI 10.3847/1538-4357/ab25ea
475. Toomre, A.: On the gravitational stability of a disk of stars. *Astrophysical Journal* **139**, 1217–1238 (1964). DOI 10.1086/147861
476. Touboul, M., Kleine, T., Bourdon, B., Palme, H., Wieler, R.: Late formation and prolonged differentiation of the Moon inferred from W isotopes in lunar metals. *Nature* **450**, 1206–1209 (2007). DOI 10.1038/nature06428
477. Tremaine, S., Dong, S.: The Statistics of Multi-planet Systems. *Astronomical Journal* **143**, 94 (2012). DOI 10.1088/0004-6256/143/4/94
478. Trilling, D.E., Bryden, G., Beichman, C.A., Rieke, G.H., Su, K.Y.L., Stansberry, J.A., Blylock, M., Stapelfeldt, K.R., Beeman, J.W., Haller, E.E.: Debris Disks around Sun-like Stars. *Astrophysical Journal* **674**, 1086–1105 (2008). DOI 10.1086/525514
479. Tsiganis, K., Gomes, R., Morbidelli, A., Levison, H.F.: Origin of the orbital architecture of the giant planets of the Solar System. *Nature* **435**, 459–461 (2005). DOI 10.1038/nature03539
480. Turner, N.J., Fromang, S., Gammie, C., Klahr, H., Lesur, G., Wardle, M., Bai, X.N.: Transport and Accretion in Planet-Forming Disks. *Protostars and Planets VI* pp. 411–432 (2014)
481. Udry, S., Santos, N.C.: Statistical Properties of Exoplanets. *Annual Reviews of Astronomy and Astrophysics* **45**, 397–439 (2007). DOI 10.1146/annurev.astro.45.051806.110529
482. Uribe, A.L., Klahr, H., Henning, T.: Accretion of Gas onto Gap-opening Planets and Circumplanetary Flow Structure in Magnetized Turbulent Disks. *Astrophysical Journal* **769**(2), 97 (2013). DOI 10.1088/0004-637X/769/2/97
483. Valencia, D., Sasselov, D.D., O’Connell, R.J.: Detailed Models of Super-Earths: How Well Can We Infer Bulk Properties? *Astrophysical Journal* **665**, 1413–1420 (2007). DOI 10.1086/519554
484. Varnière, P., Quillen, A.C., Frank, A.: The Evolution of Protoplanetary Disk Edges. *Astrophysical Journal* **612**(2), 1152–1162 (2004). DOI 10.1086/422542
485. Veras, D., Armitage, P.J.: The Influence of Massive Planet Scattering on Nascent Terrestrial Planets. *Astrophysical Journal Letters* **620**, L111–L114 (2005). DOI 10.1086/428831
486. Veras, D., Armitage, P.J.: Predictions for the Correlation between Giant and Terrestrial Extrasolar Planets in Dynamically Evolved Systems. *Astrophysical Journal* **645**, 1509–1515 (2006). DOI 10.1086/504582
487. Villeneuve, J., Chaussidon, M., Libourel, G.: Homogeneous Distribution of ^{26}Al in the Solar System from the Mg Isotopic Composition of Chondrules. *Science* **325**(5943), 985 (2009). DOI 10.1126/science.1173907

488. Walsh, K.J., Morbidelli, A., Raymond, S.N., O'Brien, D.P., Mandell, A.M.: A low mass for Mars from Jupiter's early gas-driven migration. *Nature* **475**, 206–209 (2011). DOI 10.1038/nature10201
489. Walsh, K.J., Morbidelli, A., Raymond, S.N., O'Brien, D.P., Mandell, A.M.: Populating the asteroid belt from two parent source regions due to the migration of giant planets—"The Grand Tack". *Meteoritics and Planetary Science* **47**, 1941–1947 (2012). DOI 10.1111/j.1945-5100.2012.01418.x
490. Ward, W.R.: Density waves in the solar nebula - Differential Lindblad torque. *Icarus* **67**, 164–180 (1986). DOI 10.1016/0019-1035(86)90182-X
491. Ward, W.R.: Protoplanet Migration by Nebula Tides. *Icarus* **126**, 261–281 (1997). DOI 10.1006/icar.1996.5647
492. Warren, P.H.: Stable-isotopic anomalies and the accretionary assemblage of the Earth and Mars: A subordinate role for carbonaceous chondrites. *Earth and Planetary Science Letters* **311**, 93–100 (2011). DOI 10.1016/j.epsl.2011.08.047
493. Weber, P., Benítez-Llambay, P., Gressel, O., Krapp, L., Pessah, M.E.: Characterizing the Variable Dust Permeability of Planet-induced Gaps. *Astrophysical Journal* **854**(2), 153 (2018). DOI 10.3847/1538-4357/aaab63
494. Weidenschilling, S.J.: Aerodynamics of solid bodies in the solar nebula. *Monthly Notices of the Royal Astronomical Society* **180**, 57–70 (1977)
495. Weidenschilling, S.J.: The distribution of mass in the planetary system and solar nebula. *Astrophysics and Space Science* **51**, 153–158 (1977). DOI 10.1007/BF00642464
496. Weidenschilling, S.J., Marzari, F.: Gravitational scattering as a possible origin for giant planets at small stellar distances. *Nature* **384**, 619–621 (1996). DOI 10.1038/384619a0
497. Weiss, L.M., Marcy, G.W.: The Mass-Radius Relation for 65 Exoplanets Smaller than 4 Earth Radii. *Astrophysical Journal Letters* **783**, L6 (2014). DOI 10.1088/2041-8205/783/1/L6
498. Weiss, L.M., Marcy, G.W., Petigura, E.A., Fulton, B.J., Howard, A.W., Winn, J.N., Isaacson, H.T., Morton, T.D., Hirsch, L.A., Sinukoff, E.J., Cumming, A., Hebb, L., Cargile, P.A.: The California-Kepler Survey. V. Peas in a Pod: Planets in a Kepler Multi-planet System Are Similar in Size and Regularly Spaced. *Astronomical Journal* **155**, 48 (2018). DOI 10.3847/1538-3881/aa9ff6
499. Weiss, L.M., Marcy, G.W., Rowe, J.F., Howard, A.W., Isaacson, H., Fortney, J.J., Miller, N., Demory, B.O., Fischer, D.A., Adams, E.R., Dupree, A.K., Howell, S.B., Kolbl, R., Johnson, J.A., Horch, E.P., Everett, M.E., Fabrycky, D.C., Seager, S.: The Mass of KOI-94d and a Relation for Planet Radius, Mass, and Incident Flux. *Astrophysical Journal* **768**, 14 (2013). DOI 10.1088/0004-637X/768/1/14
500. Wetherill, G.W.: Accumulation of the terrestrial planets. In: T. Gehrels (ed.) IAU Colloq. 52: Protostars and Planets, pp. 565–598 (1978)
501. Wetherill, G.W.: Why Isn't Mars as Big as Earth? In: Lunar and Planetary Institute Science Conference Abstracts, *Lunar and Planetary Inst. Technical Report*, vol. 22, p. 1495 (1991)
502. Wetherill, G.W.: An alternative model for the formation of the asteroids. *Icarus* **100**, 307–325 (1992). DOI 10.1016/0019-1035(92)90103-E
503. Wetherill, G.W.: The Formation and Habitability of Extra-Solar Planets. *Icarus* **119**, 219–238 (1996). DOI 10.1006/icar.1996.0015
504. Wetherill, G.W., Stewart, G.R.: Accumulation of a swarm of small planetesimals. *Icarus* **77**, 330–357 (1989). DOI 10.1016/0019-1035(89)90093-6
505. Wetherill, G.W., Stewart, G.R.: Formation of planetary embryos - Effects of fragmentation, low relative velocity, and independent variation of eccentricity and inclination. *Icarus* **106**, 190 (1993). DOI 10.1006/icar.1993.1166
506. Williams, J.P., Cieza, L.A.: Protoplanetary Disks and Their Evolution. *Annual Reviews of Astronomy and Astrophysics* **49**, 67–117 (2011). DOI 10.1146/annurev-astro-081710-102548
507. Windmark, F., Birnstiel, T., Güttler, C., Blum, J., Dullemond, C.P., Henning, T.: Planetesimal formation by sweep-up: how the bouncing barrier can be beneficial to growth. *Astronomy & Astrophysics* **540**, A73 (2012). DOI 10.1051/0004-6361/201118475

508. Winn, J.N., Fabrycky, D.C.: The Occurrence and Architecture of Exoplanetary Systems. *Annual Reviews of Astronomy and Astrophysics* **53**, 409–447 (2015). DOI 10.1146/annurev-astro-082214-122246
509. Wittenmyer, R.A., Butler, R.P., Tinney, C.G., Horner, J., Carter, B.D., Wright, D.J., Jones, H.R.A., Bailey, J., O’Toole, S.J.: The Anglo-Australian Planet Search XXIV: The Frequency of Jupiter Analogs. *Astrophysical Journal* **819**, 28 (2016). DOI 10.3847/0004-637X/819/1/28
510. Wittenmyer, R.A., Wang, S., Horner, J., Butler, R.P., Tinney, C.G., Carter, B.D., Wright, D.J., Jones, H.R.A., Bailey, J., O’Toole, S.J., Johns, D.: Cool Jupiters greatly outnumber their toasty siblings: occurrence rates from the Anglo-Australian Planet Search. *Monthly Notices of the Royal Astronomical Society* **492**(1), 377–383 (2020). DOI 10.1093/mnras/stz3436
511. Wolfgang, A., Rogers, L.A., Ford, E.B.: Probabilistic Mass-Radius Relationship for Sub-Neptune-Sized Planets. *Astrophysical Journal* **825**, 19 (2016). DOI 10.3847/0004-637X/825/1/19
512. Wright, J.T., Fakhouri, O., Marcy, G.W., Han, E., Feng, Y., Johnson, J.A., Howard, A.W., Fischer, D.A., Valenti, J.A., Anderson, J., Piskunov, N.: The Exoplanet Orbit Database. ArXiv e-prints (2010)
513. Wright, J.T., Marcy, G.W., Butler, R.P., Vogt, S.S., Henry, G.W., Isaacson, H., Howard, A.W.: The Jupiter Twin HD 154345b. *Astrophysical Journal Letters* **683**, L63–L66 (2008). DOI 10.1086/587461
514. Wright, J.T., Upadhyay, S., Marcy, G.W., Fischer, D.A., Ford, E.B., Johnson, J.A.: Ten New and Updated Multiplanet Systems and a Survey of Exoplanetary Systems. *Astrophysical Journal* **693**, 1084–1099 (2009). DOI 10.1088/0004-637X/693/2/1084
515. Wyatt, M.C.: Evolution of Debris Disks. *Annual Reviews of Astronomy and Astrophysics* **46**, 339–383 (2008). DOI 10.1146/annurev.astro.45.051806.110525
516. Wyatt, M.C., Kennedy, G., Sibthorpe, B., Moro-Martín, A., Lestrade, J.F., Ivison, R.J., Matthews, B., Udry, S., Greaves, J.S., Kalas, P., Lawler, S., Su, K.Y.L., Rieke, G.H., Booth, M., Bryden, G., Horner, J., Kavelaars, J.J., Wilner, D.: Herschel imaging of 61 Vir: implications for the prevalence of debris in low-mass planetary systems. *Monthly Notices of the Royal Astronomical Society* **424**(2), 1206–1223 (2012). DOI 10.1111/j.1365-2966.2012.21298.x
517. Yang, C.C., Johansen, A., Carrera, D.: Concentrating small particles in protoplanetary disks through the streaming instability. *Astronomy & Astrophysics* **606**, A80 (2017). DOI 10.1051/0004-6361/201630106
518. Youdin, A.N., Goodman, J.: Streaming Instabilities in Protoplanetary Disks. *Astrophysical Journal* **620**, 459–469 (2005). DOI 10.1086/426895
519. Zellner, N.E.B.: Cataclysm No More: New Views on the Timing and Delivery of Lunar Impactors. *Origins of Life and Evolution of the Biosphere* **47**, 261–280 (2017). DOI 10.1007/s11084-017-9536-3
520. Zhang, H., Zhou, J.L.: On the Orbital Evolution of a Giant Planet Pair Embedded in a Gaseous Disk. I. Jupiter-Saturn Configuration. *Astrophysical Journal* **714**, 532–548 (2010). DOI 10.1088/0004-637X/714/1/532
521. Zhang, Q.: Prospects for Backtracing II/ ‘Oumuamua and Future Interstellar Objects. *Astrophysical Journal Letters* **852**, L13 (2018). DOI 10.3847/2041-8213/aaa2f7
522. Zhou, J.L., Aarseth, S.J., Lin, D.N.C., Nagasawa, M.: Origin and Ubiquity of Short-Period Earth-like Planets: Evidence for the Sequential Accretion Theory of Planet Formation. *Astrophysical Journal Letters* **631**, L85–L88 (2005). DOI 10.1086/497094
523. Zhu, W., Wu, Y.: The Super Earth-Cold Jupiter Relations. *Astronomical Journal* **156**(3), 92 (2018). DOI 10.3847/1538-3881/aad22a
524. Zube, N.G., Nimmo, F., Fischer, R.A., Jacobson, S.A.: Constraints on terrestrial planet formation timescales and equilibration processes in the Grand Tack scenario from Hf-W isotopic evolution. *Earth and Planetary Science Letters* **522**, 210–218 (2019). DOI 10.1016/j.epsl.2019.07.001